Evaluation of the Stability and Suitability of Ashebeka Dam Foundation and Reservoir Area, Arsi Zone, Central Ethiopia

Alemayehu Solomon Demise

A Thesis Submitted to the Department of Applied Geology

School of Applied Natural Science

Presented in Partial Fulfillment of the Requirement for the Degree of Master's in Applied Geology (Engineering Geology)

Office of Graduate Studies

Adama Science and Technology University

February, 2024

Adama, Ethiopia

Evaluation of the Stability and Suitability of Ashebeka dam Foundation and Reservoir area, Arsi zone, Central Ethiopia

Alemayehu Solomon Demise

Advisor

Endalu Tadele (PhD.)

Co-Advisor

Dr.Yadeta chemdesa

A Thesis Submitted to the Department of Applied Geology

School of Applied Natural Science

Presented in Partial Fulfillment of the Requirement for the Degree of Master's in Applied Geology (Engineering Geology)

Office of Graduate Studies

Adama Science and Technology University

February, 2024

Adama, Ethiopia

Declaration

I hereby declare that this Master Thesis entitled "**Evaluation of the Stability and Suitability of Ashebeka Dam Foundation and Reservoir Area, Arsi zone, Central Ethiopia**" is my original work. That is, it has not been submitted for the award of any academic degree, diploma or certificate in any other university. All sources of materials used for this thesis have been duly acknowledged through citation.

______________________ ______________________ ______________________

Name of student Signature Date

Recommendation

We, the advisors of this thesis, hereby certify that we have read the revised version of the thesis entitled "**Evaluation of the Stability and Suitability of Ashebeka Dam Foundation and Reservoir Area, Arsi zone, Central Ethiopia**" prepared under our guidance by Alemayehu Solomon submitted in partial fulfillment of the requirements for the degree of Master of Science in Applied Geology. Therefore, we recommend the submission of revised version of the thesis to the department following the applicable procedures.

______________________	________________	_______
Major Advisor	Signature	Date
______________________	______________________	______________________
Co-advisor	Signature	Date

Approval Page

We, the advisors of the thesis entitled "**Evaluation of the Stability and Suitability of Ashebeka Dam Foundation and Reservoir Area, Arsi zone, Central Ethiopia**"and developed by Alemayehu Solomon, hereby certify that the recommendation and suggestions made by the board of examiners are appropriately incorporated into the final version of the thesis

Major Advisor	Signature	Date
Co-advisor	Signature	Date

We, the undersigned, members of the Board of Examiners of the thesis by Alemayehu Solomon have read and evaluated his thesis entitled"**Evaluation of the Stability and Suitability of Ashebeka Dam Foundation and Reservoir Area, Arsi zone, Central Ethiopia**" and examined the candidate during open defense. This is, therefore, to certify that the thesis has been accepted in partial fulfillment of the requirement of the Degree of Master of Science applied Geology.

Chairperson	Signature	Date
Internal Examiner	Signature	Date
Internal Examiner	Signature	Date

Finally, approval and acceptance of the thesis is contingent upon submission of its final copy to the Office of Postgraduate Studies (OPGS) through the Department Graduate Council (DGC) and School Graduate Committee (SGC).

Department Head	Signature	Date
School Dean	Signature	Date
Office of Postgraduate Studies, Dean	Signature	Date

Abstract

In the countries like Ethiopia where the economy is led by agriculture and has a huge potential of resources for such activities, the construction of dams for irrigational purposes is very essential. The Ashebeka dam irrigation project is located in Degeluna Tijo Woreda, Arsi Zone of Oromia Regional State at about 30km south east of Asela Capital city of Arsi zone. The planned dam will have a height of 28m and a dam axis length of around 550m. However, the dam encountered engineering geological problems that affected the water tightness and stability of the dam axis and reservoir area.The main objective of this work is to investigate and characterize the engineering geological aspects of the proposed dam foundation and reservoir area based on detailed geological, geotechnical and geophysical investigations. The engineering geological investigation conducted in this site includes discontiunity survey, borehole drilling and laboratory testing. The area is characterized by the different rocks such as ignimbrite, tuff, vesicular basalt, residual and alluvial soils with different geological stuctures such as joints, fractures, and columnar joints were encountered. Geotechnically four layers were identified, these are overburden which comprises highly weathered ignimbrite and soil; moderately to slightly weathered ignimbrite, decomposed tuff and highly fractured and slightly weathered basalt rock mass. The result from this study showed that the average uniaxial compressive strength values range from 7.2 MPa for tuff to 109 MPa for ignimbrite rocks and the RQD values range from 24.5-88 and the RMR value ranges from 48 to 70. The estimated modulus of deformation and allowable bearing capacity ranges from 4.2 GPa to 40 GPa and 0.46 MPa to 27 MPa respectively. The permeability result of weak and highly fractured rock mass on the surface ranges from $2.9*10^{-1}$ - $4.6*10^{3}$ cm/s and from falling head test at a shallow depth of the foundation showed pervious and from packer test result the lugeon value ranging from 0-2. Generally the permeability decreases down a depth.The soils found in the study area were dominated by clayey silt soils and they have a plasticity index ranging from 12.8% - 47%. The permeability of soils determined from falling head laboratory tests ranges from $1.12*10^{-6}$cm/s to $7.25*10^{-5}$ cm/s. From slope stability analysis, both left and right abutment is stable, however both are unstable under fully saturated condition. Based on the findings of this study, ground improvement techniques have been suggested including consolidation grouting. For the water tightness and strength problems curtain and consolidation grouting were recommended in the proposed dam site, while bench stabilisation, changing the slope geometry, drainage holes, and shotcrete systems were recommended for slope stability issues.

Keywords: *Ashebeka Dam, Discontiunity survey, Rock mass Characterization, Water tightness, Slope stability, Improvement techniques.*

ACKNOWLEDGEMENT

First of all, I would like to thank the almighty God and his mother St. Marry for their protection and success in my life. Without them, I would not have had the wisdom and ability to do so. I am also grateful to Adama Science and Technology University for offering a master's scholarship and financial support during research work. My deepest gratitude also goes to the Engineering Corporation of Oromia (ECO), Ministry of mine, Geological Survey and Ethiopian Meterological Agency for their guidance and data sharing related to Ashebeka dam project.

I would like to express my deepest gratitude to my advsor Dr. Endalu Tadele and co-advisor Dr. Yadeta Chemdesa for their guidance and supervision during the entire period of this research. Further, I would like to thank staff members of applied geology department in Adama science and technology university for their valuable support, comments and strangely Mr. Belay Belete for his material support during this research work.

Table of content

LIST OF FIGURE

LIST OF TABLES

List of Abbreviations and Acronyms

ASTM ………………………..American Society for Testing Materials Standard

ASHBH…………………….Ashebeka borehole

Ed ……………………………Modulus of deformation

ECDSWC ……………………Ethiopian Construction Design & Supervision Works Corporation.

ECO ………………..…..…Engineering Corporation of Oromia

GPS ………………………..Global Positioning System

GSI ………………………...Geological Strength Index

HEP ………………………..Horizontal Electrical Profiling

ISRM……………………….. International Society of Rock Mechanics' Standards

JV ………………………..Volumetric Joint Count

RMR………………………..Rock mass rating

RQD ……………………….Rock quality designation

UCS ………………………..Uniaxial Compression Strength

USBR …………………………U. S. Bureau of Reclamation

USCS…………………………Unified Soil Classification System

VES …………………………Vertical Electrical Sounding

CHAPTER ONE

1. INTRODUCTION

1.1. Background

Dams are built to store water for irrigation, municipal use, hydropower electricity generation, and flood prevention. It has various size and complexity ranging from small and structurally simple constructions to large and structurally more complex dams (Johansson, 1997 and Abrehet, 2017). A dam and a reservoir are complements of each other.

The importance of geology in engineering practice is highly appreciated for hydraulic structures, particularly during the investigation and construction of dams and tunnels, where many relevant problems are closely associated with the geological conditions of the area. Investigation is not limited to the dam site only, but it must also involve the reservoir and catchment area in order to gather enough and reliable information for the success of the project. According to Gangopadhyay.S (1993), engineering geological investigation involves remote sensing study, geological, geotechnical, borehole drilling, geophysical and laboratory works are carried out to identify the surface and subsurface information of the site.

Many dams constructed in different parts of the world are affected by **leakage** (Mozafari et al., 2011). In addition, the type of dam and its design is determined by the amount of available water, topography, geology and availability of local construction materials (Fell et al., 2005). Even though, a dam site falls relatively in geologically and topographically ideal terrain, construction of dam requires engineering geological investigation. If not, dam failure can cause economic damage and it can also adversely affect people's lives on the downstream side of a dam (Robin et al., 2005).

In Ethiopia the construction of micro-dams started in the late seventies to combat the recurrent drought in the country (Tiruneh, 2005) particularly in the Northern part of Ethiopia. However, in Tigray and Amhara Regions, several constructed dams have faced **engineering geological problems** such **as leakage, reservoir siltation, damages of spillway route** and dam body without giving their desired purposes (Berhane et al., 2013). These water losses could occur through the dam body, dam foundation, dam abutments and geological formations located near the dam site, the reservoir bed and at abutments, and the **excessive seepage and/or leakage** may lead to a serious problem endangering the safety of the dam (Fell et al., 2005). Similarly, **slope failure** is one of the severe hazards that leads to the destruction of engineering structures of dam. Hence, slope stability analysis is becoming important in geotechnical engineering to prevent this natural disaster (Hussain et al., 2019).These phenomena indicate that the construction of a dam requires **proper engineering geological investigations** in the country for their safe functioning.

The present research deals about the engineering geological characterization of Ashebka Dam Site in south east of Asela. To come up with a comprehensive result, this dam site investigation has undertaken electrical resistivity method, borehole drilling and measurements of Schmidt hammer rebound values of rocks. Geophysical investigation, field observations, borehole drilling, and in-situ testing have all been used to evaluate the engineering characteristics of the rocks at this dam site.

1.2. Problem of Statement

Many dam failures occur due to lack of sufficient engineering geological characterization before the construction is commenced. Geological set-up of dam sites and associated geotechnical problems are variable from place to place. **Unfavorable geological condition** can exist anywhere. Through proper engineering geological investigation in-depth understanding of the geological conditions and their effect on the planned dam must be understood and **appropriate remedial measures** must be provided. In practice the design of an efficient foundation system depends on appropriate characterization of the supporting soil and rock, and determining the proper geotechnical parameters (Robin et.al, 2005).

The proposed Ashebeka dam site is located in an area where the geology is dominated by **pyroclastic rocks mainly ignimbrite and tuff**. This indicates that the proposed dam site can possibly face **water tightness and stability problems**. Furthermore, the dam site is located in **the south eastern flank of the main Ethiopian rift**. This could increase the vulnerability of the dam site to earthquake seismicity. Any failure on Ashebeka dam could cause risk on the lives of people living at the downstream side. Furthermore, it may also cause **economic**

destruction on the dam and the surrounding areas. In addition to this, the failure of this dam causes socioeconomic problems to society.

The success of the project will depend on **the suitability and stability of ground condition**. It is essential that the dam foundation, its abutments and reservoir site must be watertight and stable to withstand the loads imposed on the dams. Thus, this research is intended to fill the gap by providing the necessary information with regard to the detail geological and geotechnical characteristics of the materials around the dam site and reservoir area with respect to different problems.

1.3. Objective of the Study

1.3.1. General Objective

- ❖ The main objective of this study is to characterize engineering geological condition of Ashebeka dam foundation and reservoir area.

1.3.2. Specific objective

- ❖ To study the Lithostrtigraphy and geological structures of the dams axis and produce engineering geological map of dam site foundation with detail scale (1:5000)
- ❖ To evaluate the stability of dam foundation and its abutments using geomechanical analysis/approaches
- ❖ To determine the foundation suitability of dam axis based on geotechnical rockmass quality analysis.
- ❖ To assess the permeable zone and watertightness conditions of dam foundation and reservoir sites.
- ❖ To forward possible engineering remedial measures for the treatment of dam foundation and reservoir area.

1.4. Significance of the study

Dam is among engineering structures that require detail engineering geological investigation on the proposed site. Therefore, this study conducts engineering geological assessment on the proposed Ashebeka dam site to minimize foundation problem, water tightness and slope instability problems. The result of the research will be helpful for the construction and post construction phase of the dam. This research work provides useful data/information for the future researchers who are intending to work in similar problem domain. The result and findings of this research will contribute in upgrading the data in the area as well as in the region which can be used by the scientific community at large. A comprehensive and systematic investigation ensures safety and long span of the project. The physical parameters of the subsurface from the site investigation are important for geoscientists and engineers to understand the geological and engineering parameters. As part of the growth and transformation plan in Ethiopia, the country is engaged in study and construction of Ashebeka dam irrigation projects. The present research showed feasible methodology to make preliminary for characterizing of the dam foundation, reservoir and geological material for safe design and identifying any geological and engineering geological problem under the dam area. Furthermore, the present study forwarded the relative feasible and practical solutions for the sustainability of the foundation layers.

1.5. Location and accessibility

The Ashebeka dam irrigation project is located in Degeluna Tijo Woreda, Arsi Zone of Oromia Regional State at about 30km south east of Asela. Only three (3) km is required to walk on foot to arrive at dam site from Sauger town. It is bounded between 39° 05' 10.1039" to 39° 11' 58.2869" E longitude and 7° 40' 17.9567" to 7° 45' 43.4636" N latitude. It is foundat a distance of about 153 km to the South eastern direction from Adama.

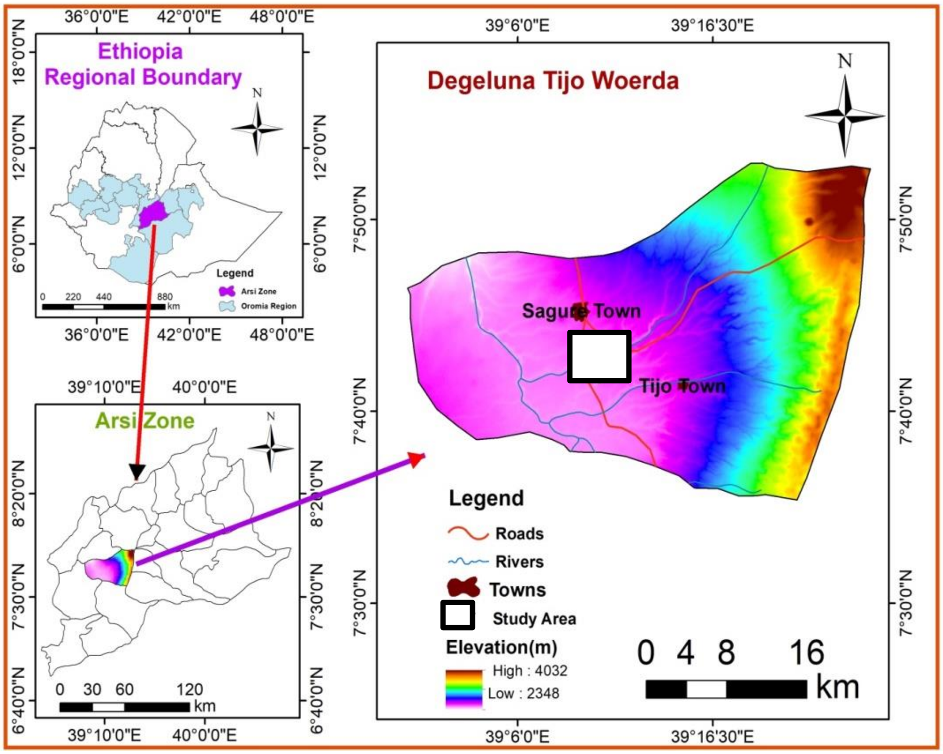

Figure 1 Location map of Ashebeka dam site

1.6. Climate

The important elements of climate for both agricultural and hydrology are evaporation, temperature and precipitation. The climate of Ethiopia ranges from equatorial desert to hot and cool steppe, from tropical Savanah and rain forest to warm temperate, and from hot low land to cool high lands (Tenalem and Tamiru, 2001).

The study area belongs to the tropical types of climate in which the first rainy peak occur in April which is known as Belg. The second major rainy season is summer. This begins in June and continues to September. The mean annual rainfall in the highland of the area is relatively high. The temperature is low in the mountains of Chilalo.

1.6.1. Hydrological data

The flow of the Ashebeka River, which is a tributary of the Lake Ziway Shala sub-basin of the Upper Rift Valley Basin, is the primary surface water supply for the irrigation needs of the proposed project area. The Ashebeka River flow gauging station in Sagure town has perennial flow, and the catchment area for the dam site for the present study project is located closer to it.

1.6.1.1. Rainfall

The National Meteorological Service Agency's (NMSA's) statistics from the Saugure Observatory Substation show that the average mean annual rainfall from 2001 to 2020, at an altitude of 2400 metres above mean sea level, was 63.59 mm.

The maximum average annual rainfall amount in the study area within twenty years interval was 79.8mm recorded in 2006 and the minimum average was 47.39mm recorded in 2009 and the average value was 63.59mm as shown below in the table1. As shown in Fig 3.1 the maximum average rain fall was 344.9mm recorded on summer season followed by 241.09 on the season autumn and minimum average rainfall was 33.2mm recorded on winter season within twinty consecutive years. The result shows that the study area characterized by large amount of rainfall.

Table 1 Distribution of rainfall amount within twenty year interval (NMSA's)

	Avg. Annual rainfall (mm)	Avg. Monthly Rainfall(mm)	Avg. seasonal rainfall (mm)			
			Winter	Autumn	Summer	Spring
Avg.Min. Rainfall(mm)	47.39	8.51	1.9	109.6	230.7	19.8
Avg.Max. Rainfall(mm)	79.8	132.235	112.7	439.8	464.2	189.3
Average value(mm)	63.59	60.55	33.2	241.09	344.9	107.56

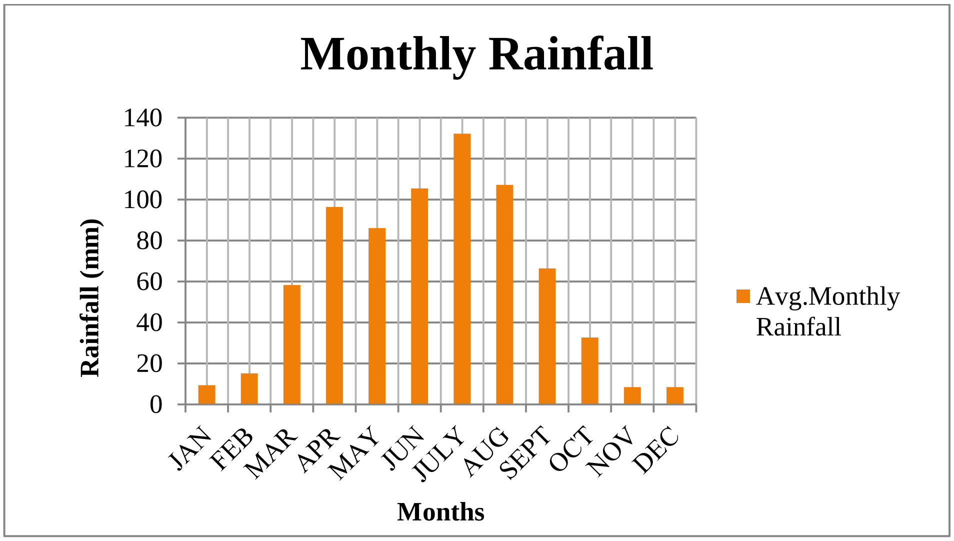

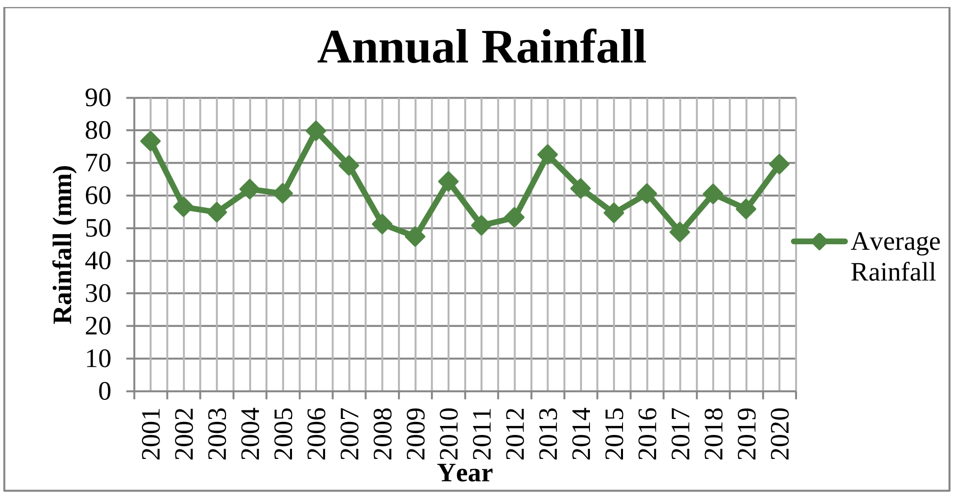

Figure 2 Monthly and annually rainfall distribution of the study area for twenty years interval.

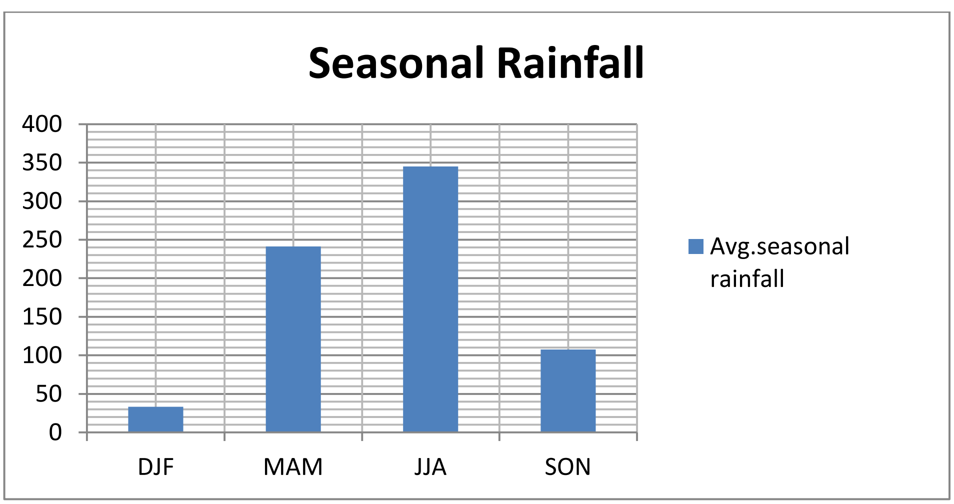

Figure 3 Distribution of seasonal rainfall amount within twenty year interval

1.6.2 Temperature

In a mountainous tropical country like Ethiopia altitude is by far the most important factor in controlling climate. It affects distribution of both temperature and rainfall. Generally, regions between 1500 - 2300 meters a.m.s.l. (categorized as 'woina dega' or sub tropical climate) have temperatures that range between 15 - 20^{o}C, areas between 500– 1500 meters a.m.s.l. (i.e. 'kola' or tropical climate) have 20 -30^{o}C and areas below 500 meters a.m.s.l. (i.e. 'bereha' or desert climate) have a temperature of 30^{o}C and above.

Table 2 Table of Temprature varation of the area from 2004 to 2020 (NMSA's) .

	Avg. Annual Tempracture(^{o}c)	Avg. Monthly Tempracture(^{o}c)	Seasonal temprature (^{o}c)			
			Winter	Autumn	Summer	Spring
Avg.Min. Tempracture	13.88	13.2	14.2	10.9	13.6	13.62
Avg.Max. Tempracture	16.12	18.1	17.3]	17.15	15.72	16.77
Average value	15	15.65	15.33	15.8	14.72	14.19

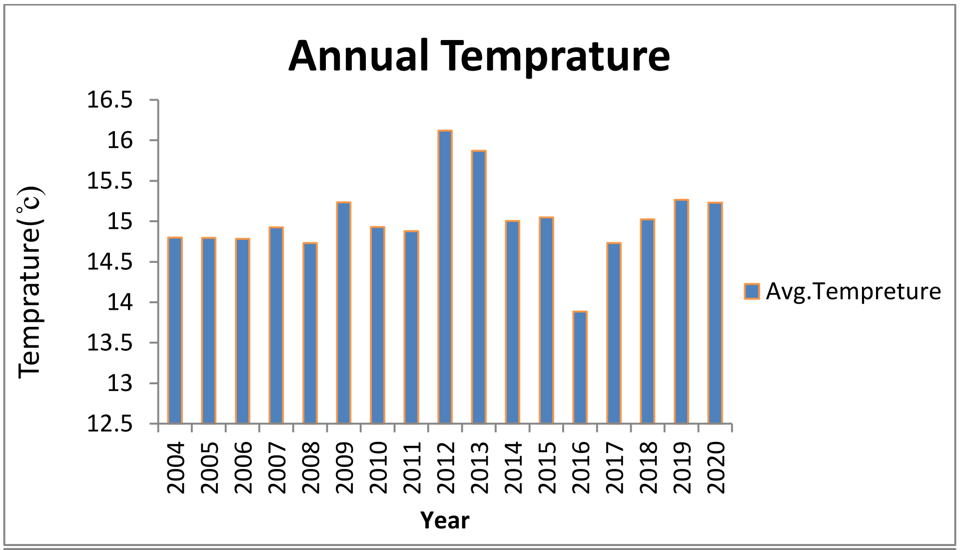

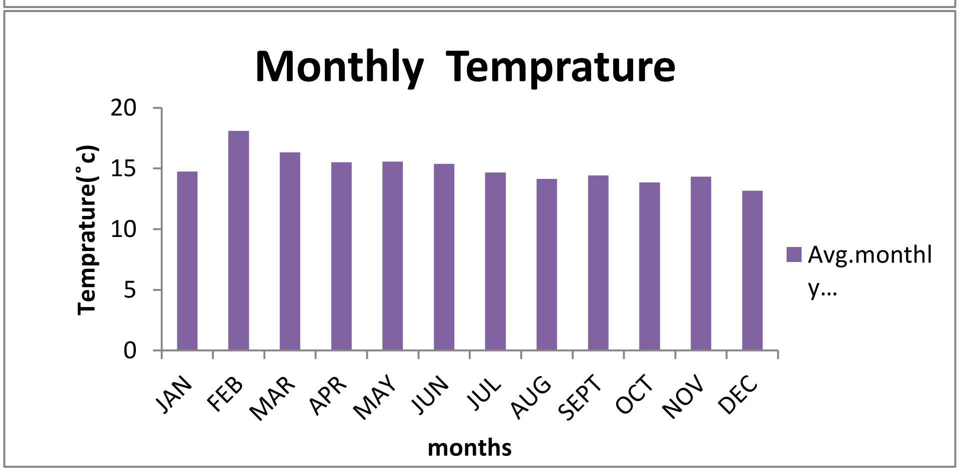

Figure 4 Monthly and annual temperature distribution of the study area for twenty years

In the study area, with an altitude ranging from 2400-2480meters a.m.s.l., has a mean minimum, mean maximum and mean average monthly temperatures of 13.2, 18.1 and 15.65°C respectively. The highest temperatures were during months of February, March, April, May and June where as August, October, and December have low temperature. Similarlly the mean minimum, mean maximum and mean average annual temperature were 13.88, 16.12, and 15 respectively. The highest annual temperature was recorded in 2012 and the lowest was in 2016. This shows the temperature variation is almost the same through out the year.

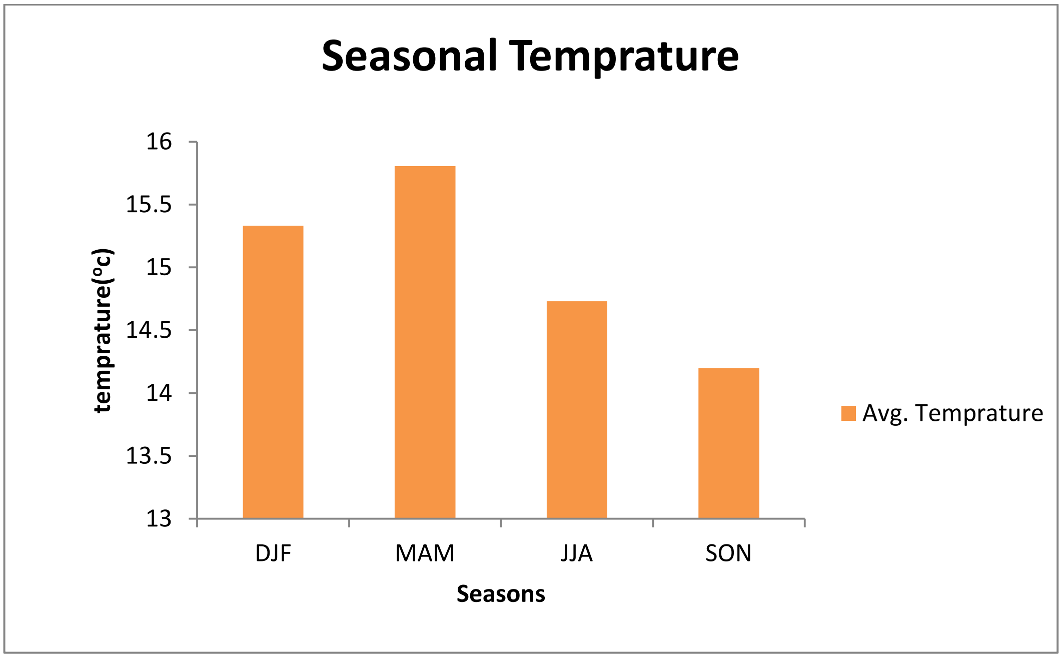

Figure 5 Seasonal temperature varation within twenty year interval

1.7. Physiography and Drainage of the study area

In Arsi Zone the plateau surface begins from rift escarpments and extends to Sagure and surrounding areas. These plateau surfaces are built of pyroclastic rocks and to a lesser extent by basalts. There are also scoria cones and basalt hills occur in the near far area. In some part of the map area, the plateau surface with almost near to the horizontal slope. The project area is surrounded exposed to residual and some alluvial deposit underlain by ignimbritic and locally basaltic bolder forming exposure. All of the river flow to the main katar river from the eastern and southern corners of the highland of the area. The command side generally situated within the low laying portions of this meandering stream extension. Topographically, it is characterized by flat to slightly undulating terrains and surrounded by medium relief mountain chains in the north and northeast. The elevation of the area ranges from 2420 to2700m.

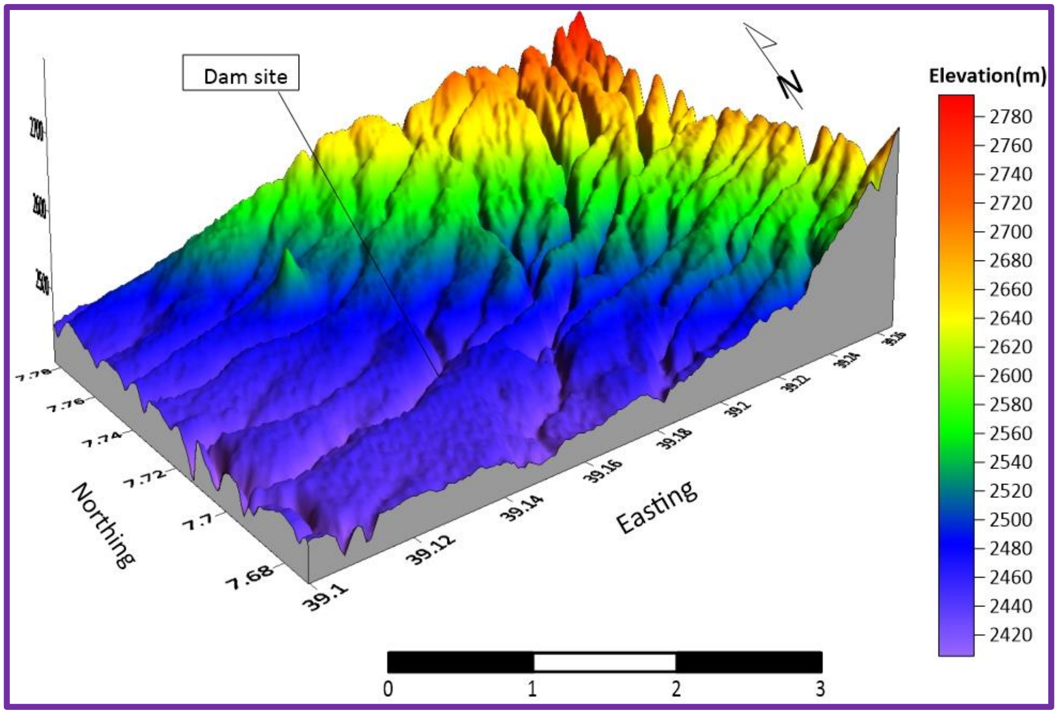

Figure 6 physiographic map of Ashbeka dam site and the surrounding

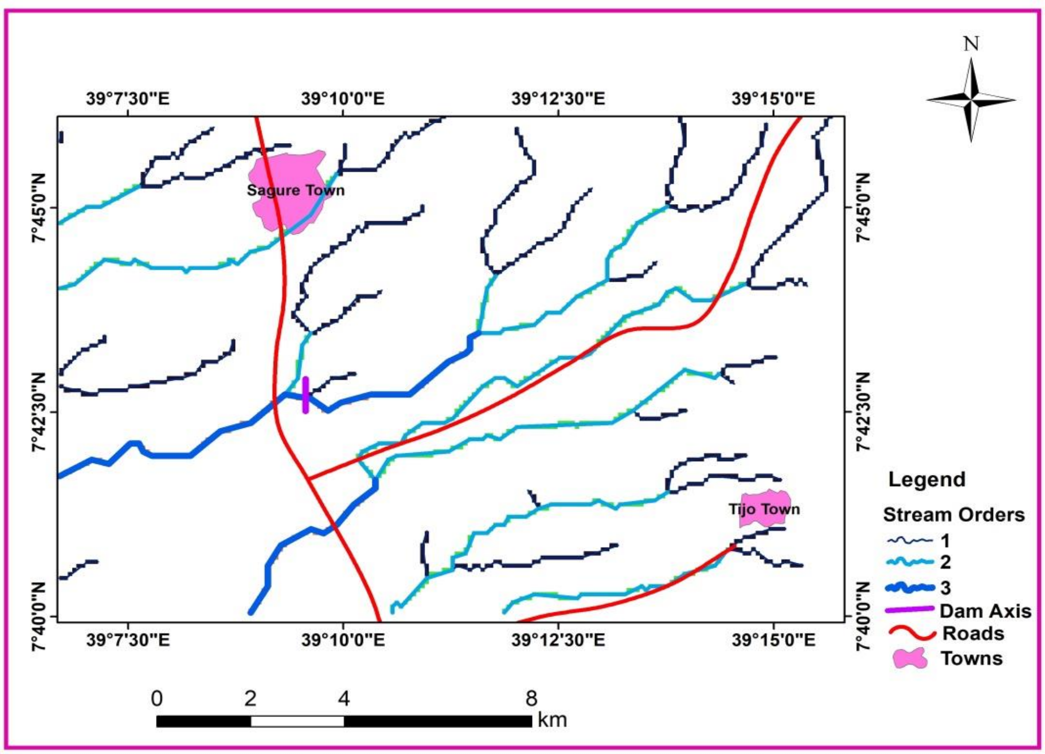

Figure 7 Drainage map of the study area with stream order.

1.8. Seismicity of Study Area

The horizontal seismic acceleration of the study area is determined from the seismic hazard map of Ethiopia. The map is based on the amplitude of ground acceleration to be expected during 100 years return period. According to the map, the country is divided into distinct seismic risk zones depending on the known history of past damaging earthquakes

The location of Ashebeka Dam site is at the eastern margin of Main Ethiopian Rift (MER), which is characterized by active tectonics. The active geodynamic nature of the MER makes the dam site vulnerable and even susceptible to seismic (earthquake) and volcanic hazards.

According to (ES EN 19981: 2015), the project area lies in Zone 3 of seismicity, where the shaking level with a 10% exceedance in 50 years matches a Peak Ground Surface Acceleration of 0.8-1.2 (m/s2).

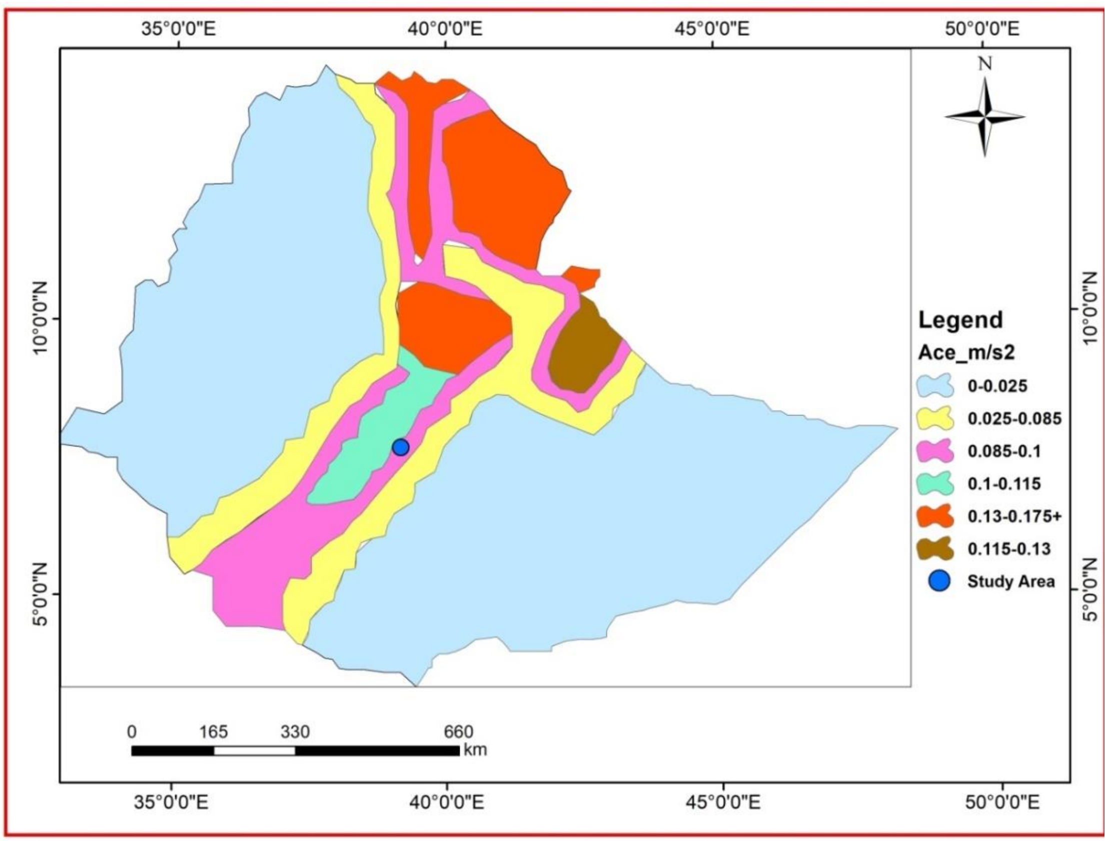

Figure 8 Ethiopia’s Seismic hazard map in terms of peak ground acceleration after (ES EN 19981: 2015

CHAPTER TWO

2. LITERATURE REVIEW

2.1. Engineering geological characterization on Dam and Reservoir

Most dam site studies revealed that inadequate engineering geological characterization is the main reason for failure (Barzegari, 2017). According to Gangopadhyay (1993), thick overburden of soft materials, presence of weathered rocks, structural defects like fault, shear zones and joints are some of common engineering geological problems that encountered during dam construction. He also stated that old slides, permeable boulder bed, buried channel and Karstic condition are adverse geological features of certain dam site. Due to the unique nature of a given dam site information regarding the engineering geological conditions plays a great role for safe design (Rajabi et al., 2014; Barzegari, 2017). Therefore, integrated surface geological surveying, core drilling, discontinuity surveying, test pits excavations, insitu testing and geophysical methods can be used to conduct engineering geological characterization to have a better understanding on the geology of the dam's foundation, reservoir area and abutments.

2.2. Rock mass characterization and classification

A rock mass classification system is intended to classify the rock mass based on their strength, discontinuity condition , weathering, structural orientation and so on which provide a basis for estimating the deformability and strength properties, supply measureable data for support estimation, and present a platform for communication between exploration, design and construction groups (Bieniawski, 1989). As stated by Sen and Sadagah (2002), the behavior of rock mass is governed by intact rock material properties and discontinuity.

Different classification systems place different emphases on the various parameters, and it is recommended that at least two methods be used at any site during the early stages of a project (Palmstrom, 2003). The rock mass classification schemes that are often used in rock engineering for assisting in designing structures are RQD, RMR, Q and GSI systems (Palmstrom, 2003).

2.2.1 Rock Quality Designation (RQD)

RQD is a modified core recovery index defined as the total length of intact core greater than 100mm in length, divided by the total length of the core run. The resulting value is presented in the form of a percentage. RQD should only be calculated over individual core runs; usually 1.5 meters long (Deere, 1988).

Table 3 Engineering classification of rock mass quality according to Deere (1968)

RQD	90-100	75-90	50-75	25-50	<25
Rock mass quality	Excellent	Good	Fair	Poor	Very poor

$$RQD = \frac{SUM\ OF\ CORE\ PIECES \geq 10cm}{TOTAL\ DRILL\ RUN} * 100\% \qquad (1)$$

RQD also estimated from the number of joints (discontinuities) per unit volume Jv using an indirect method (Volumetric Joint Count).

$$RQD = 115 - 3.3Jv, \qquad (2)$$

Where Jv is total number of joints per cubic meter.

The volumetric joint count Jv can be calculated from joint spacing which is described by Palmstrom (1982, 1985, 1986); and Sen and Essa (1992). It is a measure for the number of joints within a unit volume of rock mass

$$Jv = \sum_{i=1}^{J}(1/Si) + Nr/Sr, \qquad (3)$$

Where **Si** is the average joint spacing in meters for the **ith** joint set. Random joints may also be considered by assuming a 'random spacing'. Experience indicates that this should be set to **Sr** = 5m (Palmstrom, 1996). And **Nr** is number of random or irregular joints.

2.2.2 Rock Mass Rating (RMR)

RMR method was introduced and developed by (Bieniawski,1989) for the application of designing tunnels, dams, mines, excavation and slope stability which is based on detailed field and laboratory studies. The Rock Mass Rating system (RMR) uses six parameters as input. The respective parameters for estimating RMR are: uniaxial compressive strength of rocks

(UCS), rock quality designation (RQD), spacing of discontinuities, condition of discontinuities, groundwater conditions and orientation of discontinuities (Bienwski, 1989). The ratings for these five parameters are summed up to yield the RMR basic.

The last parameter joint orientation is treated separately because the influence of discontinuity orientations depends upon the engineering applications.

$$RMR = RMR_{basic} + \text{adjustment for joint orientation} \quad (4)$$

$$RMR_{basic} = \sum \text{parameters } (I + II + III + IV + V) \quad (5)$$

A) Uniaxial compressive strength (UCS) of intact rock

The uniaxial compressive strength of the intact rock material can be obtained from rock cores in the laboratory test. However, direct determination of the UCS is relatively expensive and it can be estimated from point load strength index I_s (50).

Broch and Franklin (1972) described the relation between uniaxial compressive strength and point load as follows.

$$UCS = 24 * Is\ (50) \quad (6)$$

Where $I_{s\ (50)}$ is the size corrected point load strength.

As a non-destructive, portable and cost-effective device for hardness testing, the Schmidt hammer is often used to obtain an indirect estimation of UCS. The Schmidt hammer rebound value may be influenced by types of hammer used, the direction of hammer impact, weathering, moisture, specimen requirements (free of any visible crack) and testing, data gathering/reduction and analysis procedures (Aydin and Basu, 2005) and all these factors should be considered during the test.

Barton and Choubey (1977) stated that uniaxial compressive strength (σc) of the rock can be estimated by multiplying the rebound number from Schmidt hammer test and the dry unit weight of the rock.

$$\log 10\ (\sigma_c) = 0.00088\gamma R + 1.01 \quad (7)$$

Where; σc is the uniaxial compressive strength in MN/m2, γ is the dry rock densities in KN/m3 and R is the average Schmidt rebound value.

B) **Discontinuity characteristics**

Which is used as a parameter of the basic RMR such as; spacing between discontinuities and condition of discontinuities (aperture, persistence, roughness, infilling, and alteration/weathering) that directly influence the characteristics of the rock mass by reducing the strength and the parameters were described and classified from surface exposure or drill core samples (Bieniawski, 1973).

C) **Groundwater conditions**

Which can strongly influence rock mass behavior. The groundwater rating varies according to the conditions encountered and the general conditions can be described as completely dry, damp, wet, dripping and flowing with a higher rating for a completely dry rock mass (Bieniawski, 1989).

Table 4 Rock mass classification based on RMR-value (After Bieniawski, 1989)

Rock Rating	100-81	80-61	60-41	40-21	20-0
Rock class	I	II	III	IV	V
Classification	Very good	Good	Fair	Poor	Very poor
Cohesion	>400kpa	300-400kpa	200-300kpa	100-200kpa	<100kpa
Friction angle	>45	45-35	35-25	25-15	<15

Bieniawski (1976) suggested the following relationships in order to determine the cohesion and angle of friction for a specific RMR.

$$C = 0.05RMR \quad (8)$$

$$\Phi = 0.5RMR + 5 \quad (9)$$

Where Φ = angle of internal friction (degree) C = cohesion (MPa).

Palmstrom et al. (2006) describes that there is no input parameter for the rock stresses in the RMR system; however stresses up to 25MPa are included in the estimated RMR value. Thus, rock mass changes because of the overstressing like rock bursting and squeezing is not included in this classification system. Therefore, it is probable that RMR does not work well for many faults and weakness zones. Also, swelling rock is not included in the RMR system (Palmstrom, et al., 2006).

2.2.3. Slope Mass Rating (SMR)

Slope Mass Rating (SMR; Romana, 1985) is calculated using four correction factors of basic RMR (Bieniawski, 1989). These factors depend on the existing relationship between discontinuities affecting the rock mass and the slope, and the slope excavation method. It is obtained using expression (10):

$$\mathbf{SMR = RMR_b + (F1 \times F2 \times F3) + F4} \tag{10}$$

Where;

F1 – depends upon parallelism between joints and slope face strikes. (α_j- α_s) where αj is joint strike and αs is slope strike

F2 – refers to joint dip angle (β_j) or plunge of intersection of two wedge forming planes (β_i).

F3 – depends upon relationship between joint dip or plunge of line of intersection of two wedge forming planes and slope inclination. (β_j - β_s) or (β_i – β_s) where, β_s is the inclination of slope face.

F4 – method of excavation. It includes the natural slope, or cut slope excavation by pre splitting, smooth blasting, poor blasting, and mechanical excavation.

2.2.4. Geological Strength Index (GSI)

Hoek et al. (1997) introduced the Geological Strength Index as a complement to the rock failure criterion and as a way to estimate the parameters s, a and mb in the criterion. Osgoui et al. (2010) improved the GSI parameters to better classify poor and very poor rock masses and is based on both geological visual impression and quantitative measures and is also used in this study due to the presence of poor rock mass. Hoek and Brown (1980) developed an empirical approach to determine the strength of the jointed rock mass and its deformation using a failure criterion for jointed rock mass.

$\sigma 1 = \sigma 3 + \sigma c\ (mb\ \sigma 3\ /\sigma c + S)$, (11)

Where mb is reduced value of the material constant mi is given by

$mb = mi\ \exp\ (GSI\text{-}100/28-14)$ (12)

S and a are the constant for the rock mass given by the following expression.

$S = \exp(\ GSI-100/\ 9-3D)$ (13)

$a = 1/2 + 1/6\ (e^{\ -GSI/15} - e^{\ -20/3})$ (14)

D is a factor which depends upon the degree of disturbance to which the rock mass has been subjected by blasting damage and stress relaxation. It varies from 0 for undisturbed in situ rock mass to 1 for very disturbed rock mass.

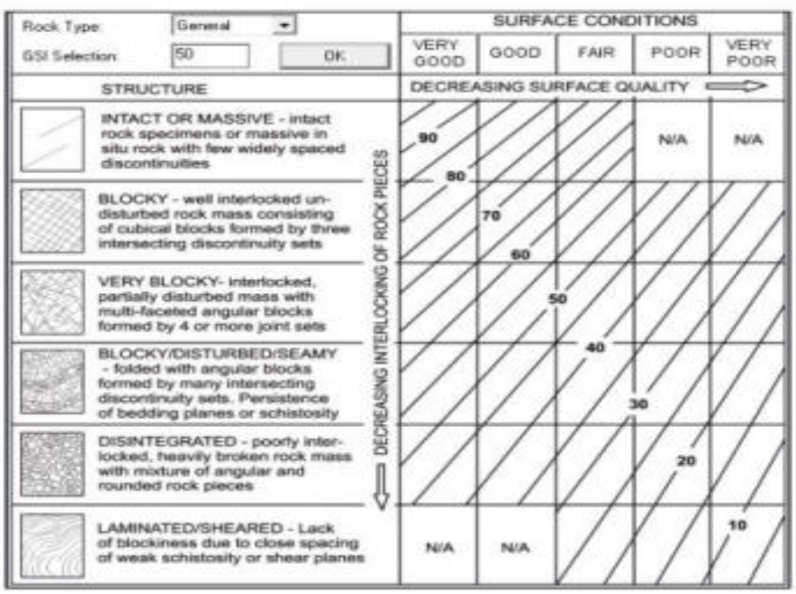

Figure 9 Estimation of Geological strength index GSI based on geological

descriptions (Hoek and Brown, 2002)

Table 5 Geological Strength Index (GSI) classification

GSI value	79-95	56-75	36-55	21-35	<20
Rock Mass Quality	Very good	Good	Fair	Poor	Very poor

2.3. Engineering classification of soils

Engineering classification of soils in short means the arrangement of soils into different groups and subgroups according to their engineering behavior. There are several types of engineering classification of soils. To mention some of the common ones are textural soil classification, the American Association of State Highway and Transport Officials (AASHTO) and the Unified Soil Classification System (USCS). Textural classification incorporates only texture but not plasticity and for this reason, it is not important for engineering classification. Although AASHTO considers both texture and plasticity, it is more useful for classifying soils for highways. The USCS considers textures and plasticity as AASHTO in classifying soils and is the most of vital all purposes. The system has also adopted by the American Society for Testing Materials (ASTM). The system is the most popular system for use in all types of engineering problems involving soils (Arora, 2004).

Properties of soil are broadly classified as Index Properties and Engineering Properties. The properties of soil which are used for identification and classification are called Index Properties of Soil such as specific gravity, water content, particle size distribution and Atterberg limits. Accordingly engineering properties of soils were permeability, shear strength, compressibility.

2.4. Bearing Capacity of the Foundation and Reservoir rocks

According to Bowles (1996), the ultimate bearing capacity (Qult) of a rock mass and the allowable bearing capacity value (qall) are determined using the following equation

$$Qult = UCSav\ (RQDav\ /100)^2 \qquad (15)$$

$$(Qall) = Qult\ /FOS \qquad (16)$$

Where Qult = Ultimate bearing capacity Qall = allowable bearing capacity FOS = factor of safety RQDav = average rock quality designation UCSav = average uniaxial compressive strength. However, this equation has its own limitations as it does not consider the shear strength parameters, slope of the ground, width of the foundation etc. Hence, the bearing capacity of the foundation rocks was further determined using equations forwarded by (Wyllie ,1992) and (Bell, 1915) as cited in (Wyllie, 1994). Accordingly, the bearing capacity of fractured and weathered condition, shallow dipping bedded plane, layered formation and karstic formations behaves in different ways.

2.5.1. Bearing Capacity of Fractured Surface

Fractured and weak foundation rocks that showed a very significant increase in the bearing capacity is produced by a small increase in the confining pressure. Hence, for fractured and weak rocks the allowable bearing capacity can be estimated by assuming curved failure surface using (Bell, 2007).

$$qa = \frac{Cf1cNc + Cf2(B\gamma/2)N\gamma + \gamma DNq}{FOS} \quad (17)$$

Where qa is allowable bearing capacity, c is rock mass cohesion, Cf1 and Cf2 are correction factors for footing shape of the foundation, B is width of the foundation, D is depth of the foundation, FOS is factor of safety and Nc, Nγ and Nq are bearing capacity factors. These bearing capacity factors were calculated using the following equations.

$$Nc = 2 * (N\phi)^{1/2}(N\phi + 1) \quad (18)$$

$$N\gamma = 0.5(N\phi)^{1/2}(N\phi - 1) \quad (19)$$

$$Nq = (N\phi)^2 \quad (20)$$

Where $N\phi = tan^2 (45 + \phi/2)$

In addition, the bearing capacity can also be estimated using Wyllie (1992) equation as follows.

$$qa = \frac{Cf1s^{1/2}\,UCS(1+(ms^{-1/2}+1)^{1/2})}{FOS} \quad (21)$$

Where UCS is the compressive strength of the intact rock and m and s; are rock mass constants.

2.4.2. Bearing Capacity of Sloping Ground

For conditions where the foundation is located on a sloping ground surface, it is necessary to modify the bearing capacity factors to account for the reduced lateral resistance provided by the smaller mass of rock on the downslope side of the footing. On shallow slopes where the slope angle is less than ϕ/2, bearing capacity or settlement will usually control the allowable working load on the footing. For slope angle greater than ϕ/2, it is seldom necessary to check the bearing capacity because the stability of the slope will be the controlling factor (Hong Kong Geotechnical Engineering office, 1981). For foundations on sloping ground surfaces, the allowable bearing pressure is calculated as follows:

$$qa = \frac{Cf1cNcq+Cf2(B\gamma/2)N\gamma q}{FOS} \qquad (22)$$

Where Ncq and Nγq are bearing capacity factors, Cf1 and Cf2 are correction factors which account for the footing shape, B is width of the foundation γ is density, c is the rock mass cohesion and H is the slope height and No is the stability number which is calculated as follows using equation.

$$No = \frac{\gamma * H}{C} \qquad (23)$$

2.5. Rock Mass Deformation

The deformation of the rock mass can be measured using the modulus of deformation, Ed (Jonson, 1988).The modulus of deformation is defined as the sum of deformation that occurs with closure of joints in the rock mass under deformation (plastic) and the deformation that occurs with continued stress application after crack closure (elastic) (Jonson, 1988).

Empirical determination of the deformability of the rock mass is given by different scholars. Based on the case histories of mostly dam foundations, (Serafim and Pereira, 1983) developed an empirical relation by back analysis of **Ed** from the measured deformation; the relation works well for the rock mass for which RMR lies between 10 to 50 and UCS of intact rock „qc‟ > 100 Mpa. The Serafim and Pereira relation for RMR89 < 50 is expressed as
(Serafim & Pereira, 1983).

$$Ed = 10^{(RMR-10)/40} \qquad (24)$$

Where, Ed is in situ modulus of deformation in Gpa and RMR is rock mass rating.

For the rock mass having RMR higher than 55 and UCS of intact rock „qc" greater than 100 Mpa the relation is in close agreement with the tested values. For RMR > 50 modulus of deformation is expressed as (Bieniawski,1978).

$$Ed = 2RMR - 100 \text{ given in Mpa} \tag{24}$$

2.6. Geological Structures

According to Gangopadhyay (1993), folding, faulting, fractures, shear zones, and joint, and other weak features are un-favorable geological structures for a dam site. In this regard, folds and faults develop several fractures and crushing of rock which are responsible for the uplift, leakage or seepage, and slope stability problems. On the other hand where shear zones and joints are present in the dam site, they bring weakness to the dam foundation. Accordingly, Barjasteh (2019) reported that structural geology has a great deal in contributing to the engineering projects, and knowledge of structural geology setting is essential for the safe design of these projects. They further document that a detailed study with a focus on the analysis orientation, their activities, movement types, the evaluation of stress relationships and possible temporal an deformations are necessary in case of structure like dams are intended to be constructed on localities where geological structures are prominent. On the other hand, weak and impermeable rocks such as shale when exposed on the abutments of the dam and overlain by permeable formation, they can also act as causative factor for sliding and cause slope instability problems. This is related to the development of pore water pressure along this weak and impermeable formation which initiates the sliding as water cannot move through these formations rather tends to move horizontally as it reaches the interface. Weathered and fractured rock formations can also lead to seepage/leakage of water through this weak formations, uplift problems and other foundation concerns.

2.7. Water Tightness Investigation

Fell et al. (2005) state that topography, geology, groundwater conditions, rainfall/climate conditions, hydraulic conductivity of lithological units, and design of the maximum full supply level of the reservoir are among the factors that affect the water tightness of storages in many areas of non-soluble rocks. The majority of non-soluble rock masses will, however, become less permeable with depth since the joint spacing and apertures tend to shut more closely with depth. Also, it is believed that the water table is near to the ground throughout the storage area's floor, and the conditions shown by the water table are those at the conclusion of the dry season (Fell et al., 2005).

2.7.1 Packer Permeability Test

The Lugeon test is widely used to estimate the average hydraulic conductivity of rock masses (Camilo, 2010) and is often considered both as the most important parameter in determining the critical permeability and as a criterion to determine the necessity of rock mass grouting (Sharghi et al., 2010). Seepage through foundation resting on fissured rock mass is strongly dependent on fracture characteristics like degree of joint spacing, joint aperture, continuity and presence of weathering and infill material (Chen et al., 2010). Numerous researches showed that water pressure/Lugeon permeability test is the suitable method to determine the permeability of the foundation rocks (Barani et al., 2014). The test is conducted at different stage at low water pressure, and increasing the pressure in each subsequent stage until reaching maximum pressure. Once maximum pressure is reached, pressures are decreased following the same pressure stages used on the way up. During the test both flow rate (q) and water pressure (P) values recorded every minute. One Lugeon value is equivalent to one liter of water flow per minute per meter.

$$\text{Lugeon Value} = \alpha * q / L * P0 / p \qquad (26)$$

Where; q is the flow rate in a liter, L is the length of the testing section in meter, P is the pressure required for the test in mega Pascal and α is a dimensionless factor and its value equal to 1 when the SI units system is used (q [L/min], L[m] and P [MPa]).

The Lugeon value results are then used to express the characteristics of discontinuity and types of rock mass in the dam foundation and the impoundment reservoirs and also the information obtained from the packer test is used to determine water/cement ration and grout injection pressure used during grouting (Ajalloeian and Azimian, 2013).

2.7.2. Permeability from Fracture Characteristics of Rock Mass

It is feasible to determine the hydraulic conductivity of rock mass from the fracture aperture and spacing, and the link between the hydraulic conductivity (k) and fracture parameters is provided by (Snow, 1965 and Louis, 1974). It is assumed that the discontinuities are parallel, smooth fractures. Yet, compared to smooth fractures, rough fractures' hydraulic conductivity is only 25% as high (El-naqa, 2000). Field observation proved this assumption.

$$K = \frac{ge^3}{12\mu s} \quad (27)$$

Where; **g** is the gravitational acceleration (9.81m/s2),**e** is the average aperture of fractures (m), **μ** is the coefficient of kinematic viscosity of the fluid ($1*10^{-6}$m2 /s for water at 20°c) and **S=1/λ**(fracture frequency) is the average spacing of fractures (m). However, the reciprocal of fracture spacing is equal to the fracture frequency (**λ**). So the above equation can be written as follows.

$$K = \frac{\lambda ge^3}{12\mu} \quad (28)$$

2.7.3 Falling Head Permeability Test Method

Less permeable soils' permeability is assessed using the falling head permeability test. Very fine sand and silt soils with (k) values between 10^{-2} and 10^{-5} are suited for it (Arora, 1997). The hydraulic conductivity(k) can be calculated using Darcy's law, which can be expressed as follows, based on the drop in the head (h0 - h1), the elapsed time (t1 - t0), and the amount of water flowing through the sample in a given time. The soil sample remolded system is the same as that used in the constant head permeability test.

$$K = \frac{2.3aL}{(t_1 - t_0)} \log_{10}{}^{(h0/h1)} \quad (29)$$

Where; A is a cross-sectional area of the vertical cylinder in which the sample is kept, a is a cross-sectional area of transparent standpipe, L is the length of the sample, h0 and h1 are initial head and final head drop respectively and t_0 is the initial time at h0 and t1 is a final time when the water level drops from h_0 to h_1.

2.8. Slope Stability Analysis

Engineering structures such as highway, railway, tunnel, dams, mines, residential and industries that are found on rugged topography and mountainous terrain needs stable slopes

(Hoek and Bray, 1981; Wyllie and Mah, 2004; Lau, 2014). Slope instability may occur due to internal and external factors. An internal factor includes adverse slope geometries, geological discontinuities, and weak or weathered slope materials conditions while external factors like human activity, heavy precipitation and seismicity could play a significant role in slope failures (Basahel and Mitri, 2018). Accordingly to Prince et al. (2007), there are four types of failures categories depending on the geometrical and mechanical nature of the discontinuity and the conditions of the rock masses. Planar failures occur when a discontinuity strikes parallel or nearly parallel to the slope face and dips into the excavation at an angle greater than the friction angle. Wedge failures involve a rock mass defined by two discontinuities with a line of intersection that is inclined out from the slope face where the inclination of the intersection line is significantly greater than the angle of friction. Circular failures occur when rock masses are highly fractured or composed of very weak material. Toppling failures involve rock slabs or columns defined by discontinuities that dip steeply into the slope face. Slope stability analysis can be implemented using rock mass rating, slope mass rating, kinematic, deterministic, probabilistic and numerical methods (Abramson et al., 2002; Raghuvanshi, 2017).

2.8.1. **Kinematic Method**

Kinematic analyses concentrate on the feasibility of translation failures due to the formation of day lighting wedges or planes of sliding. The daylight envelope is a useful method of identifying kinematic ally possible failure modes. This envelope is the locus of all the poles representing planes whose dip direction lies in the plane of the slope face. Kinematic analysis is commonly used to predict potential structural failure mechanisms (planar, wedge, and toppling) using the stereo net projection method (Prince et al., 2007). Data that used the stereographic projection method for kinematic analysis are dip and dip direction of each discontinuity.

2.8.2. **Limit Equilibrium Method (LEM)**

The limit equilibrium method compares the magnitudes of the driving and resisting forces that act along the sliding planes to estimate the factor of safety for slope instability of rock and soil where the translation or rotational movements occur on the distinct failure surfaces. All LEM share a common approach based on a comparison of resisting force and disturbing force

(Eberhardt, 2003). A limit equilibrium analysis will be taken for the structures where the possibility of kinematic instability had been identified and then shear strength parameter (friction angle (ϕ) and cohesion(c)) will be used for the FOS determination. The factor of safety is calculated as a ratio of resisting forces to driving forces. Christian (2004) stated that the factor of safety greater than and less than one indicates that the slope is stable and unstable respectively.

2.8.3. Deterministic Slope Stability Analyses

In a soil slope failure, there is no longer defined failure surface and this is free to find linear surface with least resistance and it has circular shape (Hoek and Bray, 1981; Hoek, 2000; Wyllie and Mah, 2004). Soil slope stability analysis is carried out by dividing series of slides that are usually vertical and base of the slice which is inclined at an angle with the failure plane. According to (Wyllie and Mah, 2004) factor of safety for circular mode of failure based on deterministic limit equilibrium can be calculated as follows using equation 1.

$$FOS = \frac{\text{shear strength available to resist sliding } (C+\sigma\tan\phi)}{\text{Shear stress driving the failure}}$$

Where c is cohesion and ϕ is friction angle along failure plane respectively while σ is normal stress applied onto failure plane.

Deterministic method analyzes stability of the slope based on limit equilibrium concepts which determine factor of safety from the ratio of available shear strength to mobilized shear stress (Abramson et al., 2002; Duncan, 2000).

As cited in Abramson et al., (2002), various analyses methods of slice which depends on limit equilibrium principles include (Fellenius, 1936) ordinary method, (Janbu, 1954) simplified and corrected method, Bishop (1956), Morgenstern-Price (1965), (Spencer, 1967) and (Sharma,1973). Each of these methods was described as follows.

Ordinary or Fellenius Method: It is the oldest techniques developed by (Fellenius, 1936) and which introduced the concept of limit equilibrium by dividing the failing soil mass into different slices. It satisfies moment equilibrium for circular slip surface. However, it neglects both normal and shear forces applied to the failure plane which leads to inconsistent calculation of safety factor (Abramson et al., 2002).

Janbu Simplified Method: It is another technique developed by (Janbu, 1954) which consider force equilibrium. However, the method fails to satisfy moment equilibrium and it considers zero normal and shear inter slice force.

Janbu Corrected Method: It is another method that depends on dimensionless parameter and different stability charts (Janbu, 1996). It determines safety factor by considering different conditions such as surcharge, groundwater and stress analysis and it is also applicable for non-circular slip surface.

Bishop Method: It is the technique developed by (Bishop, 1956) and it was the most common stability analysis technique for circular failure plane. This method satisfies moment equilibrium and consider inter slice normal force. However, it fails to satisfy force equilibrium and it did not consider inter slice shear force.

Morgenstern-Price Method: It is another technique developed by Morgenstern and (Price, 1965) which considers both force and moment equilibrium. In addition, it considers both inter slice normal and shear force with inclination at different angles to determine safety factor and it is applicable to slip surface of different shapes.

Spencer Method: It is a method developed by (Spencer, 1967) which is applicable to slip surface shape with different shapes. It satisfies both force and moment equilibrium. In addition, it considers both inter slice normal and shear force. However, it assumes constant inclination for both inter slice normal and shear forces.

Sharma Method: It is another technique developed by (Sharma,1973) which is applicable to both force and moment equilibrium and slip surface of any shape. It uses method of slice to calculate magnitude of horizontal seismic coefficient which is needed to bring soil mass into a state of horizontal equilibrium.

2.9. Common Dam Site Problems

Dam failures that were experienced all over the world showed the most adverse factors outlined are seepage, differential settlement and foundation defects (Barzegari, 2017). Besides these problems, soft, unconsolidated and soluble rock materials which are incapable of water storage and bearing loads of heavy structures are unfavorable for dam site. Moreover, dams and reservoirs constructed on these unfavorable geologic materials have suffered from excessive water loss in the past (Ghobadi et al., 2005; Kamal, 2007; Mohammed and Raeis, 2007; Morteza, 2012; Mohammad, 2012). According to Gurocak and Alemdag (2012), the presence of unfavorable geological structures such as joints, faults and weak planes affect the permeability of rock mass. Moreover, these structures also influence the strength and deformability of a rock to a great extent. In addition to unfavorable geological structures and geology, the presence of thick overburden increases the project cost because of the requirement for deep excavation (Ghobadi et al., 2005).

According to Adamo et al. (2020), all embankment dams will settle to some degree during and after construction. When the foundation profile is irregular and the depth of fill varies, the differential settlement will occur. When differential settlement is large enough, cracks can form in areas of tensile stress. These cracks may develop into good conduits for seepage water leading to internal erosion.

A reservoir may fail either due to excessive leakage or seepage of water, as a result of rapid sedimentation and slope instability. According to Bell (2007) when assessing the leakage and seepage problem of the reservoir; two main factors have to be taken into consideration. These are the water tightness of the basin and the stability of the bank. Seepage and leakage can be assessed and evaluated by investigating the permeability of the dam foundation, dam abutments and reservoir area and geological condition in its surrounding area.

2.10. Improvement for Common Dam Site Problems

Despite the presence of adverse geological conditions under varied geological set-up, numerous dams have been constructed and others are planned to be constructed. Through proper foundation treatment that involve grouting methods, deep soil mixing, trench excavation and backfilling with competent material, composite cut-off walls and upstream or downstream buttress structures embankment dams can be stabilized. Foundation treatment using rock-mass grouting has been utilized frequently (Warner, 2004).

Grouting is the process in which fluid material is injected and flows in to fractures or cracks within the rock mass. The execution of grouting largely depends on the result of permeability (water pressure) test to delimit foundation rock mass into zones of different rock mass quality requiring different level of treatment (Ajalloeian et al., 2012).

Stabilization Methods of Slopes

Slopes in most dam abutment, reservoirs, tunnel, mines and road cuts in the mountainous areas are prone to instability problems due to variation in the rock mass conditions and factors induced by the environments such as seismic activities and water in the slope (Pantelidis, 2009). The material characteristics of a rock slope, slope height and face angle, and the rock joint orientations play a significant role in the instability problem of the rock slopes, especially at the dam site (Basahel and Mitri, 2018). Accordingly, after identifying factor causes the instability and determining potential mode of failure, appropriate slope stabilization methods should be taken to stabilize the slopes. The most appropriate remedial measures used to stabilize rock slope at the dam site are installation of rock reinforcement (such as rock bolts, rock anchors and shotcrete), modifying geometry of the slope, and providing drainage holes (Hoek and Bray, 1981; and Abramson et al., 2002). Each of these stabilization methods are discussed as follows:

Rock Bolts: Rock bolts are steel rods, smooth or ribbed, normally held at the end of the borehole mechanically or chemically; usually of about 3m long and often fully grouted. Rock bolts can hold the loosened rock mass in place, and adopted to strengthen and stabilize the rock mass (Hoek and Bray, 1981).

Rock anchors: are used to prevent potential rockslide and rock falls on the surface (Hoek and Bray, 1981).

Concrete: Shotcrete is used frequently to preserve the integrity of a rock face by sealing the surface and inhibiting the action of weathering (Bell, 2007). It’s the mixture of cement, water and aggregate, and mainly applied to the surface of highly weathered and fractured rocks. For the shotcrete surface, it is essential to provide sufficient drain holes to remove pore pressure that is built up underneath the shotcrete surface.

Modifying the slope geometry is often done by: reducing the slope angle, reducing the weight at the head of the slope, increasing weight at the toe (“heels” or rip-rap) or constructing benches (Hoek and Bray, 1981).

The slope becomes stable by performing stabilization method for rock and soil slopes. Slope stabilization methods generally increase the factor of safety through reducing driving force by excavating material from unstable ground, installing appropriate drainage method and increasing resistive force by building retaining structure or support, chemical treatment to harden the soil (Abramson et al., 2002).

CHAPTER THREE

3. METHODOLOGY AND MATERIALS

3.1 Methodology

To accomplish the research work, the following methods and approaches were used. The methodologies were applied using integrated geological, geotechnical and borehole driling investigation techniques. Both primary and secondary data were used.

3.1.1 Pre-field Work

Collecting and reviewing published and unpublished literature, scientific journals, reports and books pertaining to geophysical investigation, the analysis and interpretation of imageries and topographic maps depicting the area of interest were perform during this stage. This were essential to develop conceptual framework which were further utilize in evolving the detail methodology for the present study. In addition, subsurface data such as borehole logs were collected from engineering corporation of oromia and utilized for subsurface investigation of the dam site.

The direct geotechnical investigation of the Ashebeka dam site required accessing of the deeper subsurface (up to 44m depth) using geotechnical core drilling technique to make boreholes, to help retrieve core samples from the subsurface, and to perform in-situ tests in the boreholes. As such, the Geotechnical Core Drilling and extraction of core samples were conducted in accordance with ASTM D2113-99: Standard Practice for Rock Core Drilling and Sampling of Rock for Site Investigation, by using rotary core drilling method. A total of Six (6) boreholes accounting to a total depth of 159m were drilled at the proposed Ashebeka dam site. These boreholes were drilled along the dam axis, at spillway and intake structure sites.

3.1.2. Field work activities

Some preliminary geological mapping, geomorphological and land form assessment, digging of few test pits at the reservoir area and the foundation, discontinuity survey, slope analysis, sampling, and water tightness analysis were conducted. Then these data were analyzed, summarized, and interpreted at the preliminary phase and the remaining works are identified. Some of the field work are includes the following activities.

3.1.2.1. Geological Mapping

Using representative traverse lines that cross numerous lithological units and significant geological features at the reservoir and dam site, geological mapping was done.

This method is very important method to decide the purposed area is suitable to construct engineering geological structures. The shape of the river and geological formation of both abutments were well identified through this method. Based on this method different rock types were classified on their genetic type. The thickness of each lithology and geological structure orientation were measured in the field in different out crops. For the detailed engineering geological study, traverses were made on and around the proposed reservoir area, dam axis, downstream, upstream and abutments. From the rocky outcrops, the rock type, discontinuities, infilling materials, weathering degree, strength and probable seepage/leakage condition were recorded. The topographic features, type of surface deposit and their depth were also be noted in the field.

3.1.2.2. Discontinuity surveys

Discontinuity surveys were mostly conducted in the reservoir area and on the dam's axis. Based on the characteristics governing the failure mechanism, which were either structurally controlled failures or non-structurally controlled failures (rock mass controlled failures), potentially unstable slopes were identified during the field investigation. When "discontinuity orientations" significantly contribute to the instability of the rock slope, structurally controlled failures happen, but non-structurally controlled failures happen when weathering is severe (Mahboubi et al., 2008). In these situations, the slope's failure was controlled by rock mass failures, and the presence of rock joints has little impact on the slope's stability behavior. Also, figuring out what influences the failure mechanism aids in choosing the best slope stability analysis approaches. According to the International Society of Rock Mechanics' Standards (ISRM, 1981), a quantitative description of the discontinuity characteristics, including orientation, roughness, spacing, persistence/continuity, aperture(openness), filling material, groundwater condition, and the number of joint sets, was gathered from the exposed rocks at the dam axis and the reservoir area. Slope height, dip, and dip direction were also measured. The Brunton compass was used to measure the joint orientations such as strike, dip, and dip direction (Figure 10).

Figure 10 Joint measurement using brunton compass and discontinuity surveying.

3.1.2.3. In-situ Rock Strength measurement

Schmidt hammer measurements on certain slope sections were used in the current investigation to determine the rocks' in-situ strength. The test was carried out in accordance with the ASTM-recommended standard (2001). Recording at least 10 single data, eliminating any that deviate from the average by more than 7 units, and then averaging the remainder is advised by ASTM (2001). The instrument's numerical scale on which the rebound distance of the plunger is immediately read is known as the rebound number (R). The steps taken during an in-situ strength test involve:

- Choosing a surface that is intact (free of obvious cracks), dry, and representative rock mass.
- Before beginning the test, Schmidt Hammer was calibrated.
- Using a grindstone to clean up debris and smooth down rough surfaces, in particular the impact points under the plunger tip.
- Placing the test hammer perpendicular to the rock surface while steadily pushing; the hammer struck the rock surface with a specified amount of force. After the impact, lock the hammer by pressing the button, and use the equipment to read the gauged rebound values.

Finally, by averaging result of representative rebound values, the uniaxial compression strength (UCS) of the rock were estimated using equation 6.

Figure 11 Insitu strength measurement using schmidit hammer on ignimbrite rock (A) and on fractured basalt rocks (B).

3.1.2.4. Sampling

In order to conduct several laboratory tests, disturbed soil samples were taken from the test pit. Four test pits were excavated by the researcher and ECO, with a maximum depth of 2.5 meters. Of these, one was located in the reservoir area (ASHTP-04), (ASHTP-02) was at river beds, and (ASHTP-01) and (ASHTP-03) was located on the left and right abutments of the dam respectively (Figure 12). The plastic bag was used to preserve the soil samples' original moisture content after they had been collected. Also, the engineering characterstics of the rocks that make up the dam site and reservoir area were described. Later, based on degree of weathering and welddness rock samples from the exposed surface were collected for laboratory analysis.

Figure 12 Test pit excavation from different part of the study area and soil sampling .

3.1.3. Laboratory Testing

3.1.3.1 Laboratory Test on Soil

The laboratory tests conducted on soil samples include gradation test (sieve and hydrometer analysis), specific gravity, natural moisture content, atterberg limit tests (liquid and plastic limit) and permeability tests at GIA Engineering PLC soil mechanics laboratory. The basic procedures followed on each laboratory testing were described as follows.

3.1.3.1.1. Gradation Test

Using sieve and hydrometer analysis, this test is conducted to estimate the percentage of various grain sizes present in a soil. The distribution of coarser grains bigger than 75µm in diameter is determined using a sieve analysis, whereas the distribution of finer particles smaller than 75µm in diameter is determined using a hydrometer analysis. The test was carried out in accordance with ASTM D 422 (1998), a standard test procedure for soil particle-size analysis. By using a hammer and pestle crushing device, dry soil samples were prepared and crushed into suitable small sizes. The pan was then placed at the bottom of all the sieves after a stack of sieves had been cleaned with a brush and positioned with the smaller aperture at the bottom and larger opening at the top. The soil retained on each sieve and the pan was then measured using balance after the test had been running for 15 minutes. Using a hydrometer, the soil sample that was kept on the pan was examined. The recorded data findings were then processed on an Excel datasheet, and the analysis result was used to plot the grain size distribution curve.

3.1.3.1.2 Atterberg Limit Test

An Atterberg limit test is performed to determine the plastic limit (PL) and liquid limit (LL) of fine-grained soil and to classify a fine-grained soil according to the Unified Soil Classification system. The test was conducted according to ASTM D 4318 (1998) standard (Figure12). Accordingly, the test was conducted in the laboratory as follows. For the liquid limit test, part of the soil samples that passed through sieve #40 (0.425mm opening size) was taken in an evaporating dish. Distilled water was added to the soil sample and mixed it to form a uniform paste with the help of a spatula and then on the cup of the liquid limit device to make a smooth surface paste of soil and divide it into two halves by using spatula and grooving tool respectively and then by rotating the handle at a rate of 2 revolutions per a second until the soil cake comes contact by flowing with the bottom of the groove along with distance approximately 13mm. The number of blows required to close the two halves of soil specimen by 13mm was recorded. From the flow portion, the representative sample was taken in moisture Cans and the moisture Cans were oven dried for 16hrs at 105°C. Finally, the results of each soil sample were recorded and analyzed. Similarly, for plastic limit determination, part of the moist sample for liquid limit determination was taken and then the sample was placed on the glass plate and rolled with the finger to form the thread of uniform diameter. The thread was then rolled until its diameter reaches 3mm and crumbled. The crumbled soil sample was collected in cans and weighted on mass balance and then put in the oven for 16hrs and the temperature of the oven was adjusted to 105°C. Finally, the moisture cans were taken out and the results of each sample were recorded and analyzed. From the liquid limit and plastic limit result, the plastic index (PI) was determined using equation 13 as follows.

PI = LL – PL

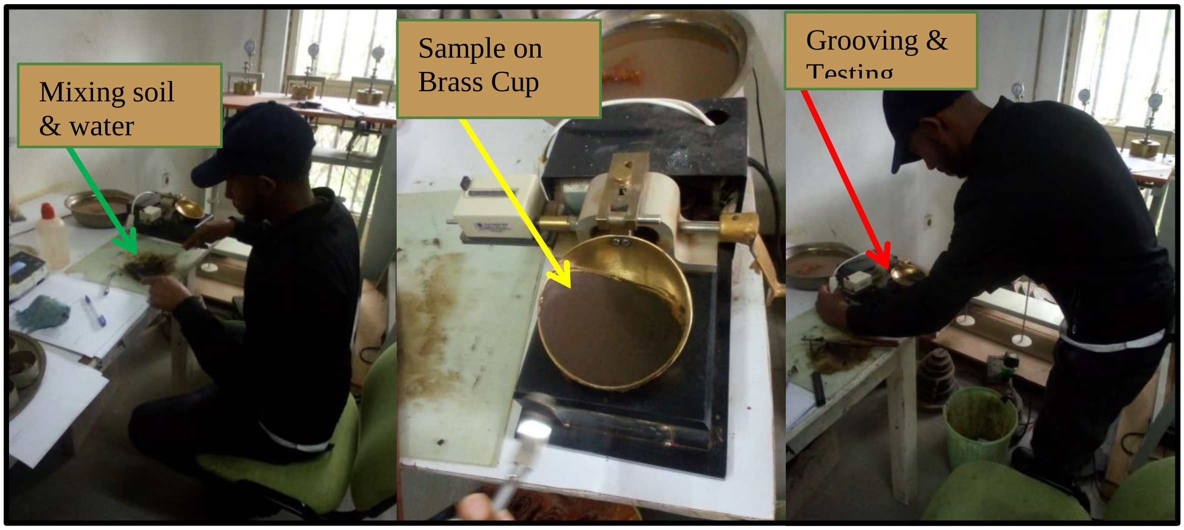

Figure 13 Liquid limit test using digital casagrande apparatus.

3.1.3.1.3 Moisture Content Test

Determination of moisture content of a soil is further required as a guide to the classification of soils. This test was conducted according to ASTM D 2216 (1998) standard by oven drying method. Accordingly mass of the wet soil sample was weighted and put in oven-dried for 24 hours at 105^0C and then the weight of oven-dried soil samples was recorded. Finally, natural moisture content was determined using the following equation.

$$w = \frac{M1-M2}{M2} * 100$$

Where; w is the natural moisture content in (%), M1 is the mass of wet soil sample in (gm.) and M2 is the mass of oven-dried soil samples in (gm.).

3.1.3.1.4. Specific Gravity Test

The test was conducted according to the ASTM D 854 (1998) standard by using a pycnometer. Accordingly, the test was conducted in the laboratory as follows. Record the weight of the empty clean and dry pycnometer (WP) using digital balance before starting the test and then place 10g of oven dried soil sample that passed through the sieve #10 in the pycnometer and again record the weight of the pycnometer containing the dry soil (WPS). Add distilled water to the pycnometer water to the level somewhat above the soil sample and soak the sample for 10 minutes and the entrapped air was removed by boiling technique. After that fill the pycnometer with distilled water to the mark and then determine the weight of the pycnometer that contained soil and water (WB). Then the pycnometer was emptied and cleaned and fill it with distilled water only to mark and measure the weight of the pycnometer and distilled water (WA). Finally, specific gravity was determined using the following equation.

$$\mathrm{Gs} = \frac{W0}{\mathrm{W0} + (\mathrm{WA} - \mathrm{WB})}$$

Where: W_0 is the weight of a sample of oven-dry soil

3.1.3.1.5 Permeability Test

The permeability test was performed to determine the coefficient of permeability of soil samples. The test was conducted according to ASTM D 5084 (1997) standard by using the falling head permeability test. Accordingly, the soil samples were first remolded and compacted by using standard proctor for determination of the optimum moisture content at which a soil become more dense in achieve the maximum dry density. Then fully saturated compacted soil samples for 24hrs. After that vacuum saturation was done by placing the sample in vacuum saturation apparatus for 15minutes to remove air from the void of soil specimen. The falling head permeability test was carried out by in placed the molded sample between the porous disc and then the standpipes filled with water and water was allowed to flow through the sample from head (h0) at a time (t0) to head (h1) at a time (t1) through known length (L) and cross-sectional area (A) of the soil sample in the standpipe of area (a). Finally, the coefficient of permeability was determined using equation 28.

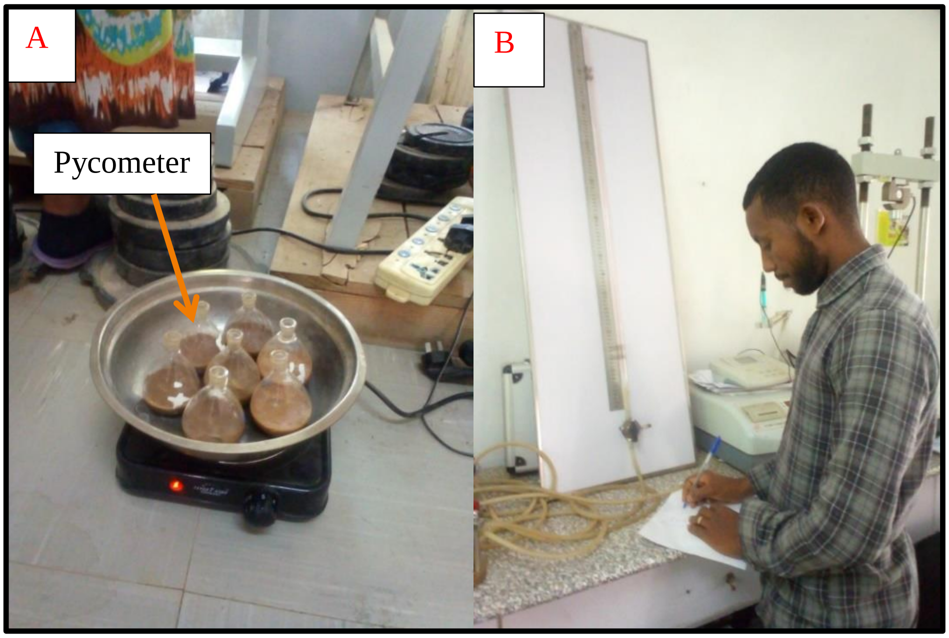

Figure 14 Specific gravity test (A) and permeability test of soil sample (B)

3.1.3.2 Laboratory Test on Rock

The laboratory tests conducted on rock samples were the point load test and unit weight test.

3.1.3.2.1 Point Load Test

The point load strength tests was conducted to determine the unconfined compressive strength of the intact rock. The test was conducted according to ASTM D 5731 (1995) standards to determine the strength of irregular rock samples. Its common method is used to estimate the uniaxial compressive strength of rock. This index test is performed by subjecting a rock specimen to an increasingly concentrated load until failure occurs by splitting the specimen (Conshohocken, 2007). The guidelines suggested that at least 10 tests per sample should be tested. In this study, a total of 6 irregular rock samples were collected from abutments of the dam and reservoir area for point load strength test. The test was conducted under natural moisture content on irregular rock sample (Figure 14) at Gia Engineering PLC (GIA EPLC) laboratory as follows.

- ✓ Using geological hammer and chisel, irregular rock samples were prepared into proper size and shape as the scale of point load testing machine.
- ✓The height, width and length of the irregular rock samples were recorded before starting the test.

✓Then insert a rock sample in the test device and continuously apply the load until the failures occur and the peak values of failure load, P were recorded.

Finally, point load test results were used to calculate the unconfined compressive strength of the intact rock using equation 6.

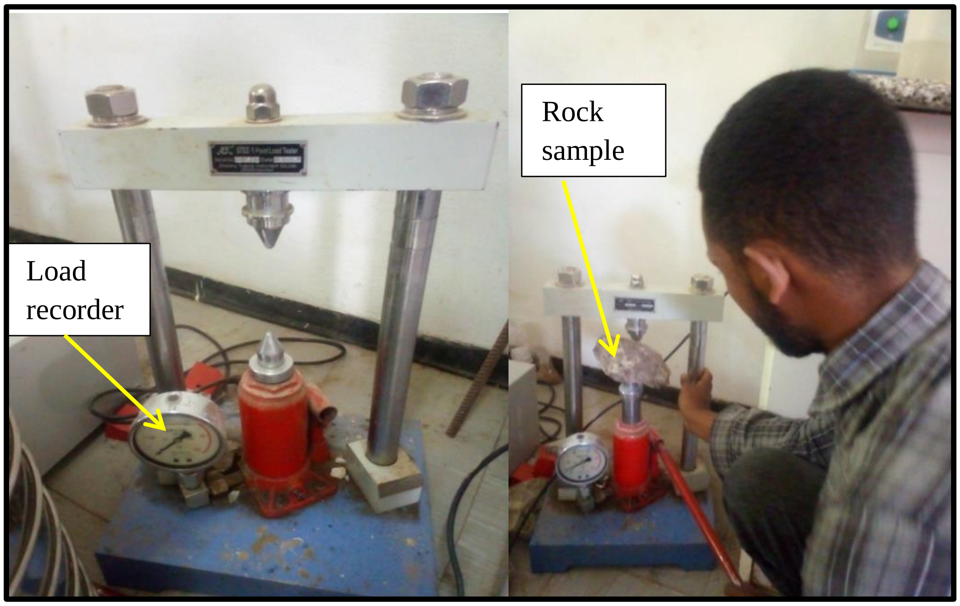

Figure 15 Point load test of rock samples collected from the study area.

3.1.3.2.2 Unit Weight Test

In the present study, the unit weight was applied on the irregular rock samples using buoyancy techniques in the Geotechnical Engineering laboratory of GIA Engineering PLC in accordance with the standard recommended by ISRM (1978).Ten irregular rock samples total from both dam abutments and reservoir area were used for the test, and the average of those samples was taken to analyse the slope stability and gauge the strength of the rocks. The test procedures followed during the unit weight test were given as follows.

✓ First the the irregular rock samples were labeled and weighted (M1) under its natural moisture content and oven-dried for 24 hours at 105^{o}c and then the weight of oven-dried rock samples was recorded (Mdry).

✓ The cylinder was filled with water and the initial volume of water (V1 in cm^3) was recorded and oven-dried samples were inserted into the cylinder filled with water and record the change in volume (V2 in cm3).

Finally, the dry density (ρd) and unit weight (γ) of each rock sample was determined by using the following equation respectively.

$$\rho d = \frac{M_{dry}}{V}$$

$$\gamma = \rho d * g$$

Where, ρd is the dry density of the rock samples in g/cm3, M_{dry} is the mass of rock samples after oven-dried in (g), V is the difference between volume of water after inserting the rock sample in and volume of water before inserting the rock sample, i.e. V = V2 –V1 (cm^3), γ is the unit weight of rock in KN/m^3 and g is the acceleration due to gravity in (m/s^2).

3.1.4 Data Analysis and Processing

3.1.4.1. Rock classification

In order to estimate the strength and deformability of the rock mass, provide measureable data for support estimation, and provide a platform for communication between exploration, design, and construction groups, a rock mass classification system is intended to classify the rock mass based on its strength, discontinuity condition, weathering, structural orientation, and other factors (Bieniawski, 1989). It is advised that at least two techniques be employed at any site during the early stages of a project because different classification systems place varying emphasis on the various factors (Palmstrom, 2003).

The shear strength parameters in this study were calculated using the rock mass rating system (RMR) proposed by Bieniawiski (1989) and the geological strength index (GSI) developed by Marinos and Hoek (2000). Five fundamental parameters were used to calculate RMR. They include the rock's Uniaxial Compressive Strength (UCS), Rock Quality Designation (RQD), the spacing and state of the discontinuities, and the groundwater. For the classification of rock masses, the uniaxial compressive strength of the intact rock (UCSi), which is estimated from the point load test, is chosen. Also, the assessment of the rock quality at the dam site using RQD estimates from the field.

Selecting a typical slope segment and measuring it using a square meter of rock mass is the first step in determining RQD. The number of joint sets in the chosen area as well as the quantity of joints inside each joint set were then determined. Equation 3 was used to find the Jv values, while equation 2 was used to determine the RQD values. Lastly, obtained rock mass classification parameters were translated into rated parameters, and the RMR value was computed.

In order to characterize the condition of the rock mass in accordance with Hoek and Marinos' (2000) GSI basic charts, the Geological Strength Index (GSI) was derived using RMR findings using equation 11. The RocLab software used the GSI values as a consequence to determine the shear strength parameters.

3.1.4.2. Rock Mass Strength and Failure Criteria

Using Generalized Hoek-Brown Failure criteria, the RocData software evaluated the shear strength and modulus of deformation of the rocks at the dam site (Hoek et al., 2002). To compute the geo-mechanical parameters of the rock mass, this software employs GSI, the material constant of intact rock (mi), UCS of intact rock, and disturbance factor (D). As a result, the GSI value was calculated from the RMR using equation 11 and the rock mass classification was done using the UCS of intact rock calculated using the point load index and the UCS value of core samples. Similar to that, the material constant for intact rock (mi) was taken from the RocData software's standard table (Hoek et al., 2002). Moreover, as no excavation occurs during the natural disaster, a disturbance factor of 0.7 has been applied.

3.1.4.3. Bearing Capacity of Foundation Rock

Estimating a foundation rock's bearing capacity is crucial for dam design. The safe load bearing capability of foundation rocks was estimated in this study using a variety of empirical methodologies. For a preliminary estimate of the safe load bearing capability of foundation rocks, Bowles (1996) developed equation 14 as the first empirical technique.

However, the shear strength parameters, ground slope, and foundation width are not taken into account by Bowles' calculation. In order to determine the foundation's carrying capacity, Wyllie (1992) and Bell (1915), who are quoted in Wyllie, developed. As a result, both methods are used to evaluate the bearing capacity for weak and fractured foundation rocks.

UCS of intact rock, rock mass constant m, and s were used to calculate the bearing capacity of foundation rocks. By employing Hoek-Brown strength criterion and the RocData program. Similar methods were used for the Bell equation's cohesion (c), friction angle (ϕ), and bearing capacity factors (N_c, N_γ, and N_q), as well as the foundation's width (B) and depth (D). Hoek and Brown strength criteria were used to determine cohesion and friction angle, and equations 15, 16, and 17 were used to derive bearing capaacity factors Nc, Nγ, and Nq from friction angle. Also, the rock mass's unit weight result was derived from the results of a laboratory test conducted by ECDSWC. Then, assuming a factor of safety of 3, the allowed bearing capacity was calculated.

Wyllie (1992) asserts that when a foundation is built on a slope, the slope's inclination has a significant impact on the bearing capacity of the ground. The strength parameters (ϕ and C) and bearing capacity factors (Ncq and Nq), as well as the unit weight of the rock (γ), the inclination, the height of the slope (H), the width of the foundation (B), and the factor of safety(FOS), are used to estimate the allowable bearing capacity.

The graph provided by the US Department of the Navy (1982) and Meyerhof (1957) was used to estimate the bearing capacity factors Ncq and Nq for the aforementioned equation.

3.1.4.4. Slope Stability Analysis

The kinematic method and limit equilibrium slope stability analysis methodologies were used to examine the slope stability of the dam abutments and the reservoir rim. Each of these slope stability methods was discussed briefly in the next sections.

3.1.4.4.1 Kinematic Method

This method predicts the likelihood of failure by using the prominent discontinuity planes within the slope mass. Using the software Dips 6.0, kinematic analysis of rock slopes for structurally controlled failure was performed in this work (Rocscience, 2004). The primary joint set, slope, dip directions, and friction angle are among the input parameters for the Dips program (Hoek, 1974 and Barton and Choubey, 1977). A bruton compass was used to measure the dip and dip directions from the surface rock mass, and RocData software was used to calculate the friction angle along the failure plane (Rocscience, 2004). Kinematic evaluations were performed on left abutment slope 1 (LASS1), and right abutment slope 1 (RASS1) sections of the structural control slope.

3.1.4.4.2 Limit Equilibrium Method

In terms of safety factors, limit equilibrium methods (LEM) can assess a variety of failure types. In this study, RocPlane and Slide software were used to analyze slope stability for both structurally and non-structurally controlled slope sections (Rocscience, 2004). Accordingly, stability analysis was carried out using the RocPlane software for the structurally controlled slope sections, left abutment slope 1 (LASS1) and right abutment slope 1 (RASS1), which are located on the left and right abutments, respectively. This was done because the possibility of kinematic instability had been identified. In light of this, the factor of safety for the planar mode of failure for each crucial slope segment was determined using the RocPlane and rock swedge software. Slope geometry (height and dip angle), upper slope face angle, waviness, and joint dip angle were measured in the field and used as input parameters for the RocPlane software.

The unit weight of the rock was calculated in a laboratory, and the horizontal seismic acceleration was taken from a seismic risk map, while the other parameters, such as the friction angle and cohesiveness, were evaluated using the RocData software (Asfaw, 1986). Furthermore, the stability analyses of the non-structurally controlled slope sections i..e on the reservoir rim(RRSS1) was also done by using slide 6.0 software (Rocscience, 2004).

The Uniaxial Compressive Strength of Intact Rocks (UCSi), Geological Strength Index (GSI), Intact Rock Constant (mi), and Disturbance Factor (D) that were calculated in the RocLab software are input parameters that are used in the slide software. Also, the slope geometry measured in the field, the unit weight of the rock determined in the lab, and external forces (groundwater and seismic stress) were taken into account as input parameters for the slide program. The crucial slip surface for a particular slope was identified in this work by analyzing individual slip surfaces using search techniques. The "auto-grid approach," which determines the minimum slip surface using Slide software's default settings, was utilized to find the crucial slip surface. In general, a 20x20 grid was defined which resulted over 4000 slip centers. Slide software was determined the factor of safety by utilizing General limit equilibrium (GLE)/Morgenstern-Price method. GLE satisfies and computes FOS for both moment and force equilibrium (Fredlund and Krahn, 1977).

3.4.3.2 Finite Element Method

One of the most suitable method for highly weathered and fractured rock mass slopes is FEM. In this study, the finite element analysis were carried out for non structural slope on the reservoir area using Phase2 software. The Shear Strength Reduction (SSR) option in Phase2 allows the user to automatically perform a finite element slope stability analysis and compute a critical strength reduction factor (SRF) for the model. The basic input parameters required for Phase2 software including rock type, slope height, uniaxial compressive strength of intact rock (σci), unit weight of rock (γ), Geological strength Index (GSI), Hoek Brown parameters (a, mb and s), cohesion (c), friction angle (ϕ), intact rock constant (mi), Disturbance factor (D), Young's modulus (Erm), Poisson's ratio (v), seismic load and groundwater condition. Slope geometry and GSI were determined in the field. Disturbance factor (D) and material constant (mi) were assumed from the chart provided by Marinos and Hoek (2000). The value of Disturbance factor(D) varies from 0 to 1 for undisturbed in-situ rock masses and very disturbed rock masses respectively (Torres and Brent, 2002). Some of the data such as uniaxial compressive strength (σci) and unit weight of rock (γ) were determined in the laboratory. Furthermore, shear strength parameters were estimated using RocLab software whereas Poisson's ratio (v) was taken from publication (Gercek, 2007) was used in the analysis. The young's modulus (Erm) of the rock mass is calculated from the Disturbance factor (D), Geological Strength Index (GSI), whereas intact modulus (Ei) (Hoek and Diederichs, 2006) were estimated by the following equation, which is already built in the Phase2 software.

Erm = Ei *(0.02 + $1-D/2$ $1+e($ $60+15D-GSI$ 11)) Where Erm is rock mass elastic modulus in KPa, D is the Disturbance factor, GSI is the Geological Strength Index and Ei is the intact modulus. The intact modulus, Ei can be expressed as follows. The intact modulus, Ei was expressed as follows.

Ei = MRσci (20) Where; MR is the modulus ratio proposed by Deere (1968) and σci is the Uniaxial Compressive Strength of the intact rock. This relationship is useful when no direct values of the intact modulus are available or where completely undisturbed sampling of measurement of Ei is difficult.

3.1.4.5. Water Tightness Analysis Method

The water tightness analysis was carried out using laboratory permeability testing of the soil sample, surface hydraulic conductivity estimation from discontinuity aperture and spacing, water tightness model and lugeon tests.

The laboratory permeability test was conducted on four representative soil samples collected from the test pits to determine the coefficient of permeability of the soil deposits in the foundation and reservoir area. The relationship between the hydraulic conductivity (k) and fracture characteristics (spacing, S and aperture, e) is given by equation 25, which is derived by Snow (1965) and Louis (1974) to estimate the hydraulic conductivity of rock mass that is exposed in the dam abutments and reservoir area. During the discontinuity surveying data collection, special attention was given for the orientation of joints that favorable for leakages. Moreover, the water-tightness of dam axis was evaluated using a water pressure test or packer tests conducted by ECDSWC.

3.1.5. Engineering Geological Mapping

After analysing primary and secondary data, the engineering geological map of the study area were prepared at a scale of 1:5000. The engineering geological mapping has been carried out based on engineering characterization of the rock mass and the soils that exist at the dam site. Soils and rocks of the dam site were characterized and classified and their classification is used to produce an engineering geological map of the dam site.

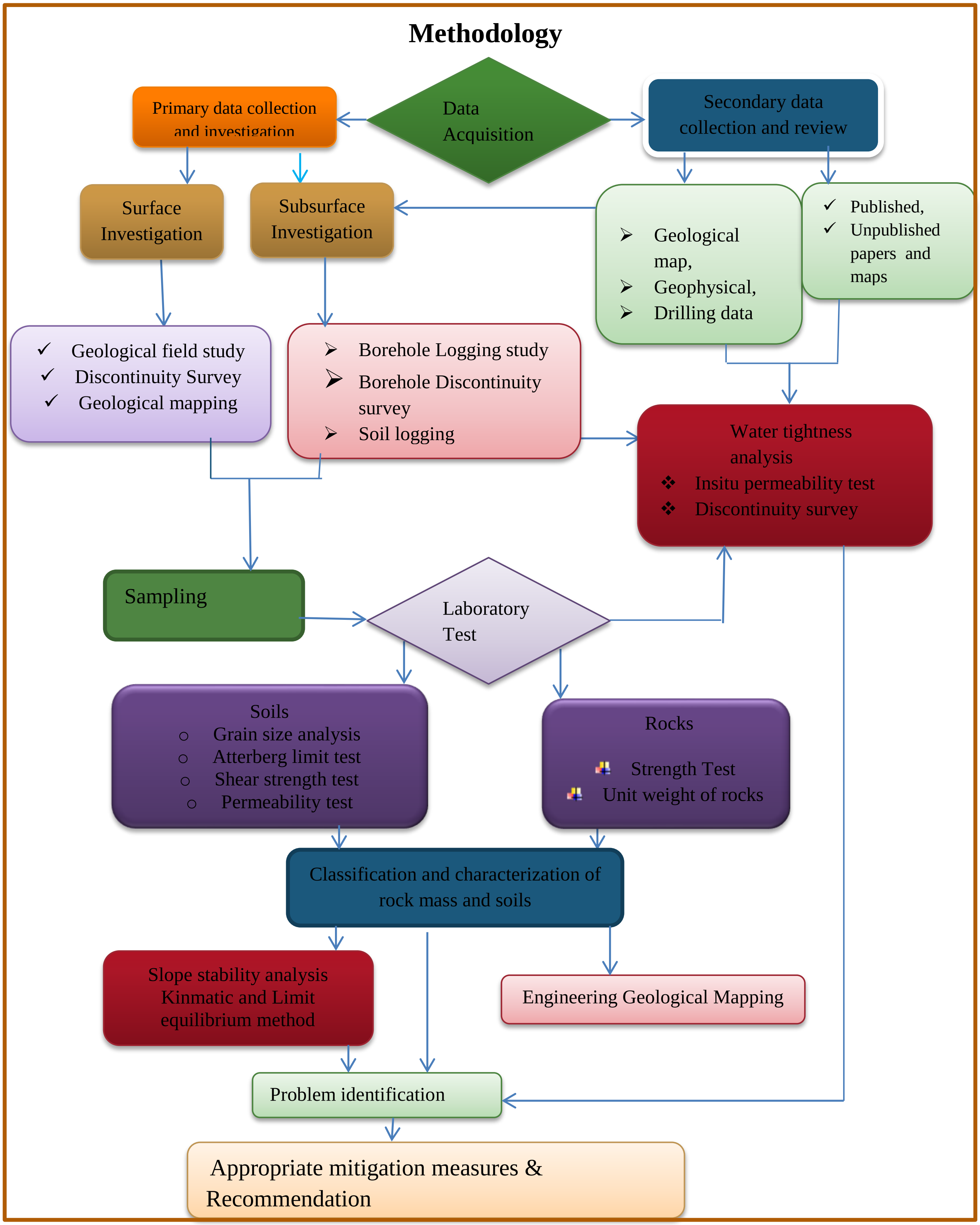

Figure 16 Flow chart of the research methodology.

3.2. Materials

There are different materials and equipment were used to conduct the research work. Some of them are:-

- Common geological instruments such as geological and Schmidit hammer, Burton compass, GPS, meter tape, sample bag for soil and rock sampling.
- Geological, hydro-geological map and Topographic map of Ethiopia prepared by the Ethiopian Mapping Agency.
- Laboratory equipment's such as atterberg limit test apparatus, soil permeability test apparatus, soil shear strength test apparatus, rock strength test (UCS) apparatus.
- Geophysical equipment, in-situ permeability and strength test equipment's.
- Computer software programs such as ArcGIS software, dip software, slope stability analysis software will be used.
- Shovels, hoes, buckets during digging test pits.

CHAPTER FOUR

4. GEOLOGY OF THE STUDY AREA

4.1 Introduction

According to Alen and Taddesse (2003), Ethiopia's geology comprises Precambrian basement rocks to more recent volcanic rocks. The following geological formations make up this group of rocks. Rocks from the Precambrian, Paleozoic-Mesozoic, and Cenozoic epochs, as well as related sediments (Alen and Taddesse, 2003). Precambrian metamorphic and related intrusive igneous rocks are visible in the country's northern, western, southern, and eastern regions.

Geological map of Ethiopia were first compiled by Kazmin (1973) at scale of 1:2,000,000, and was modified later by (Tefera et al.,1996) provide some broad and basic information about the geology of the central part of Ethiopia.

4.2. Regional Geology

Geology of Asela map sheet is mainly plateau volcanics belonging to the southeastern Ethiopia and associated lowlands. Minor areas occurring to the northwestern part belong to the Main Ethiopia Rift (MER). This contains faulted plateau volcanics which are mainly pyroclasts, previously known as Nazreth series. Later young Quaternary lava flows (mainly basalts) covered localized areas of the rift. The north eastern Asela map sheet contains upper limestone, upper sandstone which are overlain by lower Tertiary volcanics. In the Asela map sheet Tertiary volcanic Formations, known in central and northwestern Ethiopia, previously previously known as Ashanghi Formation, Aiba Formation, Alajae Formation and Termaber Formation are encountered. There are trachytic dikes, especially on Bale mountains cutting many of the earlier volcanics. At places, the Asela map sheet is covered by volcanic mountains of younger Plio-Pleistocene trachyte flows, scoria cones and Quaternary basalt flows. Quaternary volcanics and sediments occur in the MER to the NW part of the map sheet.

Volcanics of central Ethiopia are not only flood basalts, but also include, thick succession of pyroclastic flows and falls, mainly ceasing the major known flood basalts (Workineh, 2006). There are also pyroclastic flows or pyroclatic falls within the major episodic flood basaltic volcanism. Also occur paleosoils and wood fossils, at various stratigraphic levels, indicating hiatus in volcanism. Therefore, volcanism in central Ethiopia didn’t commence and ended within short period of time as some investigators concluded.

The sedimentary units were ended by cretaceous Upper sandstone (Ambaradom Formation. The Mesozoic sedimentary rocks are unconformably overlain by the lower lava flows correlable to the Ashanghi Formation (Mengesha et al., 1996). Upward in the section comes the middle lava flows, correlable to the Aiba Formation of northern Ethiopia. Thick succession of pyrocastics are lacking in the southeastern plateau. The Aiba basalts are unconformably overlain by plateau basalts and pyroclastics correlable to the Alajae basalts and rhyolites of northern Ethiopia. These later ones cover large parts of Arsi and Bale plateau.

The Mesozoic sedimentary rocks are unconformably overlain by the lower lava flows correlable to the Ashanghi Formation (Mengesha et al., 1996)

Thick succession of pyrocastics are lacking in the southeastern plateau. The Aiba basalts are unconformably overlain by plateau basalts and pyroclastics correlable to the Alajae basalts and rhyolites of northern Ethiopia. These later ones cover large parts of Arsi and Bale plateau. These basalts are previously known as Arsi and Bale basalts (Merla et al., 1979 and Mengesha et al., 1996). The whole volcainic terrain to the east of Asela, except the trachytic peaks, were mapped as Ashanghi Group (Kazmin, 1972).

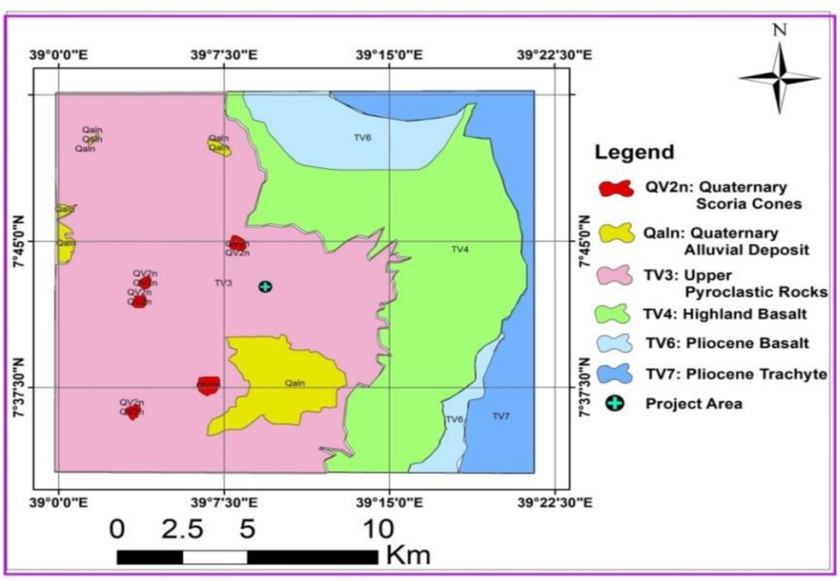

Figure 17 Geological map of the study area and the surrounding.

4.3. Geology of the study area

The geology of the dam site has been mapped from river cut, hillside, quarry site and road cut exposures. The geology of the area are consists three geological formations including pyroclastic material, basalt, and residual soil. Moreover, fresh ignimbrite, moderately weathered ignimbrite and slightly weathered ignimbrite with different rate of fracturing are the dominant lithology in the area. The dam site is covered by slightly to moderately weathered and moderately to highly fractured ignimbrite.

4.3.1. Ignimbrite

Ignimbrite rock unit is exposed most part of the study area incliding both right and left abutment, reservoir and spillway with different rate of fracture and weathering. In the right abutment of the dam it is more fresh with slightly fracture. The rock unit is mostly with the tuff, ash-fall or ash-flow deposits. The thickness varies from place to place.

The rock is welded to highly welded and massive in most places with different degree of fracture and some coarser fragments are visible in some parts of the area. The rock is characterized by different type of geological structures including columnar joints.

Figure 18 Ignimbrite rock with different fracture and weathering rate.

4.3.2. Tuff

Tuff is volcano clastic rock composed of solid volcanic ash that contain particles of volcanic glass (vitro-clasts), small fragments of crystals formed in lava (crystal clasts) and/or fragments of volcanic rock and lava (lithoclasts). The rock has light gray color and fine texture. The rock mostly occurred intercalation with the ignimbrite rocks in the reservoir area.

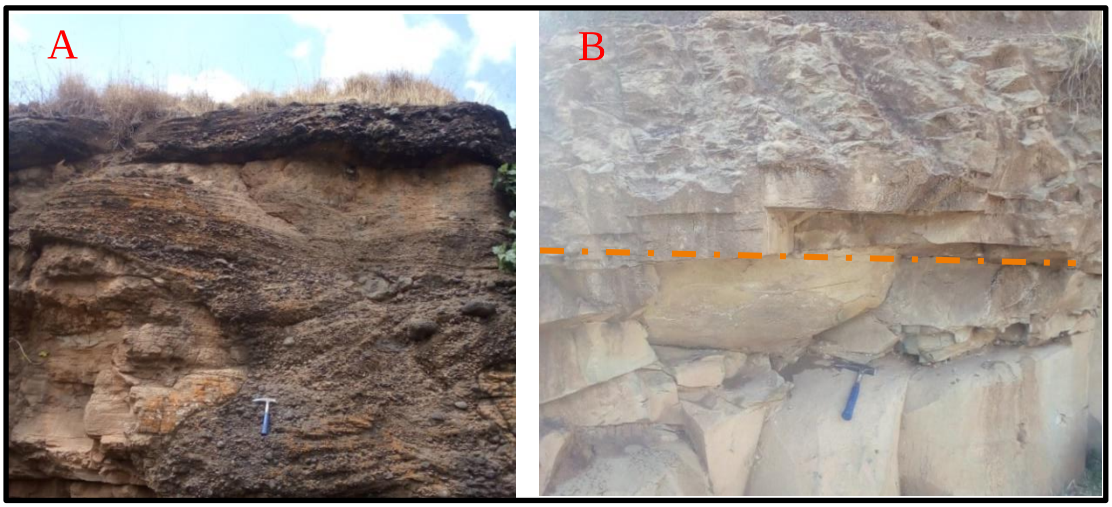

Figure 19 Tuff with large size rock fragments in the reservoir area (A) and tuff units underline by the ignimbrite rock units at down stream side(B).

4.3.3. Basalt rocks

The basalt units are mostly bolder forming and fresh to slightly weathered rocks. They are found in the reservoir area and thin layer near the axis of the dam. This rock is vesicular in texture and amygdaloidal with light to dark gray color.

Figure 20 Basaltic rock with vesicular texture (A) and bolder forming outcrop in the reservoir (B) and near the dam axis (C).

4.3.4. Soil cover

Two types of soil exposure were seen in the study area in addition to locally exposed organic soil. They are soil that was originally created from the region's weathered bed rock (residual) and soil that was brought by water (alluvial).

4.3.4.1. Alluvial Deposit

Soils deposited in riverbeds are known as alluvial deposits. The size of particles deposited in river beds depends on the speed of flow. If the flow of a river is strong, only large cobble-type material can get deposited. Unconsolidated gravel layer comprising rock blocks, boulders, cobble, gravel, sand, and silt are visible on the riverbank.

4.3.4.2. Residual Soil

This unit is cover large part of the main canal routes and the right and left abutments of the dam. According to sections from an excavated pit and a valley, the soil material is between 0.3 and 2.80 meters thick. This soil is silty clay, clay silt, sandy silty, and silt sandy, according to its physical characteristics and from preliminary geothecnical investigation . Residual soils formed from parent rocks of ignimbrite and tuff rocks at the original place by physical and chemical weathering processes which are formed at the place of origin. A geological map of the study area is given in Figure 24 below.

Figure 21 Alluvial soil cover in the study area on the side of Ashebeka river(A) and Pit excavated Residual soil deposit at the side of Ashebeka river (B).

4.4. Geological structure

The study area included under a portion of the main Ethiopian rift (MER). As a result, rift-related geological structures were discovered at the Ashebeka dam site. These structures are characterized by brittle deformation, which led to the formation of fractures, faults, and joints.

4.4.1. Joints

Joints are the dominant geological structures in the study area, which is observed mostly on ignimbrite rocks. Several strike orientations of the joints are seen in the rock mass in the study area. Most joints have three sets of striking directions: NE-SW, NW-SE, and WNW-ESE on the left abutment, and NNW-SSE, and NE-SW on the right abutment. They have medium continuity/persistence and moderately spaced, represented by vertical/sub-vertical rough surfaces, no filling material, and slightly weathered wall. Joints with stike orientation of ENE-WSW and WNW-ESE are favorable for leakage, becouse they are parallel to sub parallel with the river directions. Some joints are parallel to the dam axise and cross with perpendicular joints causes leakage by connecting to the neighbor valleys.

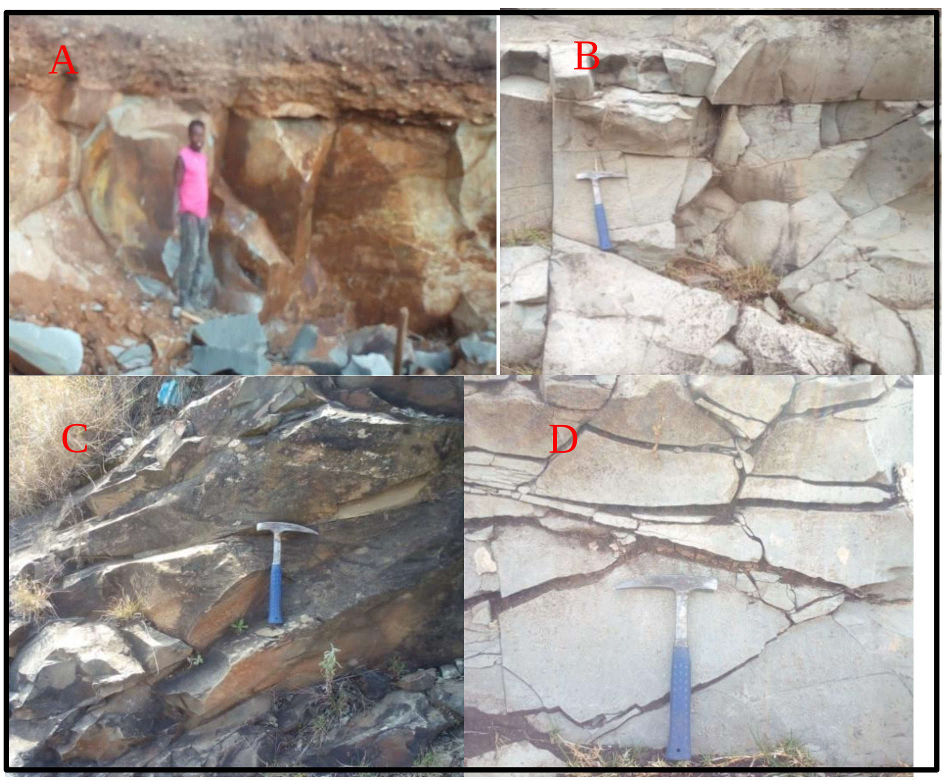

Figure 22 Different joint sets a) in reservoir area b) on the right abutment c and d) on the left abutment.

4.3.2 Columnar Joint

These geological structures are observed at the dam site and in the reservoir area on the ignimbrite rock unit. Columnar joint on the ignimbrite rocks is clearly visible at the right abutment of the dam and at the quarry site the area. These are formed from the hot pyroclastic material when it reaches the ground with the hot temperature. These joints deep up to 2.5m from the surface. Most of the joints are pentagonal in shape and some are hexagonal.

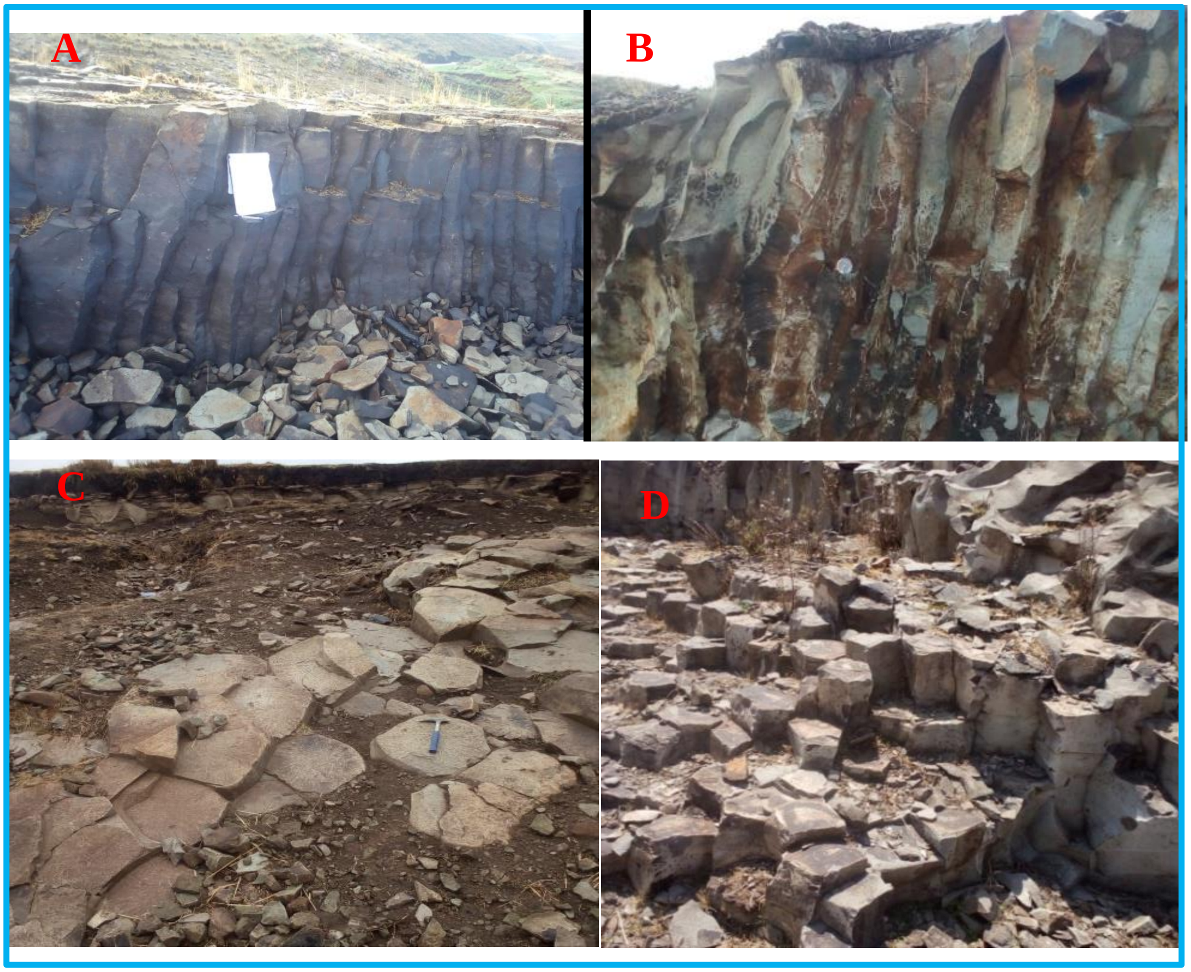

Figure 23 Columnar joint at right abutments of the dam (A&B) and at different parts of the reservoir area(C&D).

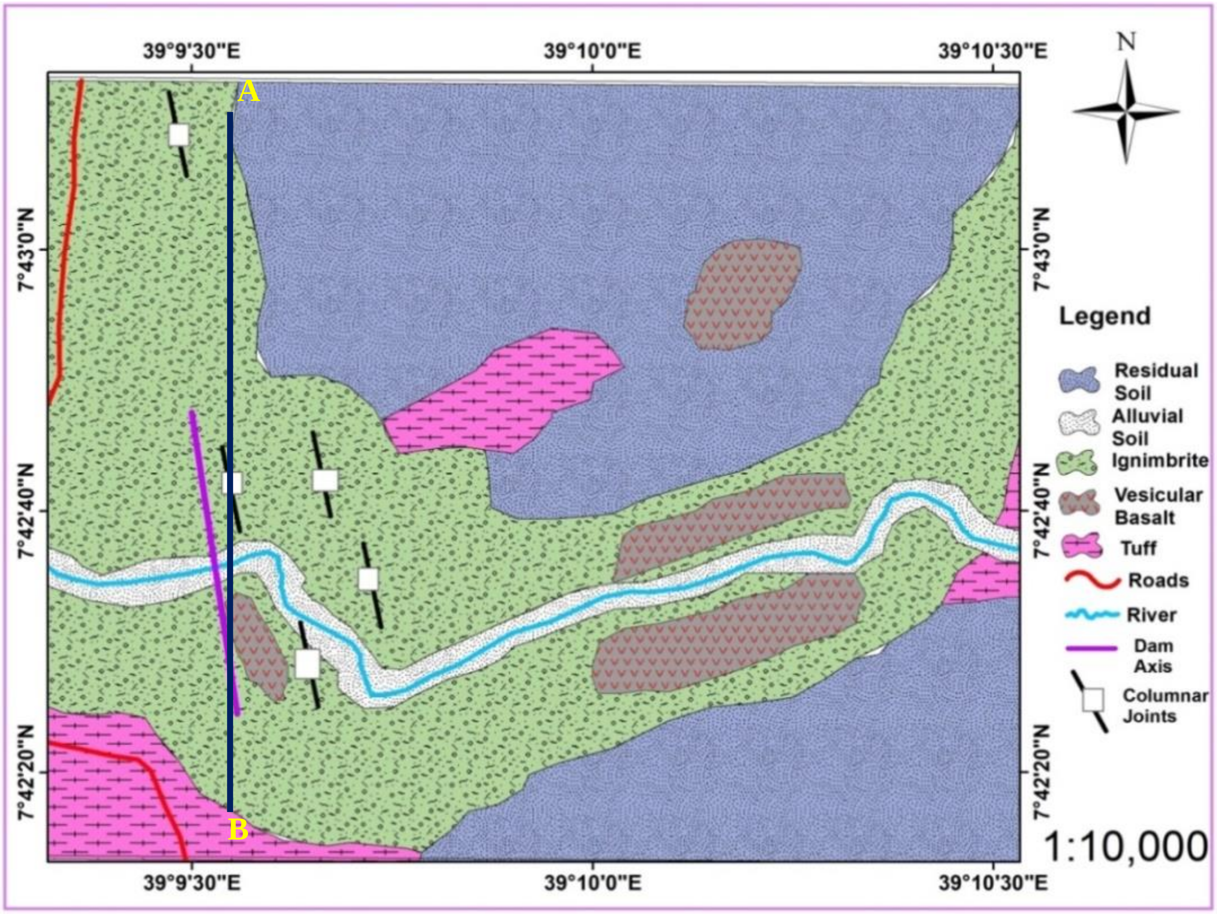

Figure 24 Geological map of Ashebeka dam site at a scale of 1:10000

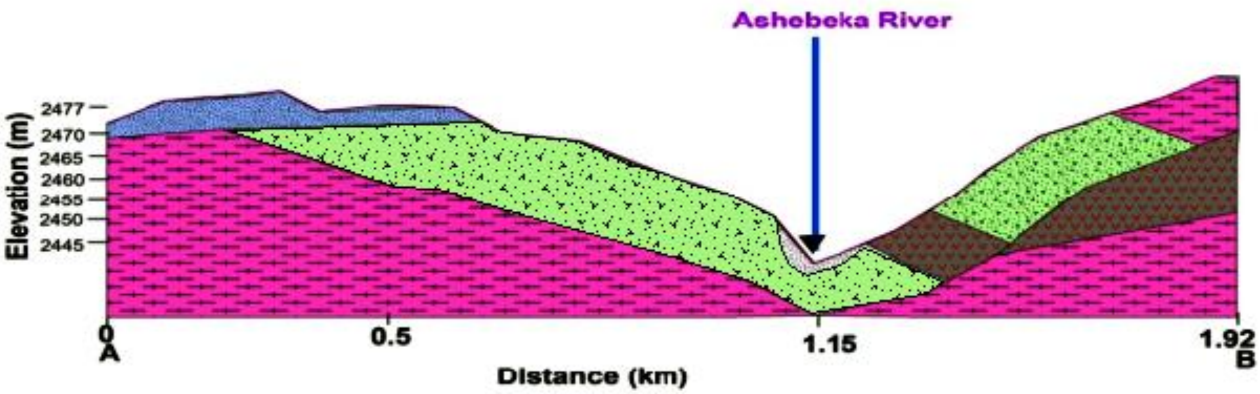

Figure 25 Geological cross section a cross the river and along the dam axis of AB line

CHAPTER FIVE

5. RESULTS AND DISCUSSION

5.1 Description and Characterization of Geology of the Area

From field observation, the study area is characterized by a moderately wide river valley which topographically surrounded by slightly elevated ground in the upstream and downstream of the dam site and flat to gentle slope which form abutments of the dam site. Abutments of the dam comprises of fractured ignimbrite rock. The ignimbrite rock is exposed at both abutments and covered by residual soil deposits at the top flat part of the area. The ignimbrite rock that exposed at the abutment was characterized by moderately to highly jointed and fractured with slightly to moderately weathered rock masses. In addition, some part of the ignimbrite rock formed intercalation with tuff units in the reservoir area. The basaltic rock is exposed along the Ashebeka river bed and underline by ignimbrite rock at the dam axis and in the reservoir area. It characterized by highly fractured and moderately weathered. Moreover, the reservoir area is dominantly covered by residual soils and ignimbrite rocks in some localities covered by tuff units which form gentle slopes and by basaltic rocks.

5.2 Surface Rock Mass Characterization

5.2.1 Discontinuity Survey

The discontinuity survey was undertaken according to the International Society of Rock Mechanics (ISRM, 1978) standard to characterize the rock mass conditions of the dam site and reservoir area. During the fieldwork, discontinuity data such as joint spacing, orientation, conditions (apertures, infill material and roughness) and the number of joints were collected and interpreted from exposed rocks at the slope face of the two abutments and from the reservoir area. These discontinuity data are used for slope stability analysis, water tightness assessments and also for rock mass classification as basic input parameters for the calculation of rock mass rating values and to determine the engineering properties of rocks. From field observation, one critical slope section namely RRSS1 nonstructural controlled on the reservoir area was identified.

5.2.1.1 Orientation of discontinuity

Furthermore, the discontinuity analysis result revealed that three dominant joint sets were having WNW-ESE (JS1), NNW–SSE (JS2), and NE-SW (JS3) strike directions on the left abutment, whereas NNE- SSE (JS1), WNW–ENE (JS2) and NE–SW (JS3) striking joints were found on the right abutment. From these results, it can be deduced that JS3 and JS1at left and JS2 and JS3 at right abutment and JS1 in the reservoir have very favorable orientation for leakage as their orientations are near parallel to the direction of the river flow. Some joints are parallel to the dam axise and cross with perpendicular joints causes leakage by connecting to the neighbor valleys.This scenario is also associated with potential leakage of water from the reservoir. Therefore, special treatment is required at the both abutments during the construction stage to prevent the potential leakage.

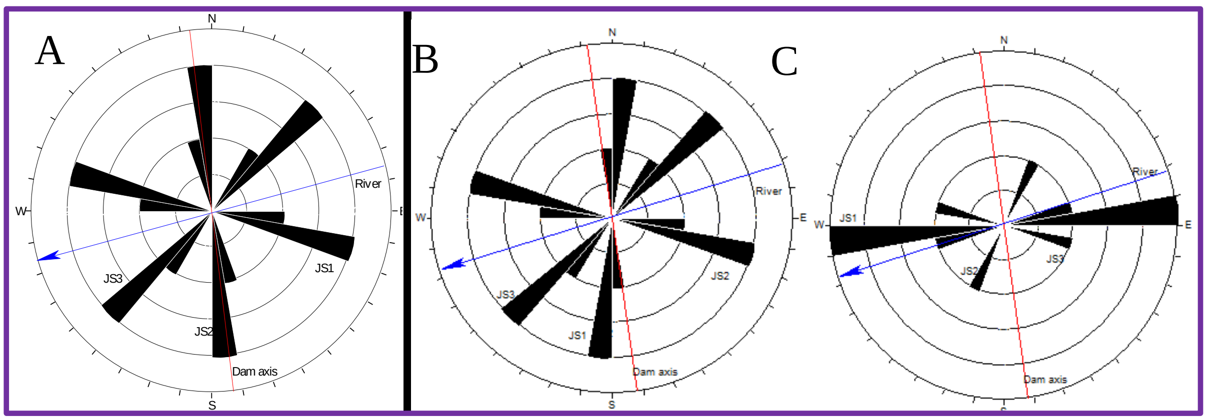

Figure 26 Rose diagram for left abutment (A) and for right abutment (B) for reservoir area (C)

5.2.1.2 Spacing and continuity of discontinuity

The strength of the rock mass declines and the permeability of the rock mass increases as the distance between two successive discontinuities decreases, according to Bell (2007). At the right abutment majority of joint sets are characterized by closely spaced, vertical to sub-vertical oriented, slightly rough to rough surfaces, tight with no filled materials. Similarly, at left right abutment the joint planes are mostly planar, rough and slicken sided surface were also observed. Summary of representative discontinuity measurements was presented in table 8.

5.2.1.3 Aperture and filling of discontinuity

Discontinuities can be open or closed, particularly joints. The degree of weathering the rocks have undergone has a significant impact on how open they are, which in turn affects the mass's overall strength and permeability. There may be partial or total filling in certain joints.

Table 6 Description of the aperture of discontinuity surfaces Anon (1977).

Aperture (mm)	0	<2	2-6	6-20	20-60	60-200	>200
Description	Tight	Extreamly narrow	Very narrow	Narrow	Moderately narrow	Moderately wide	Wide

Based on the above classification at the left abutment are classified extreamly narrow to narrow, at the right abutment are classified under extreamly narrow to tight and very narrow to tight class at reservoir area dominantly on ignimbrite rocks. The other geotechnical units have narrow aperture width.

Table 7 Some of representative surface discontinuity characteristics for the study area

Location	Joint sets	Coordinate		Orientation			Avg. Spacing (cm)	Avg. Aperture(cm)	Persistence(cm)	Filling material	Ground water condition	Roughness condition	Degree of weathering
		N	E	Strike	Dip	Dip direction							
Left abutment	J1	7°42'28"	39°9'36"	280	31	190	14	<0.1	10	No	Dry	Slightly rough	Slightly. weathered
	J2			170	85	80	15	1	40	No	Dry	Slightly rough	Slightly. weathered
	J3			220	50	130	25	<2	100	No	Dry	Rough	Slightly. weathered
Right abutent	J1	7°42'36"	39°9'33"	180	45	90	30	No	50	No	Dry	Slightly rough	Slightly. weathered
	J2			280	85	190	20	No	52	No	Dry	Slightly rough	Slightly. weathered
	J3			220	72	130	35	No	1m	No	Dry	Slightly rough	Slightly. weathered
Reservoir area	J1	7°42' 29"	39°10'02"	260	45	170	30	1	>100	Void	Dry	Slightly rough	Slightly. weathered
	J2			20	60	290	95	3	>100	Void	Dry	Slightly rough	Slightly. weathered
	J3			300	10	30	20	5	>200	Soil	Dry	Rough	Moderately weathered

5.2.2 Rock Quality Designation (RQD)

Rock Quality Designation has been estimated from joint volumetric count (JV) for rock mass that are exposed at the dam site and in the reservoir area using equation 2 as suggested by Palmstrom (1982). Accordingly, the average RQD values on the left abutment range from **31.3% to 47.46%** (Table 8). Similarly, on the right abutment, the average RQD values range from **52.2% to 63.62%** (Table 8) and in the reservoir RQD values range from **54.94% to 94.15%**. Based on this, it can be concluded that the rocks exposed at both abutment slopes have poor to fair rock qualities and fair to good in the reservoir area according to Deer (1968). This indicated that the rock mass found at both abutments and reservoir area are fractured and affected by numerous joint and degree of weathering.

Table 8 RQD estimated from surface discontinuity frequency

Location	Observation section	Jv	RQD	Average RQD	Rock quality according to deere(1968)
Right abutment	RAMS1	17.5	57.25	59.45	Fair
		18	55.6		
		15	65.5		
	RAMS2	21.21	45	63.62	Fair
		12	75.4		
		13.5	70.45		
	RAMS3	19.58	50.4	52.2	Fair
		17.5	57.25		
		20	49		
Left abutment	LAMS1	25	32.5	31.3	Poor
		23.6	37.12		
		27.5	24.25		
	LAMS2	18.2	54.94	47.46	Poor
		21.2	45.04		
		22	42.4		
Reservoir	RRMS1	9.3	84.31	61.65	Fair
		16.7	59.89		
		22.5	40.75		
	RRMS2	6	95.2	90	Good
		5.45	97		
		7.5	90.25		
	LRMS1	19	52.3	54.94	Fair
		15.6	63.52		
		20	49		
Where RAMS and LAMS are right and left abutment measurement section					

respectively and RRMS and LRMS are right and left side reservoir measurement section

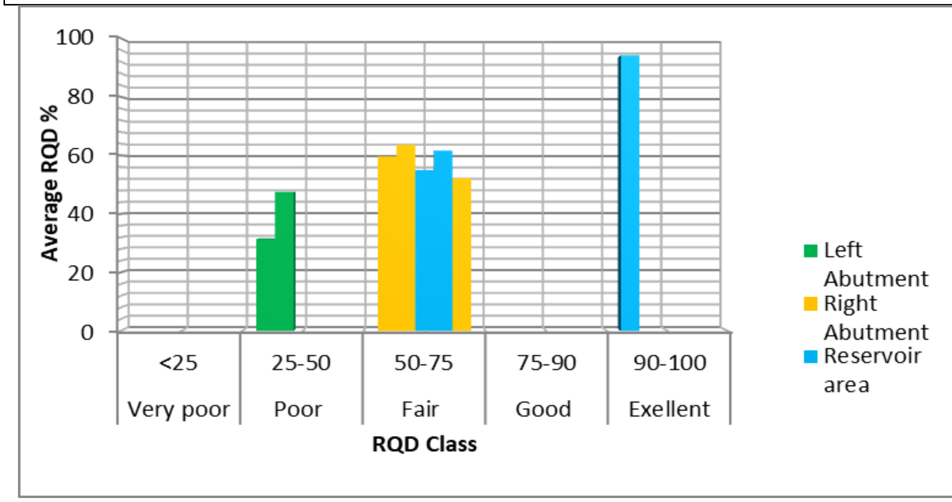

Figure 27 Graphical presentation of RQD value in the abutments and reservoir area.

5.2.3 In-Situ Rock Strength Test

The strength of rocks adjacent to joint walls at the dam abutments and in the reservoir area has been measured in the current study using Schmidt hammer (SH) in accordance with the standard recommended by ASTM (2001).

Measurements should be made using at least 10 readings, according to ASTM (2001), before averaging the remaining values and eliminating any that deviate from the average by more than 7 units. As a result, the test was conducted on fresh and slightly weathered rocks, and at least ten Schmidt rebound values were gathered for each observation location. The resulting rebound values were averaged, and those values that deviated from the average by more than 7 units were then discarded. The remaining rebound values were then transformed into the rocks' uniaxial compressive strength (UCS) using equation 7.

According to the results, the strength of the rock on the left abutment ranges from 24.54 MPa to 54.95 MPa, which is classified as very low strength to low strength rock, while the strength of the rock on the right abutment ranges from 61.65 MPa to 109.39 MPa, which is classified as medium strength rock, according to Deere and Miller (1966) .These results are shown in Table 10. Based on the Schmidt hammer results, it can be said that the rocks at the dam abutments range in strength from weak to medium strength rocks. Additionally, the uniaxial compression strength (UCS) values in the reservoir area range from 41.68 MPa to 69.18 MPa, which is categorised as low to medium strength rock according to Deere and Miller (1966) classification.

Table 9 Shemidit hammer result of rocks from the study area.

Location	Observation point	Average SHV	UCS (MPa)	According to Deere and Miller (1966)
Riht abutment	RAMS1	40.54	104.71	Medium strength
		46.90	109.39	Medium strength
		45.5	100	Medium strength
	RAMS2	35.75	61.65	Medium strength
		37.66	67.60	Medium strength
		38.50	70.79	Medium strength
	RAMS3	40.81	79.43	Medium strength
Left abutment	LAMS1	33.3	54.95	Low strength
		32	51.28	Low strength
	LAMS2	17.54	24.54	Very low strength
		33.63	44.67	Low strength
	LAMS3	32.6	42.66	Low strength
		34.2	46.77	Low strength
		32.7	43.65	Low strength
Reservoir	RRMS1	37.90	54.95	Low strength
		41	63	Medium strength
		33.58	44.67	Low strength
	RRMS2	43	69.18	Medium strength
		42.90	67.6	Medium strength

		32.08	41.68	Low strength
Where **RAMS and LAMS** are right and left abutment measurement section respectively and **RRMS** and **LRMS** are right and left side reservoir measurement section.				

5.2.4 Laboratory results for rock samples

To calculate the uniaxial compressive strength of intact rocks using equation 5, the point load test was carried out on irregular rock samples in accordance with ASTM D 5731 (1995) standards. A total of five irregular rock samples that were taken from the reservoir and dam abutments were examined. As a result, according to Deere and Miller (1966), the obtained UCS values of the rocks range from 21.12 MPa to 123.12 MPa (Table 10). Which are classiffied as low strength to medium strength, respectively, according to Deer and Miller's 1966 classification.

The findings of the point load strength test on the rock sample generally indicated that ignimbrite rock varies from welded to moderately welded and slightly to moderetly weathered rocks.

Similarly the unit weight test, which was carried out on eight irregular rock samples obtained from the dam's two abutments and the reservoir area were carried out using the buoyancy techniques recommended by ISRM (1978). The result is displayed in Table 10 and the average unit weights range from 19.58 KN/m3 to 27.3 KN/m3.

Table 10 Result of point load value of rocks determined in the laboratory

Sample Id	Load (Mpa)	Diameter, D_e(mm)	Correction factor $F=(De/50)^{0.45}$	Corrected point load	UCS (Mpa)	Water absorption	Rock Quality according to Deere(1966)
ASHRS-1	20	65	1.13	5.13	123.1	0.95	High strength
ASHRS-2	3.6	55	1.04	1.24	29.76	6.81	Medium strength
ASHRS-3	35	105	1.39	4.4	105.7	2.5	Medium strength

ASHRS-4	4.7	82	1.25	0.88	21.12	7.11	Low strength
ASHRS-5	8.46	52	1.02	3.2	76.8	3.76	Medium strength
Where **ASHRS** is Ashebeka rock sample.							

Table 11 Result of unit weights of rocks determined in the laboratory

Sample Id.	$M_{dry\ (g)}$	$V(cm)^3$	ρdry (g/cm3)	γ = ρdry *g (kN/m3)	Average γ = ρdry *g (kN/m3)
Fresh to Slightly weathered ignimbrite	299.00	105	2.848	28.48	23.45
	308.40	200	1.542	15.42	
	402.00	152	2.644	26.44	
Moderately weathered ignimbrite	285.00	170	1.67	16.7	19.58
	386	176	2.19	21.9	
	192.35	101	1.904	19.04	
	465.54	225	2.069	20.69	
Vesicular basalt	625.52	229	2.73	27.3	27.3
Where: **Mdry** is oven dried mass of rock, **V** is change in volume of water, **ρdry** is dry density and γ is dry unit weight of rock.					

5.2.5 Engineering Classification of the Rock Mass

The three most popular methods for classifying rock masses, RMR (rock mass rating) Bieniawski, (1989) , SMR (slope mass rating) Romana, (1985) and GSI (geological strength index) Marinos and Hoek, (2000), have been used in the current study to characterize rock masses and determine the quality of the rock masses at the dam foundation.

5.2.5.1 Rock mass rating (RMR)

The RMR system is consist of five fundamental parameters, such as (1) the UCS of intact rock, (2) RQD, (3) spacing between discontinuities, (4) condition of discontinuities, and (5) groundwater condition, and (6) orientation of the discontiunity that indicate various conditions of rock mass and discontinuities. The classification of rock masses utilizes UCS values from schmidt hammer rebound values and RQD results from volumetric joints. Rock mass categorization factors such as joint spacing, discontinuity condition, and ground water condition were determined in the field. As a result, the left abutment's rock mass quality ranges from fair rock to good rock, with rock mass rating values ranging from 48 to 63(Table

12). Similar to the left abutment, the right abutment's rock mass quality varies from fair rock to good rock, with ratings ranging from 58 to 68 (Table 12). Table 12 lists the specific discontinuity parameters with rating values and computed RMR. The deformability modulus of the rock mass ranges from 8.9Gpa at the left abutment to 40Gpa at the reservoir area. The result shows that low to high deformable rocks. Therefore during construction special treatment is required.

Table 12 Rock mass rating (RMR) values and classification of rocks at the dam site (After Bieniawski, 1989).

Section points	UCS(Mpa)		RQD(%)		Spacing (cm)		Discontinuity condition	Ground water condition		Orientation	RMR value	Rock mass class	Deformation modules , Ed
	Avg. UCS	Rating	Avg. RQD	Rating	Avg. Value	Rating	Rating	Condition	Rating	Rating			
RAMS 1	104.7	12	59.45	13	25	10	25	Dry	15	-7	68	Good	36
RAMS 2	66.68	7	63.42	13	29	10	25	Dry	15	-7	63	Good	26
RAMS 3	79.43	7	41.3	8	24	10	25	Dry	15	-7	58	Fair	16
LAMS 1	53.12	7	52.2	13	23	10	25	Dry	15	-7	63	Good	26
LAMS 2	34.60	4	31.3	8	15	8	20	Dry	15	-7	48	Fair	8.9
LAMS 3	44.36	4	47.5	8	20	8	20	Dry	15	-7	48	Fair	8.9
RRMS 1	54.2	7	94.2	20	85	15	20	Dry	15	-7	70	Good	40
RRMS 2	59.48	7	61.7	13	44	8	20	Dry	15	-7	56	Fair	12

Where **RAMS and LAMS** are right and left abutment measurement section respectively and **RRMS** and **LRMS** are right and left side reservoir measurement section.

5.2.5.2 Slope mass ratings (SMR)

The slope mass rating rock mass classification system utilized the relationship between representative discontinuity sets and slope face, the rock mass rating basic (RMR) and slope excavation methods as an input parameters. The result revealed from the calculation of SMR ranges from 28 to 49.6 which is bad to normal rockmass at the left abutment which reperesents unstable to partially stable areas. Similarlly at the right abutment the SMR value ranges from 70 to 90 which shows that good to very good rockmass and characterized by stable to completely stable rockmass. Also SMR value at the reservoir area shows that very good rockmass characteristics with completely stable.

Table 13 parameters used for estimation of slope mass rating (SMR).

Slope section	**Representative Discontinuity sets and Slope face**	**Dip**	**Strike**	**F1 (α_j–α_s) or ($\alpha_i - \alpha_s$)**	**F2 (B_j or B_i)**	**F3 (B_j-B_s) or (B_i-- B_s)**	**F4**
Left Abutment	**Slope face**	**65**	**20**	**-**	**-**	**-**	**-**
	JS1 with JS3	**50**	**5**	**-15**	**50**	**-15**	**15**
	JS2 with JS3	**45**	**10**	**-10**	**45**	**-20**	**15**
	JS3	**42**	**40**	**-20**	**42**	**-23**	**15**
Right Abutment	**Slope face**	**40**	**250**	**-**	**-**	**-**	
	JS1	**65**	**180**	**-70**	**65**	**25**	**15**
	JS2	**30**	**100**	**-150**	**30**	**-10**	**15**
	JS3	**85**	**220**	**-30**	**85**	**45**	**15**
Reservoir area	**Slope face**	**30**	**230**	**-**	**-**	**-**	**-**
	JS1	**45**	**260**	**30**	**45**	**15**	**15**
	JS2	**60**	**200**	**-30**	**60**	**30**	**15**
	JS3	**10**	**300**	**70**	**10**	**-20**	**15**

Table 14 Estimated **SMR** values at the abutment and reservoir areas**.**

Slope section	**Discontinuity set**	**Ratings/Values**				**RMR b**	**SMR value**	**SMR description**	**Stability**
		F1	**F2**	**F3**	**F4**				
Left Abutment	**JS1 with JS3**	**0.7**	**1**	**-60**	**15**	**55**	**28**	**Bad**	**Unstable**
	JS2 with JS3	**0.7**	**0.85**	**-60**	**15**	**55**	**34.3**	**Bad**	**Unstable**
	JS3	**0.4**	**0.85**	**-60**	**15**	**55**	**49.6**	**Normal**	**Partially stable**
Right Abutment	**JS1**	**1**	**1**	**0**	**15**	**75**	**90**	**Very good**	**Completely stable**
	JS2	**1**	**0.4**	**-50**	**15**	**75**	**70**	**Good**	**Stable**
	JS3	**1**	**1**	**0**	**15**	**75**	**90**	**Very good**	**Completely stable**
Reservoir area	**JS1**	**0.4**	**0.85**	**0**	**15**	**77**	**92**	**Very good**	**Completely stable**
	JS2	**1**	**1**	**0**	**15**	**77**	**92**	**Very good**	**Completely stable**
	JS3	**0.15**	**1**	**-60**	**15**	**77**	**83**	**Very good**	**Completely stable**

5.2.5.3 Geological strength index (GSI)

Also, GSI values were estimated from RMR using empirical equation (Hoek and Brown, 1997). GSI = RMR $_{basic}$ – 5 Where; RMR $_{basic}$ is the basic Rock Mass rating value and GSI is Geological Strength Index.

These results were compared with GSI values calculated in the field through eye observation using the quantitative GSI chart proposed by Marinos and Hoek (2000).

The state of discontinuity surfaces and structures in the rock masses was used to determine the value of the GSI of the rock mass at the surface outcrops and excavated slope faces on the abutments. The rock mass on the left abutment can be categorized as disintegrated to blocky/disturbed rock mass with GSI values ranging from 50 to 65, according to the GSI data. Similar to the left abutment, the right abutment's rock mass has GSI values between 60 and 70 and is categorized as very blocky to blocky rock mass. On the other hand, the reservoir area's disintegrating rock mass has GSI values ranging from 50 to 72 (Table 13). Generally, the result of RMR and GSI rock mass classification showed that the rock mass on the left abutment has low quality as compare to right abutment.

Table 14 Estimated GSI values at left and right abutment.

Location	Section Points	RMR_b	GSI values determined from RMR_b	Rock quality	Rock units
Right Abutment	RAMS1	75	70	Good	Slightly weathered ignimbrite
	RAMS2	70	65	Good	Slightly weathered ignimbrite
	RAMS3	65	60	Good	Slightly weathered ignimbrite
Left Abutment	LAMS1	70	65	Good	Slightly weathered ignimbrite
	LAMS2	55	50	Fair	Moderately to highly weathered ignimbrite
	LAMS3	55	50	Fair	Slightly weathered ignimbrite
Reservoir area	RRMS1	77	72	Good	Slightly weathered ignimbrite
	RRMS2	63	58	Good	Slightly weathered ignimbrite
	RRMS3	55	50	Fair	Slightly weathered ignimbrite
Where **RMR_b** = basic rock mass rating and **GSI** = geological strength index					

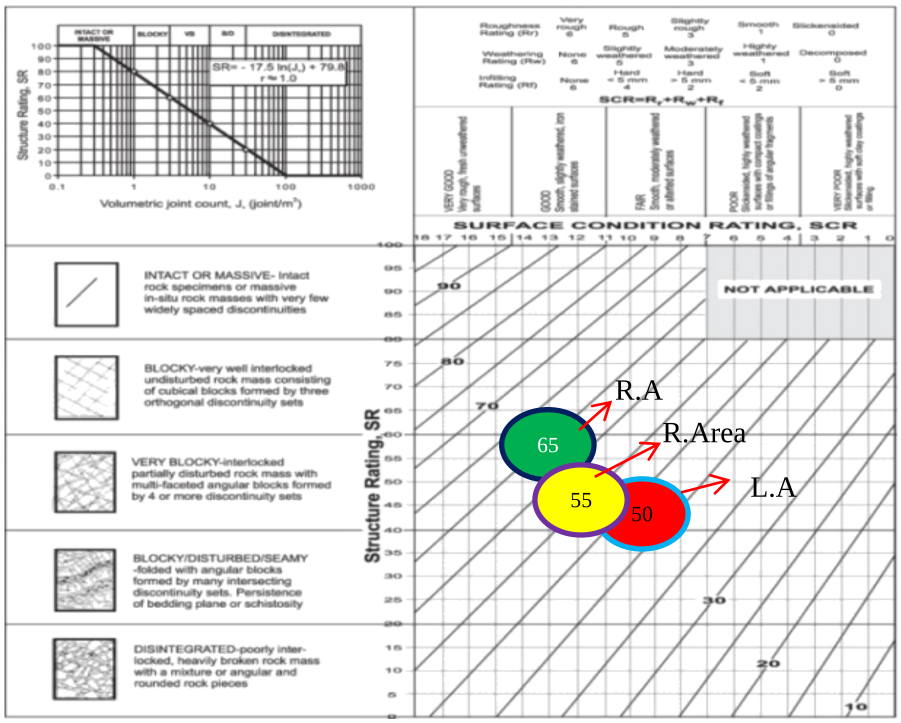

Figure 28 Rock mass classification of dam abutments based on GSI system (after Marinos and Hoek, 2000).

5.2.6 Rock Mass Shear Strength and Deformation parameters Estimation

In this study, RocLab and RocData software were used to determine various geo-mechanical parameters of rock mass for structurally controlled and non-structurally controlled slope sections. The Geological Strength Index (GSI), Uniaxial Compressive Strength of Intact Rocks (i), Material Constant of Intact Rock (mi), and Disturbance factor (D) are the input parameters for the RocLab software (Table 14). As input parameters for the application of slopes, slope height and unit weight of rock were also used. Equation 5 was used in this work to determine the RMR value, and the quantitative GSI chart was used to estimate the GSI value. However, the GSI derived from the field was employed in the analysis of slope stability. In the lab the Uniaxial Compressive Strength of intact rocks (UCSi) and rock unit weight (γ) values were determined. The dam abutment slope was mechanically excavated. Because D has a default value of 0.7 in the RocLab software was used for this study. Similarly, the material constant of intact rock (mi) was also taken from different published works (Rocsience, 2002) and for ignimbrite rock the value of mi is considered to be 20 which is already built in the RocLab software. For non-structurally controlled slope sections, the input parameters of RockLab software and the results of the output parameters are given in the Table 15.

Table 15 Values of input parameters of RocLab software for different rock samples.

Rock type	Input parameters						Output parameter			
	UCS(Mpa)	RMR	GSI	Mi	γ(kN/m3)	H (m)	Hoek-Brown Failure Criteria			
							UCSrm (MPa)	Cm (MPa)	ϕm(^{O})	Em (Mpa)
Fresh to slightly weathered ignimbrite on right abutment										
Fresh to slightly weathered ignimbrite	83.6	70	65	20	23.45	28	6.552	4.97	34.76	14093.12
Ignimbrite with different degree of weathering and vesicular basalt on the left abutment										
Fresh to slightly weathered ignimbrite	53.12	70	65	20	23.45	10	4.16	3.16	34.79	11234.21
Moderately to highly weathered ignimbrite	31.3	50	50	20	19.58	25	0.802	1.36	27.92	3636.05
Vesicular basalt	65.6	51	46	22	27.31	15	1.235	2.87	28.27	4181.82
Fresh to slightly weathered ignimbrite on reservoir area										
Fresh to slightly weathered ignimbrite	54.2	65	56.6	20	23.45	21	2.28	2.7	30.9	6997.02
Where, **Mi** is material constant for intact rocks, **H** is slope height, **UCSrm** is uniaxial compressional streangth of rock mass, **Cm** is cohesion, **Φm** is angle of friction and **Em** is elastic modules.										

5.2.7. Bearing Capacity of the surface rock units

Bearing capacity for each rock units are first determined using Bowles (1996) equation from the average computed RQD and UCS values of corresponding geotechnical layers. Accordingly, the analysis result shows that the safe load bearing capacity of the surface rock ranges from 0.97MPa to 7.63 MPa. The result shows the bearing capacity of geotechnical units possess very low safe bearing capacity.

Table 16 Allowable bearing capacity of the foundation rock mass using Bowles equation.

Rock type	Average UCS (MPa)	Average RQD (in Decimal)	Qult(MPa)	FOS	Qall(MPa)
Fresh ignimbrite	63.64	60.1	22.9	3	7.63
slightly weathered ignimbrite	45	51.5	11.9	3	3.97
Moderately to highly weathered ignimbrite	31.3	30.5	2.9	3	0.97
Vesicular basalt	65.6	24.5	3.9	3	1.31

The rock mass that makes up the dam foundation is weak and fragmented. In considering this idea, the allowed bearing capacity of foundation rocks was further calculated using an equation provided by Wyllie (1992), which is based on the Hoek-Brown strength requirements and the Bell equation as described in Wyllie (1992).

Accordingly, the allowable bearing capacity analysis result ranges from 3.59MPa for vesicular basalts to 27.7MPa for fresh ignimbrite rocks from the computed Wellie equation. Further, allowable bearing capacity of ignimbrite on sloping ground surface result 10.3MPa and 4.3MPa in right and left abutment respectively. From the result the allowable bearing capacity of the area is varies very low to low.

Table 17 The calculated bearing capacity of rocks as Wyllie (1992)

Allowable Bearing Capacity for fresh ignimbrite rock on the right abutment as per Wyllie (1992)						
UCS	GSI	S	M	FOS	qult (MPa)	qa (MPa)
83.6	65	0.0063	2.9	3	83.3	27.7
Allowable Bearing Capacity for fresh to slightly weathered ignimbrite on the left abutment as per Wyllie (1992)						
53.12	65	0.0063	2.9	3	30	10
Allowable Bearing Capacity for moderately to highly weathered ignimbrite on the left abutment as per Wyllie (1992)						
31.3	50	0.007	1.28	3	13.14	4.3

Allowable Bearing Capacity for vesicular basalt on the left abutment and in the reservoir area as per Wyllie (1992)						
65.6	46	0.0004	1.029	3	10.79	3.59
54.2	56.6	0.0019	1.84	3	17.87	5.9

Table 18 Bearing capacity of rocks on sloping ground on both right and left abutments.

Allowable bearing capacity of ignimbrite rock on the sloping ground at right abutment										
C (MPa)	$\phi(^o)$	Bearing capacity factor			γ(MN/m3)	H(m)	β (°)	B(m)	FOS	qa (MPa)
		No	Ncq	Nyq						
4.9	34.8	0.134	4.3	25	0.02345	28	40	34	3	10.3
Allowable bearing capacity of ignimbrite rock on the sloping ground at left abutment										
2.26	29.6	0.156	4.1	12	0.02345	15	30	26	3	4.3

5.3 Engineering Characterization of Soils

In order to conduct laboratory tests on the soil index properties, such as particle size distribution (sieve and hydrometer analysis), atterberg limits (liquid and plastic limit), natural moisture content (NMC), and specific gravity, representative soil samples were taken from the test pit. The test pits' depths range from 0.40 to 2.8 meters.

5.3.1 Natural Moisture Content (NMC)

Determine the amount of water or moisture present in the specified quantity of soil in terms of its dry weight. The obtained results show that the natural moisture content of the soils at the left abutment ranges from 17.5% to 19.4%. Similar to the left river bank, the natural moisture content of the soils in the right abutment and reservoir area ranges from 21.8% to 32.4%, and 15.2% to 37.4% respectively. In the test pits, the moisture content of the soils in the research area often rises with depth. Higher soil moisture levels suggested that the soils had low permeability.

5.3.2 Specific Gravity Test

The test was conducted according to the ASTM D 854 (1998) standard by using a pycnometer. Results of the specific gravity of the soil samples from the study area vary from 2.37 to 2.78 (Table 18).

Table 19 specific gravity and permeability results of soil samples from different parts of the study areas.

Location	Sample code	Sample interval(m)	Moisture content (%)	Specific gravity
Left Abutment	ASHTP-01A	0-0.7	17.5	2.78
		0.7-1.5	19.4	2.56
In river bed	ASHTP-02	0-0.5	26.75	2.70
Right Abutment	ASHTP-03A	0-2	32.4	2.63
	ASHTP-03B	0-0.6	21.8	2.56
At Reservoir Area	ASHTP-04A	0-0.44	15.2	2.46
	ASHTP-04B	1-1.65	31.8	2.37

5.3.3 Soil Particle Size Analysis

The percentages of various grain sizes in the soil have been determined using particle size analysis. The analyses were done on disturbed soil samples taken from the test pits. The percentage of soil particle size coarser than 0.075mm is determined by using sieve analysis where as those less than 0.075mm are determined by hydrometer analysis. Based on the particle size analysis result, particle size distribution curves/gradation curves are plotted. From the curve, the distribution of soil particles was determined and it also gives an idea regarding the gradation of the soil whether it is well graded or poorly graded. From hydrometer and sieve analysis results the soil samples revealed 20-16% sand, 23-42% silt and 38-61% clay at the left abutment, 16.5-21.4% sand, 40-42% silt and 34-65% clay in the reservoir area at the right of Ashebeka river, 18 %, 30% silt, and 52% clay at the river bed and32-37% sand, 33-34% silt, and 30-34% clay at the right abutment of the dam site (Table 19). Accordingly, the results obtained from grain size analysis indicated that the soil in the reservoir area was classified as clayey silt at ASHTP-04A and ASHTP-04B on the right side of the river. Similarly, at the right abutment, the soil was classified as clayey silt with sand at ASHTP-03A and clayey silt at ASHTP-03B. For the left abutment the soil was classified as silty clayey at ASHTP-01A and clayey silt at ASHTP-01B and silty clay soil at ASHTP 02 near the river bed. In general, based on grain size distribution analysis, the soil types found in the study area are identified as fine-grained soils.

5.3.3.1 Grain Size Analysis from the Left Abutment

From the curve below, the distribution of soil particles was determined and it also gives an idea regarding the gradation of the soil whether it is well graded or poorly graded. The soils in the left abutment of the dam site are poorly graded soils. From hydrometer and sieve analysis results the soil samples revealed 16- 20% sand, 23-42% silt and 38- 61% clay at the left of Ashebekariver.

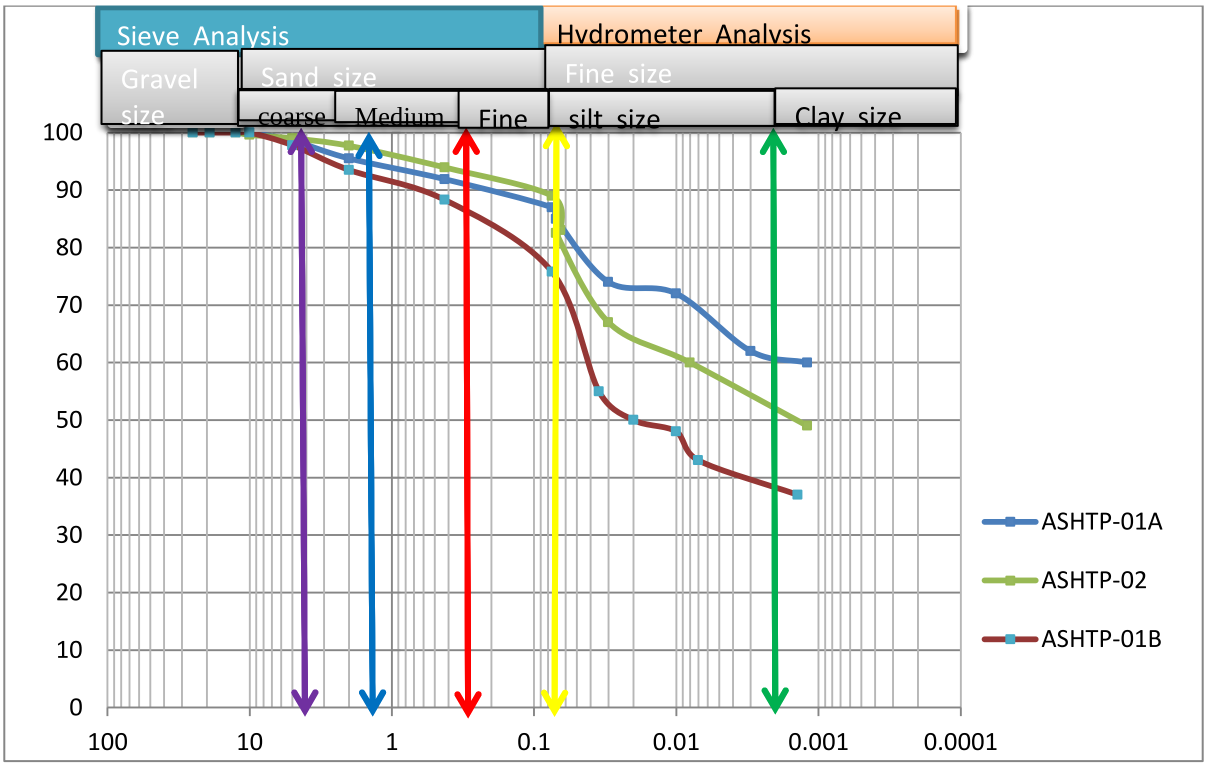

Figure 29 Grain size distribution curves of soil from the left abutment of the study area.

5.3.3.2 Grain Size Analysis from Right Abutment

The soil samples taken from ASHTP-03A, and ASHTP-03B, at the right abutment with a depth of 0 to 2m, and 0 to 0.60m respectively are well graded soil. The percentage of fine grain particles is more than coarser particles in ASHTP-03B than ASHTP-03A. The percentage of sand, silt, and clay for ASHTP-03A are 32%, 34%, and 34%, for ASHTP-03B are 37%, 33%, and 30% respectively as shown in Figure 30 below.

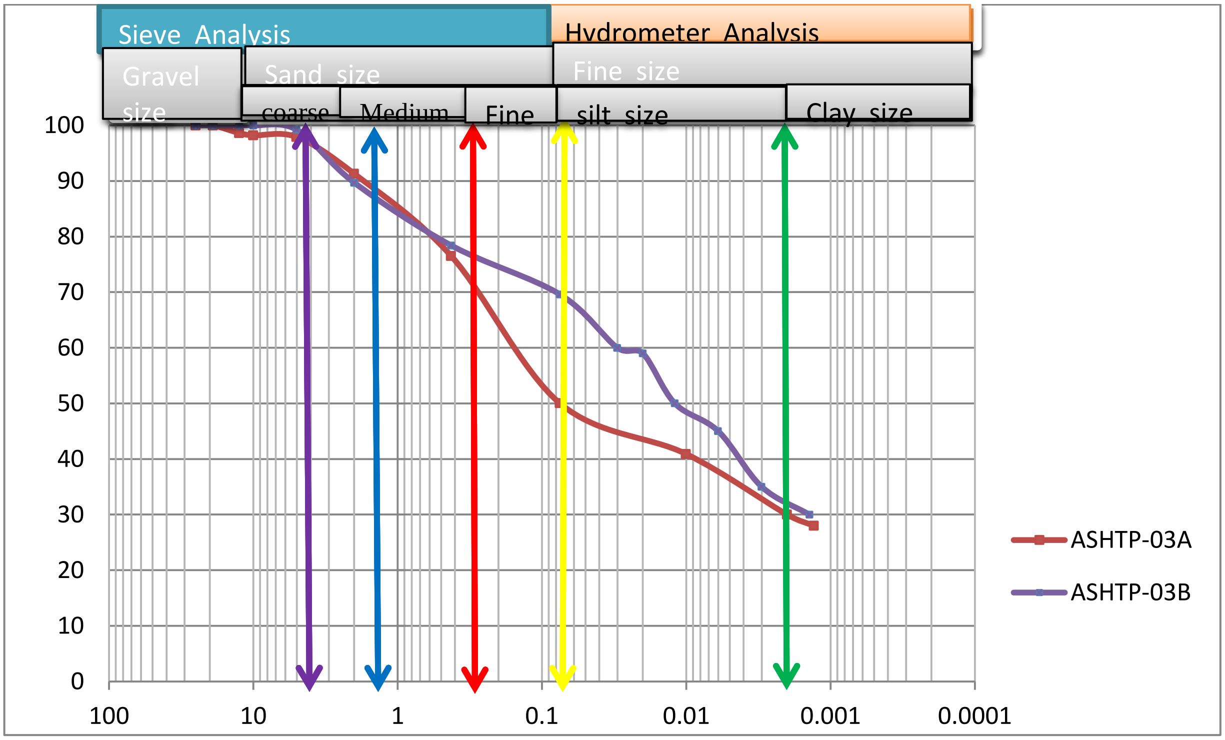

Figure 30 Grain size distribution curves of soil from the right abutment of the study area.

5.3.3.3 Grain Size Analysis from the reservoir area

The soil in the reservoir area was classified as clayely silt and clayey silt with sand at ASHTP-04A and ASHTP-04B respectively.The percentage of gravel, sand, silt, and clay for ASHTP-04A are 0.95%, 16.5%, 42%, and 40%, for ASHTP-04B are 4.3%, 21.4%, 40%, and 34.53% respectively as shown in Figure 31 below.

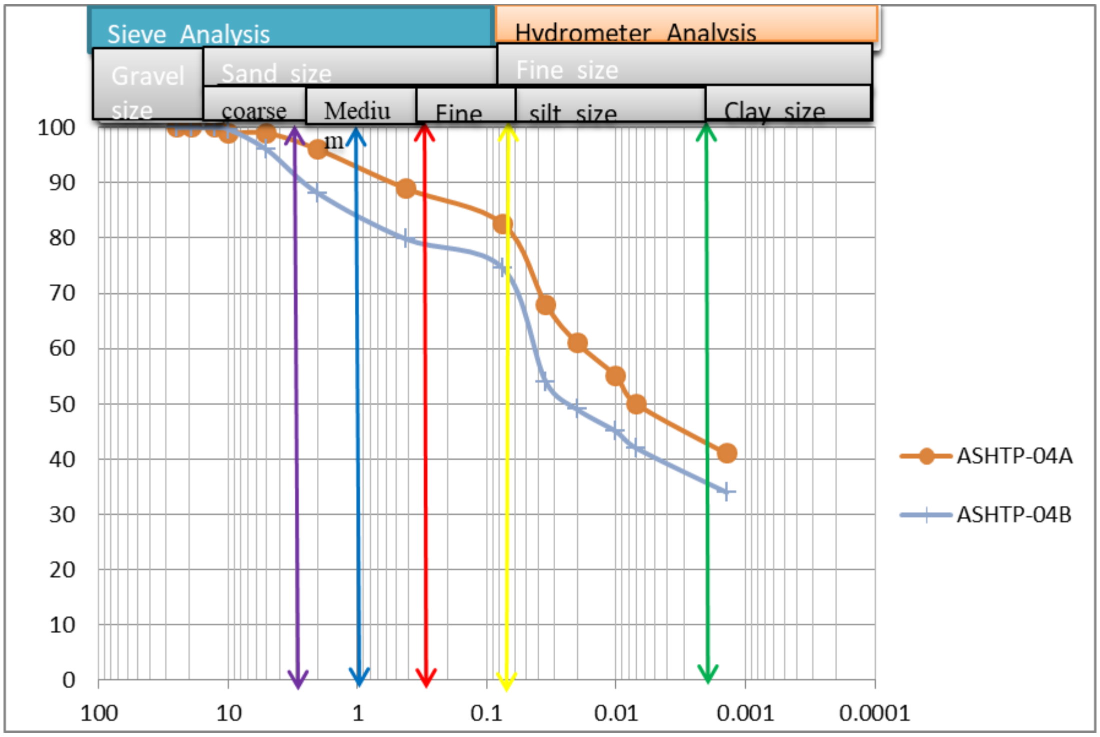

Figure 31 Grain size distribution curves of soil from the reservoir area.

5.3.4 Atterberg Limit Test

The amount of moisture in the soil has a significant impact on its consistency. When the moisture level of the soil is very high, it acts more like a liquid state, and as the moisture content progressively drops, the behavior of the soil changes from one state to the other. An Atterberg limit test is used to categorize soil using the Unified Soil Classification System and to establish the liquid limit, plastic limit, and plasticity index of fine-grained soil (Ramana, 1993). In the present study, the representative soil samples were collected from test pits dug in the reservoir area and dam site. The results of the Atterberg limit test are presented in Table 19. According to the result obtained from Atterberg limit tests, the soil in the reservoir area had a liquid limit (LL) varying from 42.81% to 81.4% which indicated intermediate to high plasticity soils (Ramana, 1993) and the plasticity index (PI) ranges between 17 to 47% showing medium to high plasticity. Similarly on the right abutment in the the Liquid Limit (LL) varies from 36.77% to 47.1% and the plasticity index (PI) varies from 12.8% to 13.8% which shows low plasticity classes (Ramana, 1993) and 62.6 to 75.5% liquid limit and 21.5 to 35.8% shows medium to high plasticity soil in the left abutment.

Table 20 Grain Size Distribution and Atterberg Limits test results.

Location	Sample code		Sample interval(m)	Grain Size Distribution (%)				Atterberg Limits (%)			plasticity Class (Ramana, 1993)
				Gravel	Sand	Silt	clay	LL (%)	PL (%)	PI(%)	
Left abutment	ASHTP -01	ASHTP-01A	**0-0.7**		**16**	**23**	**61**	**75.50**	**38.7**	**36.80**	High plastic
		ASHTP-01B	**0.7-1.5**		**20**	**42**	**38**	**62.60**	**41.1**	**21.50**	Medium plastic
At river bed	ASHTP -02	ASHTP-02	**0-2**		**18**	**30**	**52**	**73.90**	**39.1**	**34.80**	High plastic
Right abutment	ASHTP -03	ASHPT-03A	**0-2**		**32**	**34**	**34**	**36.70**	**23.9**	**12.80**	Medium plastic
		ASHTP-03B	**0-0.6**		**37**	**33**	**30**	**47.10**	**33.3**	**13.80**	Medium plastic
In reservoir	ASHTP -04	ASHTP-04A	**0-0.44**	**0.95**	**16.5**	**42**	**40**	**42**	**25**	**17**	Medium plastic
		ASHTP-04B	**1-1.65**	**4.03**	**21.4**	**40**	**34.53**	**81.4**	**34**	**47.4**	High plastic

5.3.5 Activity of soil

The activity of soil is a ratio of the plasticity index of soil to the percentage of clay size fraction in the soil. It is widely used for identifying the type of clay mineral in the soil and for the estimation swelling potential of soil. The activity value of soil samples is presented in table 28 below. The computed activity result for the study area ranges from 0.37 to 1.37. Accordingly, all clay content of soil samples obtained from the study area was classified as inactive, except soil sample ASHTP-04B. Based on Mitchell's (1976) range of activity value to determine the type of clay mineral, Kaoline and illite are clay minerals for the representative soil samples. Therefore, the clay portion of these samples has inactive to moderate activity and less swelling potential.

Table 21 Classification of soil samples based the activity values.

Sample code	PI (%)	% of clay fraction	Activity	Classification	Expected dominant minerals
ASHTP-01A	36.80	61	0.60	Inactive	Kaolinite and Illite
ASHTP-01B	21.50	38	0.56	Inactive	Illite
ASHTP-02	34.80	52	0.67	Inactive	Kaolinite and Illite
ASHPT-03A	12.80	34	0.37	Inactive	Kaolinite
ASHTP-03B	13.80	30	0.46	Inactive	Kaolinite and Halloysite
ASHTP-04A	17	40	0.42	Inactive	Kaolinite and Halloysite
ASHTP-04B	47.42	34.53	1.37	Active	Illite

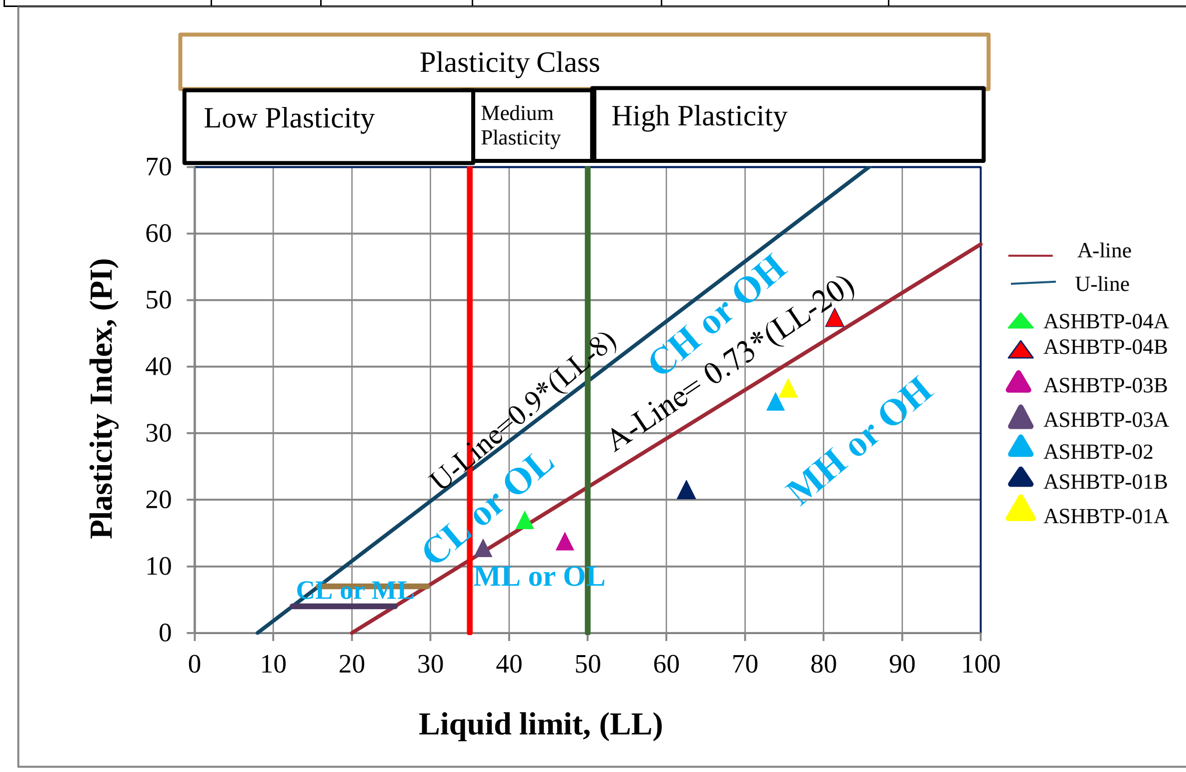

Figure 32 The plasticity chart to show the distribution of soil samples from the study area

5.3.6 Soil Classification by USC systems

The Unified Soil Classification System (USCS) is the most widely used soil classification system for engineering purposes. According to USCS, the soil samples from the reservoir area fall in ML/OL and CH/OH soil types (Figure 41) which implies clayey-silt and silty clay soils respectively. Accordingly, on the left abutment at ASHTP-01A, ASHBTP-01B and ASHBTP-02 test pits, the soil is a high plasticity silt soil (MH) while at ASHBTP-03A and ASHBTP-03B on the right abutment of the dam site, the soil is classified as low plasticity silty soil (ML).

Table 22 USCS classification of soil samples from four test pit of the study area (ASTM D 2487).

Location	Sample code		Grain Size Distribution (%)				Atterberg Limits (%)			USCS	Plasticity Class(Ramana,1993)
			Gravel	Sand	Silt	Clay	LL(%)	PL(%)	PI(%)		
Left abutment	ASHTP-01	ASHTP-01A		**16**	**23**	**61**	**75.50**	**38.7**	**36.8**	MH	Highly plasticity
		ASHTP-01B		**20**	**42**	**38**	**62.60**	**41.1**	**21.5**	ML	Medium plasticity
At river bed	ASHTP-02	ASHTP-02		**18**	**30**	**52**	**73.90**	**39.1**	**34.8**	MH	Highly plasticity
Right abutment	ASHTP-03	ASHPT-03A		**32**	**34**	**34**	**36.70**	**23.9**	**12.8**	MH	Medium plasticity
		ASHTP-03B		**37**	**33**	**30**	**47.10**	**33.3**	**13.8**	ML	Medium plasticity
In reservoir	ASHTP-04	ASHTP-04A	**0.95**	**16.5**	**42**	**40**	**42**	**25**	**17**	ML	Medium plasticity
		ASHTP-04B	**4.03**	**21.4**	**40**	**34.53**	**81.42**	**34**	**47.42**	CH	Highly plasticity

5.3.7 Compaction Characteristics

The compaction test findings for the samples taken from the dam site are summarised in Table 22. The Optimum Moisture Content range for the laboratory tests was 19.89-34.3%, while the Maximum Dry Density range was 1.17-1.54g/cm3 . In general, soils with lower activity levels (ASHTP-03A, and ASHTP-04A) are compacted to a higher density at a lower moisture content than soils with higher activity levels (ASHTP-02, ASHTP-01A and ASHTP-01B).

Table 23 MDD and OMC of soil samples collected from the dam axis and reservoir area.

Compaction Characteristics	Sample code						
	ASHTP-01A	ASHTP-01B	ASHTP-02	ASHTP-03A	ASHTP-03B	ASHTP-04A	ASHTP-04B
Max Dry Density (g/cm^3)	1.428	1.122	1.311	2.025	1.215	1.67	1.54
Optimum Moisture Content (OMC)%	29.11	24.25	34.3	22.49	20.19	19.89	27.5

5.3.8 Shear Strength parameters

One of the significant engineering characteristics of soils is their shear strength. Cohesion and friction together make up the shear resistance of soil. The direct shear test was conducted for two soil samples (ASHTP-04A and ASHTP-04B) by the researcher and five samples from the dam axis (ASHTP-01A, ASHTP-01B, ASHTP-02, ASHTP-03A, and ASHTP-03B) by ECO. The cohesion of of soils ranges from 2 KN/m^2 at ASHTP-04A to 33.6 KN/m^2 and their friction angles were ranges from 17.2 at ASHTP-01A to 26.1 at ASHTP-04A degrees, according to the interpretation of the laboratory data (Table 23). Both the analysis of slope stability and the determination of bearing capacity utilise these two shear strength factors as input variables.

Table 24 The shear strength parameters of soils at the dam site.

Sample code	Shear Strength Parameters		Soil type
	Cohesion, C (kN/m^2)	Friction angle, ϕ (^{0})	
ASHTP-01A	33	17.2	MH
ASHTP-01B	12	20.4	MH
ASHTP-02	30	16.9	MH
ASHTP-03A	28	22.75	ML-OL
ASHTP-03B	26	21	ML-OL
ASHTP-04A	2	26.1	ML-OL
ASHTP-04B	33.6	18	CH-OH

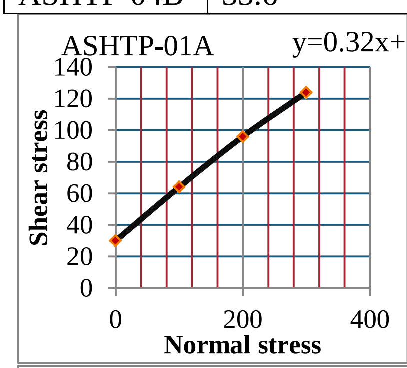

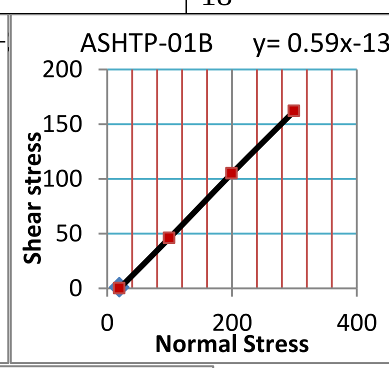

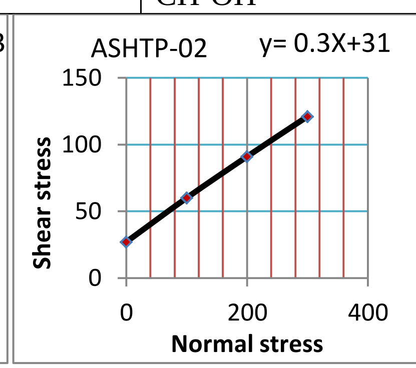

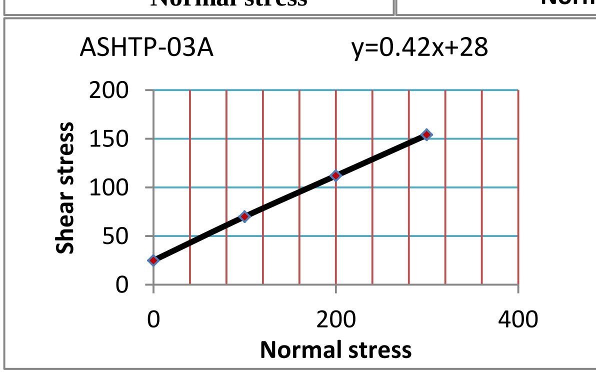

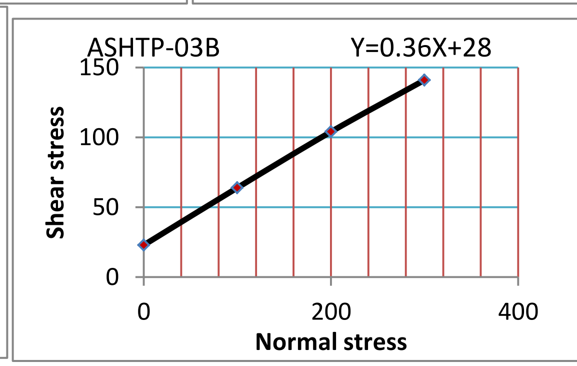

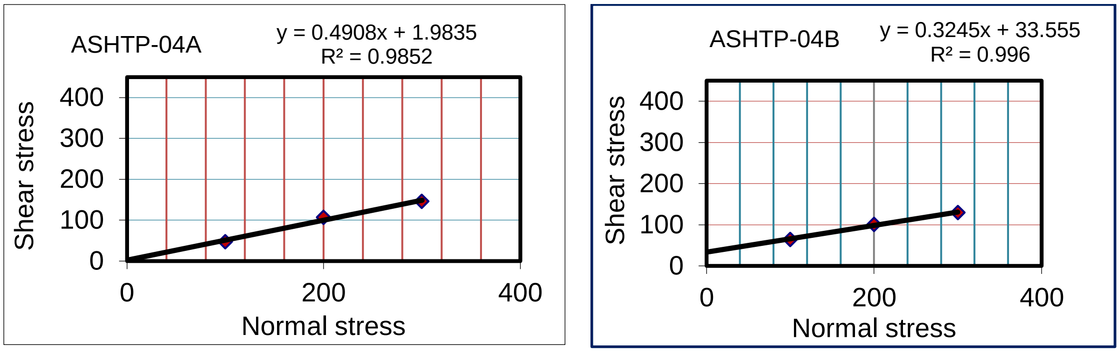

Figure 33 Graphical presentation of shear streangth parameters of soil with shear versus Normal stress curve.

5.3.9 Bearing Capacity and Permeability of the Soil

The foundation of a dam is a vital component. The stability of the supporting soil affects the stability of the structure. For purpose of the study, assuming a square footing foundation of 3m width at 2m depth, the ultimate bearing pressure (qu) according to Terzhagi is:

$$qu = 1.3cNc + \Upsilon DfNq + 0.4\Upsilon BN\Upsilon$$

Due to the following issue, the computed bearing capacity shown in table 24 are not appropriate. Since the project area's overall dam height is about 30 m high, so subsurface that extends more than 10 m below the surface needs to be addressed. The overall depth of the excavation in this study around the dam site ranged from 1 to 3 metres. The majority of the material that is exposed along the riverbed has been transported in locally. Before construction starts, a layer of 1 to 3 metres will be removed.

The conducted results of permeability of soil from the dam axis and reservoir area were ranges from $1.12*10^{-6}$ cm/s to $7.25*10^{-5}$ cm/s. According to USBR (1987) the permeability class of the soil ranges from semi pervious to impervious.

Table 25 Bearing capacity and Permeability of soil samples

Sample code	Depth (m)	Unit weight	Shear Strength Parameters		Bearing Capacity (KN/m^2)	Permeability (K) (cm/sec)	According to (USBR, 1987)
			Cohesion, C (kN/m^2)	Friction angle, ϕ (^{0})			
ASHTP-01A	0.7	14.38	33	17.2	213.8	$1.12*10^{-6}$	Impervious
ASHTP-01B	1.5	11.77	12	20.4	370.5	$4.36*10^{-5}$	Semi pervious
ASHTP-02	0.5	13.11	30	16.9	212.7	$6.07*10^{-6}$	Impervious
ASHTP-03A	2	13.15	28	22.75	338.1	$3.84*10^{-6}$	Impervious
ASHTP-03B	0.6	10.25	26	21	216.3	$7.25*10^{-5}$	Semi pervious
ASHTP-04A	0.44	24.6	2	26.1	427.2	$5.65*10^{-5}$	Semi pervious
ASHTP-04B	1.65	23.7	33.6	18	312.4	$2.24*10^{-6}$	Impervious

5.4 Subsurface Investigation

5.4.1 Subsurface Rock Mass Characterization

Drilling boreholes were used in the subsurface exploration of the Ashebeka dam site to investigate into the subsurface rock mass (ECDSWC, 2022). A total of six boreholes were drilled at the locations of the main dam, and planned spillway to evaluate the state of the subsurface geology, groundwater level, and to conduct in-depth experiments.

Table 26 Location and depth of boreholes with GPS value.

	Location	Borehole Id	N	E	Elv(m)	Maximum depth (m)
1	Left abutment	ASHBH-01	852212	517554	2443.75	35
2	Near the river	ASHBH-02	852212	517560	2428	29
3	Right abutment	ASHBH-03	852272	517554	2438.75	44
4	Intake	ASHBH-04	852054	517628	2438.25	20
5	Dam & S.W junction	ASHBH-05	852440	517567	2445.50	15
6	S.W(chute)	ASHBH-06	852822	517418		15

Accordingly, subsurface geological condition, rock-quality designation (RQD) values and permeability of rock mass have been determined for each borehole.From the direct geotechnical investigation, geotechnical core drilling, the following geotechnical layers were recovered.The subsurface geological units are explored by core drilling of boreholes as described below.

Top formation/top soil: This layer is top most layer in the site, the layer is very thin and found in all drilled borehole; it relatively thick in ASHBH-05 and reached up to 1.50m, the minimum thickness of this layer is 0.50m. It is characterized by dark brown, dry – wet, medium plastic, soft.

Welded Ignimbrite: it is found immediately underlying the top soil formation, it penetrated in and recovered from the ASHBH-01, 02 and 06. It is thick and reached up to 11.20m below the thin soil formation of the ASHBH-06. It reached 2.70m and 7.0m in the ASHBH-01 and ASHBH-02 respectively below the top soil. Grayish color, slightly weathered to fresh, dominantly fractured, joints closely spaced/, dense, medium strong. A sample taken from ASHBH-06 depth 4.89-5m, the laboratory data shows the unit weight is 24.0 and the UCS is 83Mpa.

Vesicular basalt: this geotechnical layer is penetrated in the ASHBH-01, 03 and 04. It is from 3.70m up to 9m below the decomposed tuff in the ASHBH-01. And it immediately under the top soil in the ASHBH-03 and ASHBH-04. Grayish color, dominantly fresh, slightly fractured to intact, and strong.

Aphanitic basalt: this section is also penetrated in the three boreholes, in ASHBH-01, 03 and 04. It is just below the vesicular basalt in the mentioned boreholes. There is no time gap between the two basalt layers. Dark gray, slightly weathered to fresh, slightly fractured to massive, and strong. Unit weight of this layer is ranges from 15.0 to 22.7 and the strength from the laboratory data, ranges from 83.52Mpa to 96.6Mpa.

Decomposed/loose to poorly welded tuff: This layer is penetrated in all drilled boreholes of the dam site. It is relatively thick and immediately found below the top formation in the ASHBH-05. In the ASHBH-01, 03 and 04 this formation is found below the basalt. It is below the welded ignimbrite in the ASHBH-02 and ASHBH-06.

Lithic Tuff: This layer is penetrated in the boreholes ASHBH-01, 02 & 03. In the ASHBH-01, this formation is found as thin layer between the channel deposits. In the ASHBH-02 the formation overlies by alluvial deposit and underlies by channel deposit. It is found as last layer of the ASHBH-01. Light color, weathered, dominantly intact, strength very soft. The laboratory data of this layer shows unit weight ranges from 13.1 to 17.4 and the strength ranges from 7.20Mpa to 13.92Mpa.

Alluvial deposit: This formation is clearly visible in the borehole ASHBH-02. It is found between the layers decomposed tuff/ poorly welded tuff and the channel deposit. It is composed of sand, gravels, cobbles and boulders size fragments originated from different volcanic environment. Generally very dense.

Alluvial/ flood plain deposit/dense to lose silty sand: This is the bottom section of the dam site, it is penetrated in two boreholes, ASHBH-02 and ASHBH-03. It is visible two times in the ASHBH-03 that is separated by the lithic tuff. In the ASHBH-02, this layer is logged as bottom layer. This formation is mainly recognized by its dark colour and composed of fine sand and it is dense. Maximum LL is about 40 at ASHBH-02. The PI is very low.

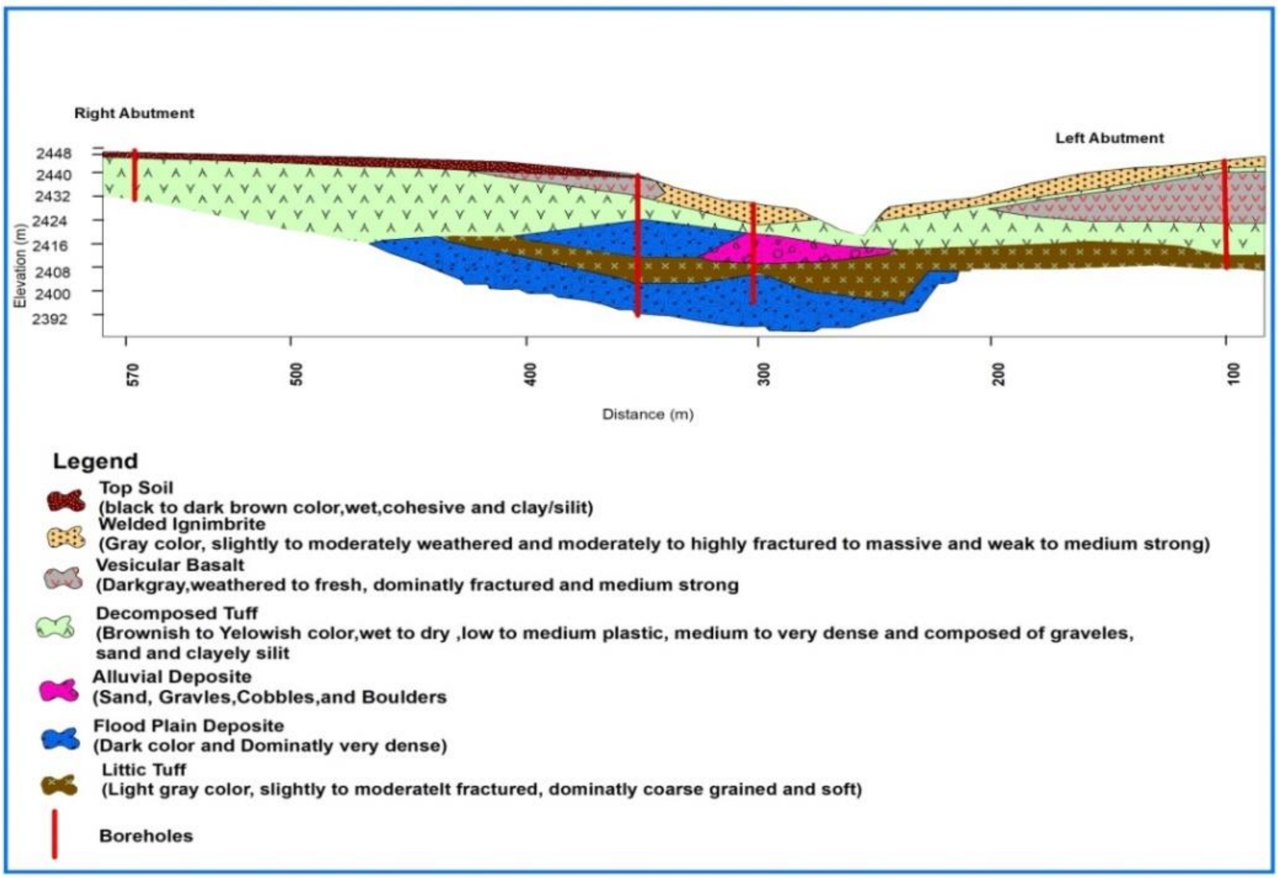

Figure 34 Surface and subsurface geological crassection from the borehole data.

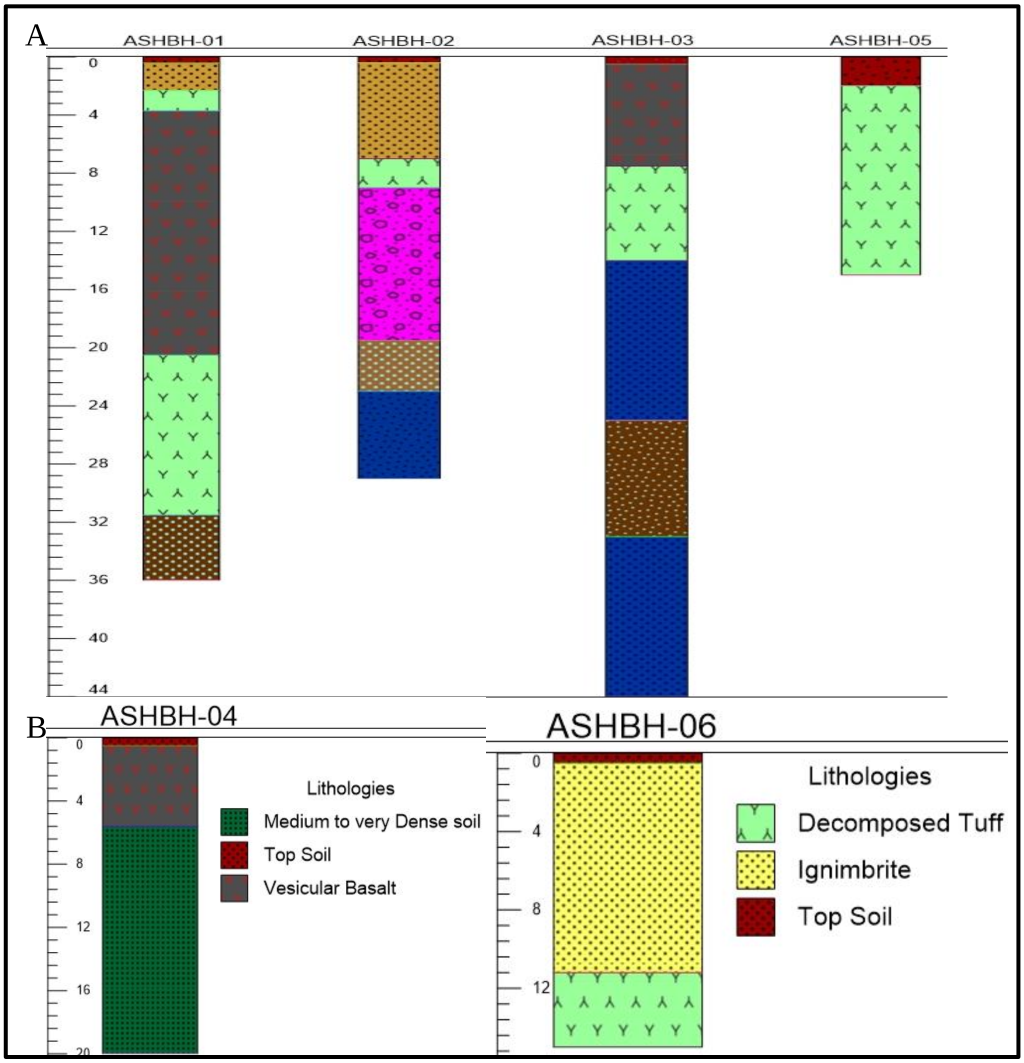

Figure 35 Geological log of the six boreholes on the dam axis(A) and on the intake and spillway (B)

5.4.1.1 Subsurface discontinuity survey

For the subsurface geotechnical units at ASHBH-01 discontiunities are classified under extreamly narrow to very narrow, at ASHBH-02 are very narrow to narrow, at ASHBH-03 are very narrow, at ASHBH-04 are narrow and ASHBH-06 are narrow classes. Open discontinuities without filling are more prone to seepage than the one with close opening and filling. From the subsurface unit at ASHBH-02, ASHBH-06 and ASHBH-04 and from the surface at the left abutment and at the reservoir area are wider aperture and more prone to seepage relatively.

Table 27 Discontiunity survey of subsurface rock units at different boreholes.

Borehole-ID	Depth	Orientation W.r.t dam axis	Spacing (cm)	Aperture (mm)	Filling material	Roughness condition	Discontinuity type
ASHBH-01	0.4-2.6	Normal	35.0	tight		Rough	Fracture
	2.6-3.7						Soft formation
	3.7-9.0	Normal	70.0	<2	Ca/Fe	Rough	Fracture joint
	9-20.5	Normal/paralle l		<3	Ca/Fe	Rough	Fracture joint
	20.5- 32						Soft formation
	32-36	Normal	100	<1	SC	Rough	Fracture
ASHBH-02	0.4-7.0	Norma, oblique, and parallel	<5	>5		Rough	Fracture joint
	7.0-17						Soft formation
	17.0-23	Normal	15	2	SC	Rough	Fractured joint
	23-29						Soil formation
ASHBH-03	9-14.20	Oblique, Normal	13.0	2.0	Ca/Fe	Rough	Fracture joint
	14.20-32	Parallel, Oblique & Normal	10.0	2.0	Ca/Fe	Rough	Fracture joint
	32-44						Soft formation
ASHBH-04	0.6-4.6	Oblique & Normal	6.0	>4	Ca/Fe	Rough	Fractures
	4.6-20						Soft formation
ASHBH-06	0.5-11.2	Oblique, Normal & Parallel	5.0	>5	Ca	Rough	Fracture joint
	11.2-20						Soft formation

5.4.1.2 Subsurface Rock Quality Designation (RQD) and UCS value

The RQD values ranged from 34 to 88% for ASHBH-01 at the left abutment, 30 to 58% for ASHBH-02 at the right river bank, 30 to 73% for ASHBH-03 at the right abutment, and 49 to 78% for ASHBH-04 at the intake in the rock mass beneath the river bed during the entire drilled depth. These suggested that the rock masses contained narrow to widely dispersed joints. The findings of the laboratory test on average uniaxial compressive strength (UCS) for rock samples are ranges from 9.36-96.96Mpa for ASHBH-01, 7.20Mpa for ASHBH-02, 13.92Mpa for ASHBH-03, and 83Mpa for ASHBH-06 (Table 27). According to Deere and Miller (1966) the strength of subsurface rock units ranges from Very low to medium strength and decrease to depth as shown in the figure 40.

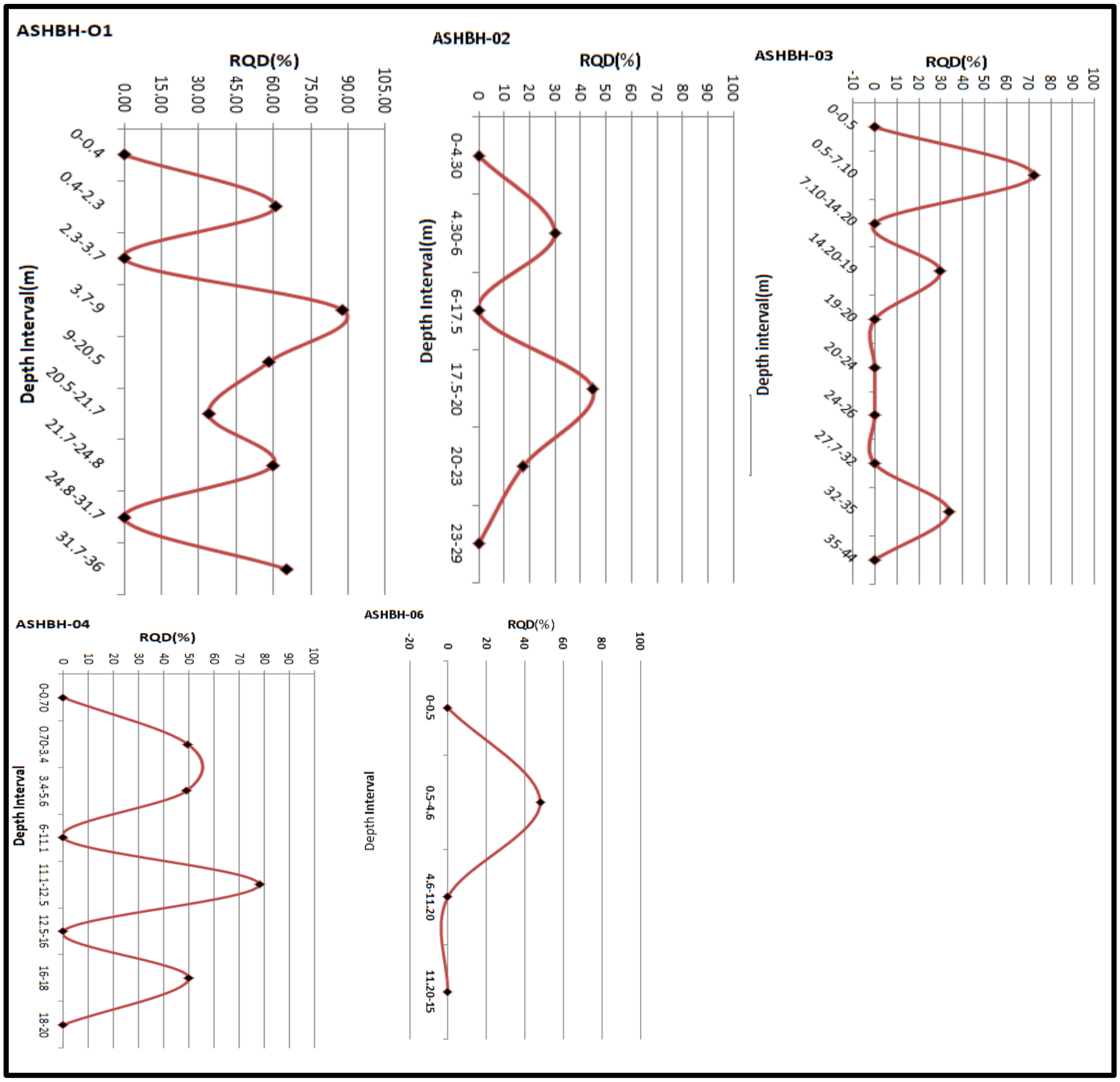

Figure 36 RQD values versus depth for selected boreholes at both Abutment and intake .

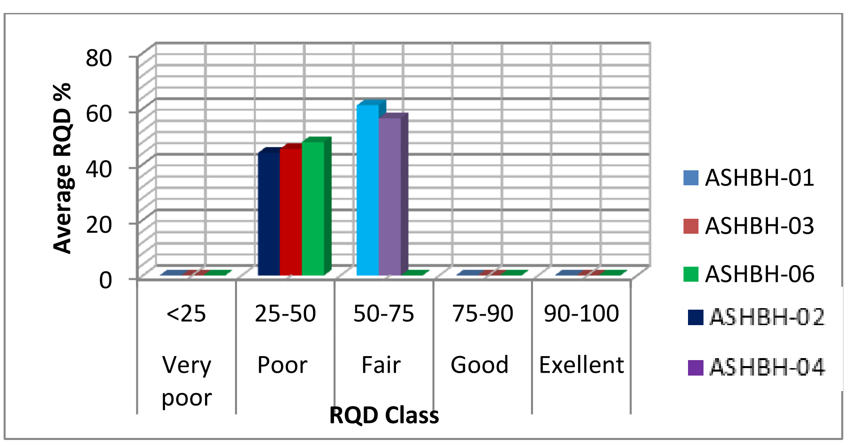

Figure 37 Graphical presentation for RQD value of rocks with classes at different boreholes.

Table 28 UCS and dry unit weight of rock samples from different boreholes.

Location	Borehole No	Depth Interval (m)	Average UCS (MPa)	According to Deere and Miller (1966)
Left Abutment	ASHBH-01	4.6 - 4.9	96.96	Medium strength
		6.7 - 6.9	89.28	Medium strength
		9.3 - 9.5	83.52	Medium strength
		14.5 -14.7	84.56	Medium strength
		34.5 -35	9.36	Very low strength
At the river bank	ASHBH-02	21.75-22	7.20	Very low strength
Right Abutment	ASHBH-03	9.85-10.10	13.92	Very low strength
S.W(chute)	ASHBH-06	2.4	83.04	Medium strength

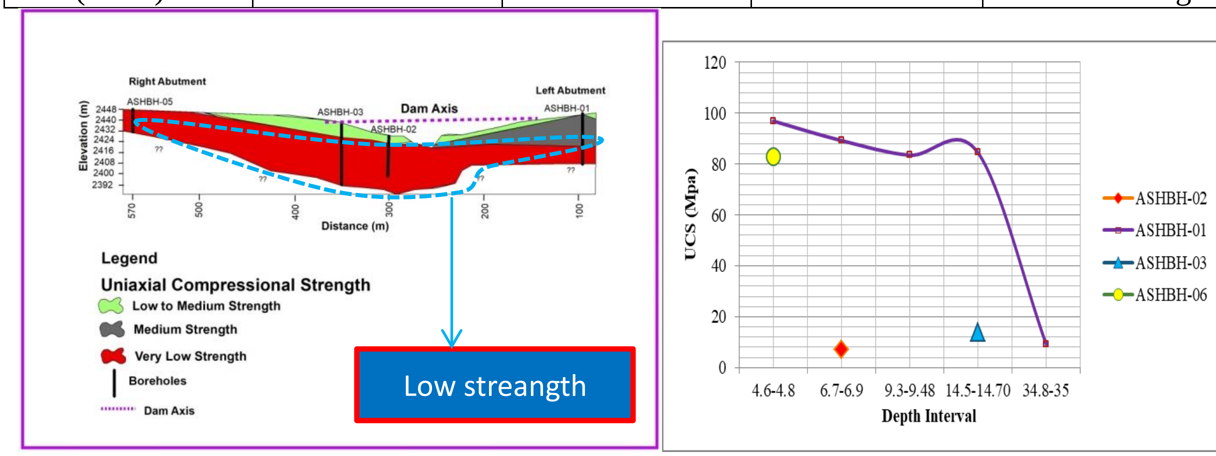

Figure 38 UCS varations from the integrated surface and subsurface value.

5.5. Deformability and bearing capacity of foundation rocks

The characteristics of intact rock were determined through laboratory testing on samples that were collected. The geomechanical rock mass rating, which takes into account the characteristics of intact rock properties and the effect of discontinuities, degree of weathering, and groundwater condition, was used to calculate the rock mass class. Drill cores recovered from boreholes were measured and examined to determine these characteristics of the rock mass. The RMR values of Ashebeka dam site were calculated by summing the rating of five parameters (Table 28), which can be obtained, through core logging and laboratory test results. The RMR values of the rocks in the study area range from 35 to 70, which can be categorized under class IV (poor rock) and class II (good rock) respectively.

The other engineering parameter to be determined in the area is the deformability of the rock mass. The calculated modulus of deformation was found to be in the range of 4.2 to 40 GPa as shown in table 28. Along the dam axis the deformability values were different and the deformability of the rock in the dam site were classified in to low, and high deformability classes. Low deformability was identified at the left abutment from borehole ASHBH-01, whereas high deformability was observed at the right abutment from borehole three (ASHBH-03), at the riverbed from borehole two (ASHBH-02), at the intake from borehole four (ASHBH-04), and at the spillway from drill six (ASHBH-06). As a result, the rock mass at the right abutment, riverbed, intake, and spillway has low values for the modulus of deformation and high deformability. Therefore, these places require ground modification in order to increase their values for the modulus of deformation.

Table 29 Subsurface rock mass rating and deformation analysis

Location	Borehole ID	Description	Average UCS (Mpa)	Average RQD (%)	Joint spacing(m)	Discontinuity condition	Water flow	RMR	Class no.	Description	Modulus of deformation	Deformation
Left abutment	ASHBH-01	Condition	72.82	61.2	0.35-0.7		Dry	70	II	Good	40	Low
		Rating	7	13	10	25	15					
Near the river bed	ASHBH-02	Condition	7.20	44.2	0.05-0.15		Dry	43	III	Fair	6.68	High
		Rating	2	8	8	10	15					
Right abutment	ASHBH-03	Condition	13.92	45.5	0.1-0.13		Dry	53	III	Fair	6	High
		Rating	2	8	8	20	15					
Intake	ASHBH-04	Condition	10.5	56.7	0.06		Dry	48	III	Fair	8.9	High
		Rating	2	13	8	10	15					
S.W(chute)	ASHBH-06	Condition	83.04	48	0.05		Dry	35	IV	Poor	4.2	High
		Rating		8	5	10	15					

The allowable bearing capacity of different rock units from different borehole locations ranges from 0.46 Mpa to 25 Mpa from the computed Bowles equation.The bearing capacity result at ASHBH-01, which is determined in foundation depth shows small decrease in bearing capacity when depth increase as shown in the table 29. The result reveals that the bearing capacity of different units is very low to medium safe bearing capacity. Therefore different type of streangth improvement technique should be required on both abutment.

Table 30 The calculated result of bearing capacity of subsurface rock units at different boreholes

Location	Borehole ID	Depth Interval(m)	Average UCS (MPa)	Average RQD (%)	Qult (MPa)	FOS	Qall (MPa)
Left Abutment	ASHBH-01	4.6-4.9	96.96	88	75	3	25
		6.7-6.9	89.28	88	69.1	3	23
		9.3-9.5	83.52	58.4	28.4	3	9.5
		14.5-14.7	84.56	58.4	28.8	3	9.6
		34.5-35	9.36	65.5	4.01	3	1.33
Near River bed	ASHBH-02	21.75-22	7.2	44.2	1.40	3	0.46
Right Abutment	ASHBH-03	9.85-10.10	13.92	45.5	2.88	3	0.96
Intake	ASHBH-04		10.5	56.7	3.37	3	1.12
S.W(chute)	ASHBH-06	4.89-5.0	83.03	48	19.13	3	6.4

5.6. Permeability of rock mass and soils

5.6.1 Permeability of surface rock mass

Hydraulic conductivity (k) of the rock mass exposed in the study area were determined using equation (26). The result shows highly dependant on the value of average spacing and aperture of the discontinuity. Permeability of the rocks on the right abutment ranges from $2.9*10^{-1}$ to $6.1*10^{2}$ cm/s, on the left abutment ranges from $9.45*10^{2}$ to $4.3*10^{3}$cm/s and on the reservoir area the permeability ranges from $6.0*10^{2}$ to $4.6*10^{3}$ cm/s. Surface permeability of the rockmass in the project area were classified as Moderately permeable and Highly permeable as shown in the table 30.

Table 31 Hydraulic conductivity (k) of rock mass on the surface of the study area using (Bell, 2007) equation.

Location	Observation section	Avg. Spacing (cm)	Avg.Aperture, e (cm)	Gravity, g (cm/s^2)	Viscosity of water (cm^2/s)	Permeability (cm/s)	Classification of permeability according to (Bell, 2007).
Left abutment	LAMS1	10	0.15	980	$1*10^{-2}$	$0.27*10^{-1}$	Highly permeable
	LAMS2	15	0.5	980	$1*10^{-2}$	$6.8*10^{-1}$	Highly permeable
	LAMS3	18	1.53	980	$1*10^{-2}$	$1.6* 10^{3}$	Highly permeable
Right abutment	RAMS1	28	0.1	980	$1*10^{-2}$	$2.9*10^{-1}$	Highly permeable
	RAMS2	17	1	980	$1*10^{-2}$	$4.8*10^{2}$	Highly

							permeable
	RAMS3	23	0.65	980	$1*10^{-2}$	$9.7*10^{-1}$	Highly permeable
Reservoir Area	RRMS1	48	0.55	980	$1*10^{-2}$	$2.8*10^{-1}$	Highly permeable
	RRMS2	16	2	980	$1*10^{-2}$	$4.1*10^{3}$	Highly permeable
	RRMS3	19	1.12	980	$1*10^{-2}$	$6.0*10^{2}$	Highly permeable

5.6.2 Permeability of subsurface rock mass and packer test analysis

A packer test for rock mass and a falling head permeability test for soils were used to estimate hydraulic conductivity, which was used to determine the state of the dam site's water tightness.

5.6.1.1 Falling Head Test Result

The in-situ falling head permeability test was used to assess the hydraulic conductivity of the highly fractured rocks and soils at the dam site. As a result, the test was carried out at three boreholes (ASHBH-02, ASHBH-03, and ASHBH-05) in the right abutment of the dam. The test results revealed that hydraulic conductivity ranges from $1.09*10^{-1}$cm/sec to$1.43*10^{-0}$cm/sec, in the class of pervious material according to USBR Rating (1987) .

Table 32 Falling head test result for soil samples

Borehole ID	Test section(m)	Permeability value (cm/s)	USBR Rating (1987)
ASHBH-02	6-11	$2.38*10^{-1}$	Pervious
	12-17	$1.31*10^{-0}$	Pervious
	18-23	$1.43*10^{-0}$	Pervious
ASHBH-03	6-11	$1.28*10^{-1}$	Pervious
ASHBH-05	1-6	$2.03*10^{-1}$	Pervious
	6-11	$1.09*10^{-1}$	Pervious

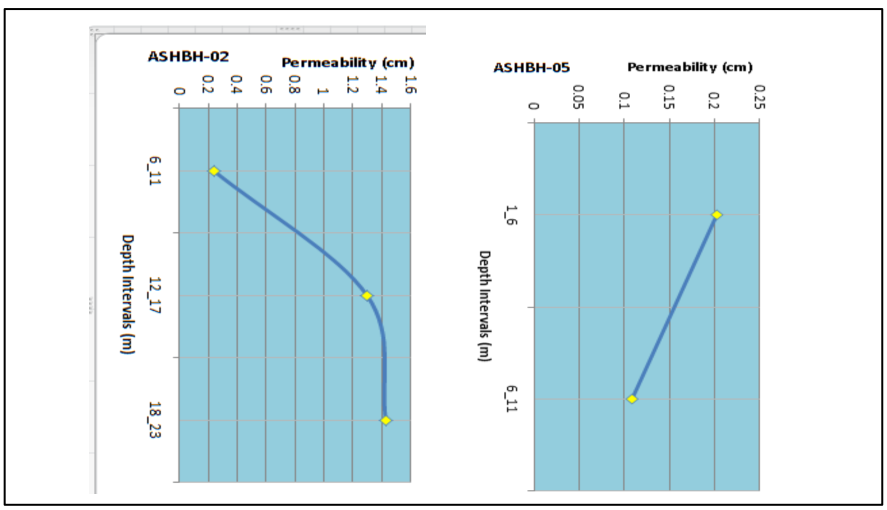

Figure 39 Graphical presentation of permeability results with depth intervals.

5.6.1.2 Packer Test Result

The hydraulic conductivity of the subsurface rock mass was evaluated at the dam site using the lugeon or packer test.

Ethiopian Construction Design and Supervision Works Corporation conducted these tests (ECDSWC, 2022). Three boreholes were used for the water pressure (Lugeon) testing at the dam's two abutments. On the left abutment, these tests were performed at boreholes of ASHBH-01, and on the right abutment, at ASHBH-03 and ASHBH-05. Table 25 shows that the average minimum and maximum lugeon values at the left abutment vary from 0 to 2 at ASHBH-01. Beside, on the right abutment at ASHBH-03 the lugeon value varies from 0 to 1 and on ASHBH-05, it is 0. This suggests that the presence of highly impermeable and closed joints within the rock mass on both abutment of the dam.

These findings indicate that the permeability of rock mass decreases with depth, and several studies have suggested that this is because of the effects of overburden (Lee and Farmer, 1993; Nappi et al., 2005; Hamm et al., 2007; and Berhane, 2013). As illustrated in Figure 26, the lugeon values along the dam axis generally decline to less than one below an elevation of 2438 m, and grouting treatment is typically needed for depths above that height.

The types of flow was further determined from the packer test data. The features of discontinuities and grouting types can be determined using the flow type. Thus, the dominating flow types at the left abutment are washout (40%), void filling, laminar, and dilatation, and turbulent flows were not recorded. Laminar and dilation flows are dominant in the right abutment, with minor portions of turbulent flow.

The laminar flow in the right abutment indicated the presence of parallel joint opening with low lugeon values. In addition laminar flow occurs when the Lugeon value of a rock mass is independent of the test pressure. In the case of dilation similar hydraulic conductivities were observed at low and medium pressures and much greater values at the maximum pressure (Houlsby, 1976). On the other hand, turbulent flow type shows the presence of either open joints with high discharge or tight joints with low discharge (Ajalloeian, 2013). Similarly, on the left abutment void filling observed in the left abutment indicated that presence of the larger joint aperture in the rock mass. In addition, void filling behavior indicated that during the test water is progressively filling isolated/non-persistent open discontinuities or swelling occurs in the discontinuities (Houlsby, 1976). Washout behaviour is observed dominantly at the left abutment. The permeability was classified according to Fell et al. (2005) where one Lugeon is equivalent to 1.3 x 10^{-5} cm/sec.

Table 33 Permeability results and representative lugeon value from packer test

Location	Borehole -ID	Test section	Representative lugeon value	Flow pattern	Permeability Class (Fell et al., 2005)	Permeability of rocks(cm/s)	Condition of rockmass discontinuity
Left abutment	ASHBH-01	5.7-10.1	2	Dilation	Moderate	$2.78*10^{-5}$	Tight
		10-15	0	Void filling	Low	$1.07*10^{-6}$	Very tight
		15-20	2	Washout	Moderate	$2.99*10^{-5}$	Tight
		20-25	0	Laminar	Low	$5.21*10^{-6}$	Very tight
		31-36	1	Washout	Low	$1.69*10^{-5}$	Very tight
Right abutment	ASHBH-03	11-16	0	Laminar	Low	$6.52*10^{-6}$	Very tight
		16-21	0	Laminar	Low	$3.94*10^{-6}$	Very tight
		21-26	0	Dilation	Low	$4.99*10^{-6}$	Very tight
		30-35	1	Dilation	Low	$9.91*10^{-6}$	Very tight
	ASHBH-05	10-15	0	Turbulent	Low	$8.73*10^{-7}$	Very tight

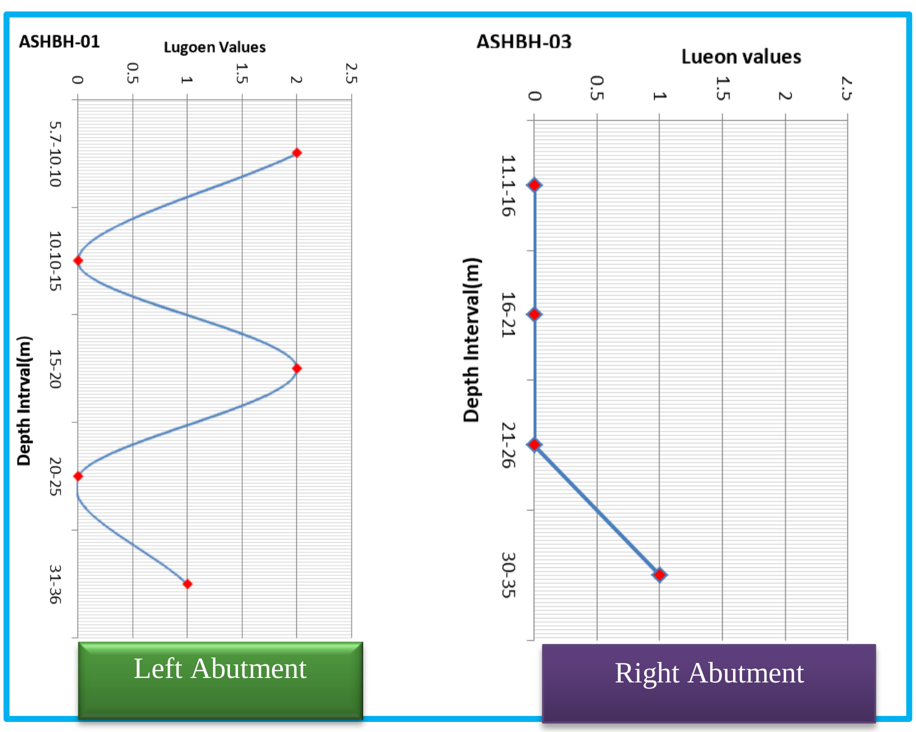

Figure 40 Graphical presentation of permeability results at borehole 01 and 03 with depth intervals.

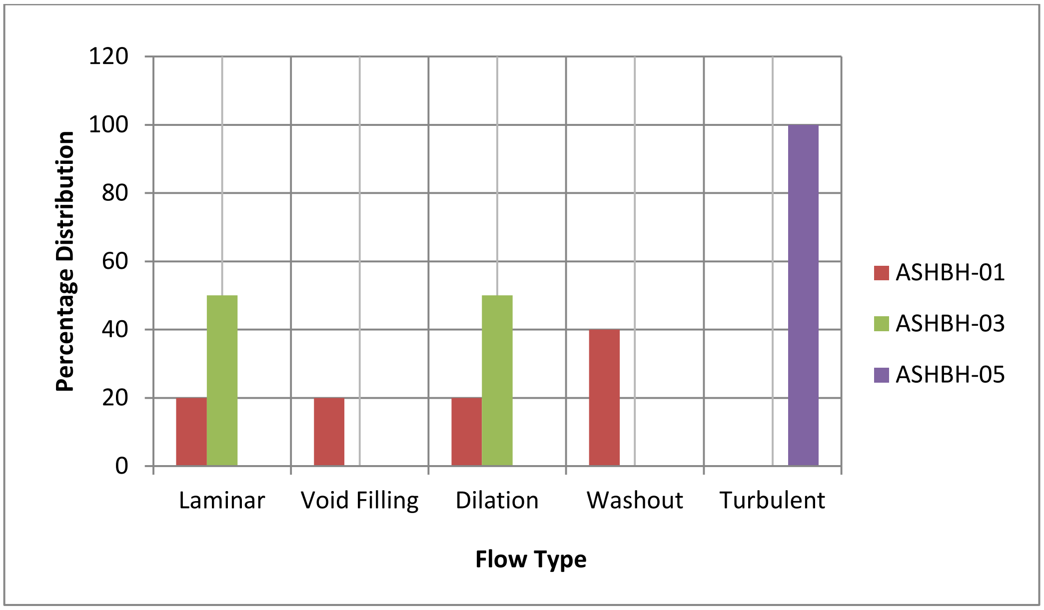

Figure 41 Relation between representative lugoen value and depth at borehole ASHBH-01 and ASHBH-03.

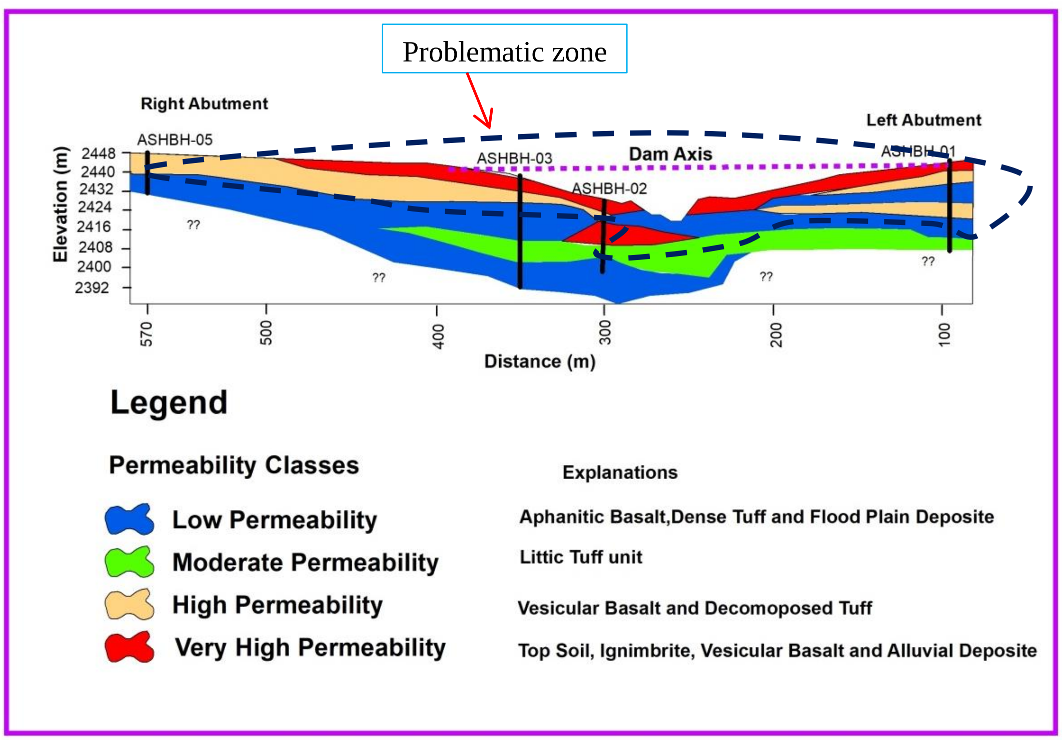

Figure 42 Permeability of rock mass along the Dam axis through integration of surface and subsurface permeability data.

5.7 Engineering Geological Map and Cross-section

To characterize the dam site's, including the distribution of different soil and rock types, as well as to provide a full picture of the area's geology, an engineering geological map should be created (Bell, 2007). The engineering geology map of the dam site is created at a scale of 1:5000. The results of the categorization of the surface soil and rock masses are utilised to produce the engineering geological map at the dam site. Based on the rock mass categorization, the engineering geological cross-section is created. Figure 44 and Figure 45 below, respectively, show the resulting engineering geology map and cross-section respectively.

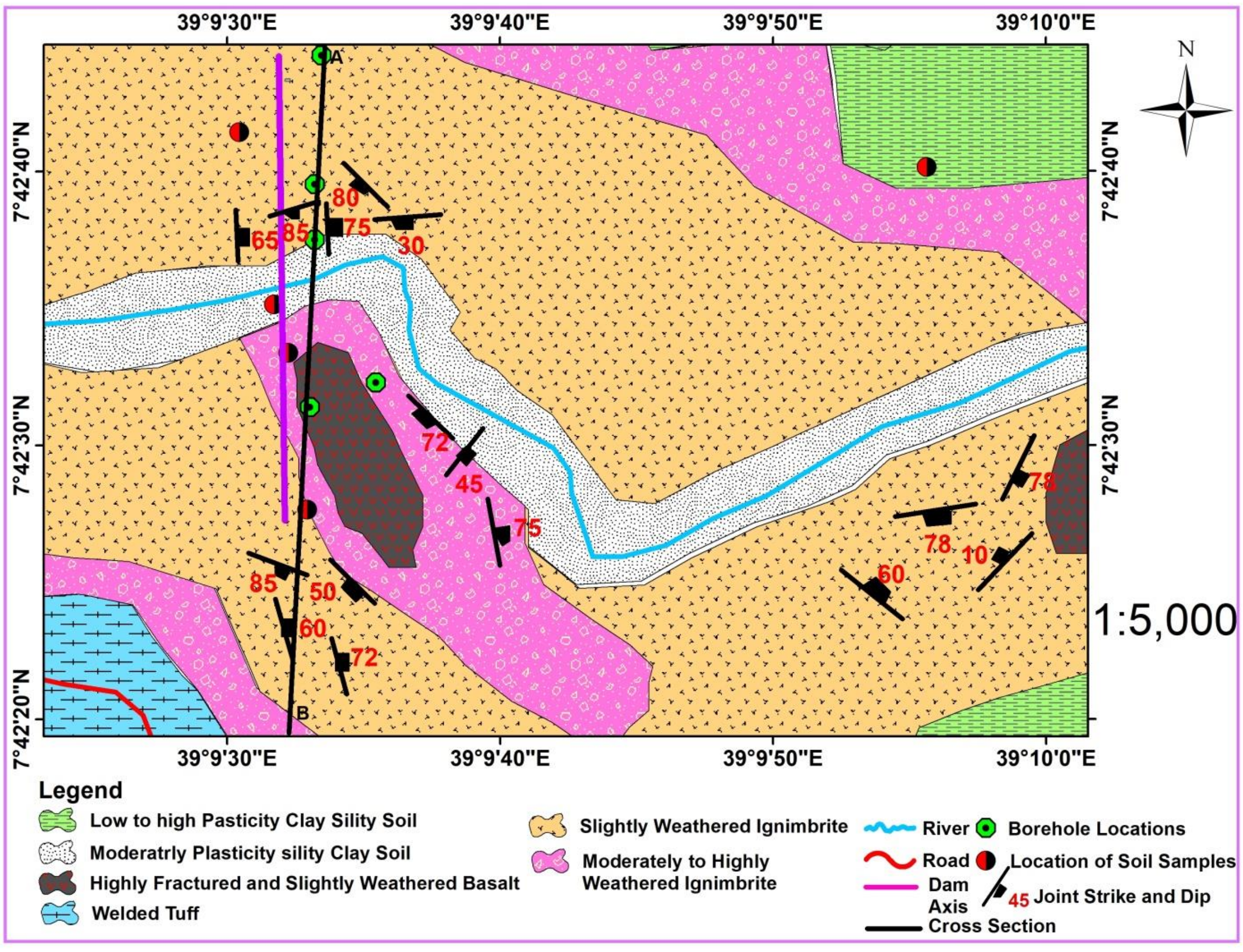

Figure 43 Engineering geological map of the study area at a scale of 1:5000.

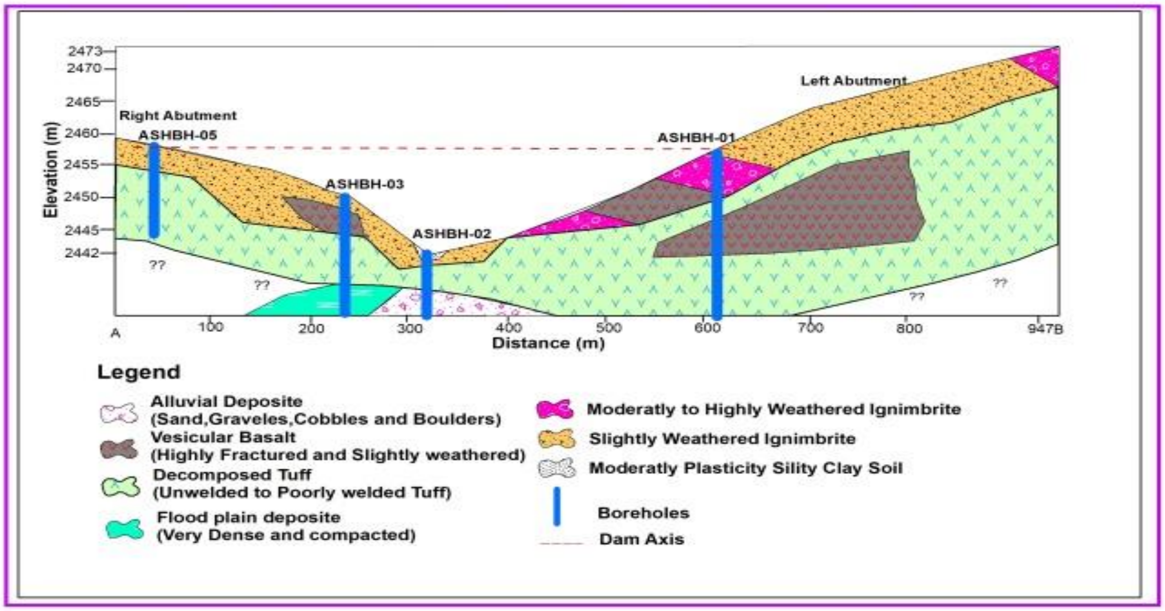

Figure 44 Engineering geological crossection a long the dam axis on AB line.

5.8 Slope Stability Analysis of the Study Area

5.8.1. Structurally (Discontinuity) Controlled Slope Sections

The structural (discontinuity) controlled and non-structural (rock mass) controlled slope portions have been determined as the crucial failure slope sections. Based on the discontinuity surveying the left abutment slope section 1 (LASS1), and the right abutment slope section 1 (RASS1) are structural controlled slope sections, while the reservoir area slope section 1 (RRSS1) is non-structural controlled slope sections.

5.8.1.1 Kinematic Analysis .

In order to perform kinematical analysis for the structurally controlled slope failure, Dips 6 software was used to examine the slope sections, which are located at the study area.There is prerequisite for the occurrence of planar mode of failure along joint (JS2) at the right abutments of dam, toppling modes of failure are not anticipated in both the left and right abutment. On the stereonet are also drawn a daylight envelope and a friction angle cone that corresponds to the angle of shear resistance (Figure 45). While friction angle along the failure plane was measured using RocData software, dip and dip direction of joints and slope were determined on-site (Table 33). Table 33 lists the specific input parameters used in the Dips software.

Table 34 Input parameters used in Dips software for kinematic analysis.

Slope section	Slope orientation (dip/dip direction(°)	The orientation of discontinuity (Dip/ Dip direction) (°)			Friction angle	Output Possible mode of failure
		JS1	JS2	JS3		
RASS1	40/160	65/90	30/190	85/130	35.23	planar mode of failure (JS2)
LASS1	65/100	72/200	75/80	42/130	28	Planar mode of failure (JS3) and wedge failure (JS1,JS2,JS3)
Where **JS1** is joint set one, **JS2** is joint set two, **JS3** is joint set three , **RASS1** and **LASS**1 are right and left abutment slope section						

As a result, the wedge failure and planar mode of failure were kinematically analysed at the left abutment's LASS1 slope section. The results of the study show that joint set 3 (JS3) caused a planar mode of failure at this slope section, and wedge failures occurred at (JS3 and JS2) and (JS3 and JS1) (Figure 48a). If we simplify the lateral limit to 20^o, the planar mode of failure were not occurred (Figure 48b). In order to calculate the factor of safety, the stability analysis of the planar mode of failure was performed using the deterministic approach by RocPlane software.

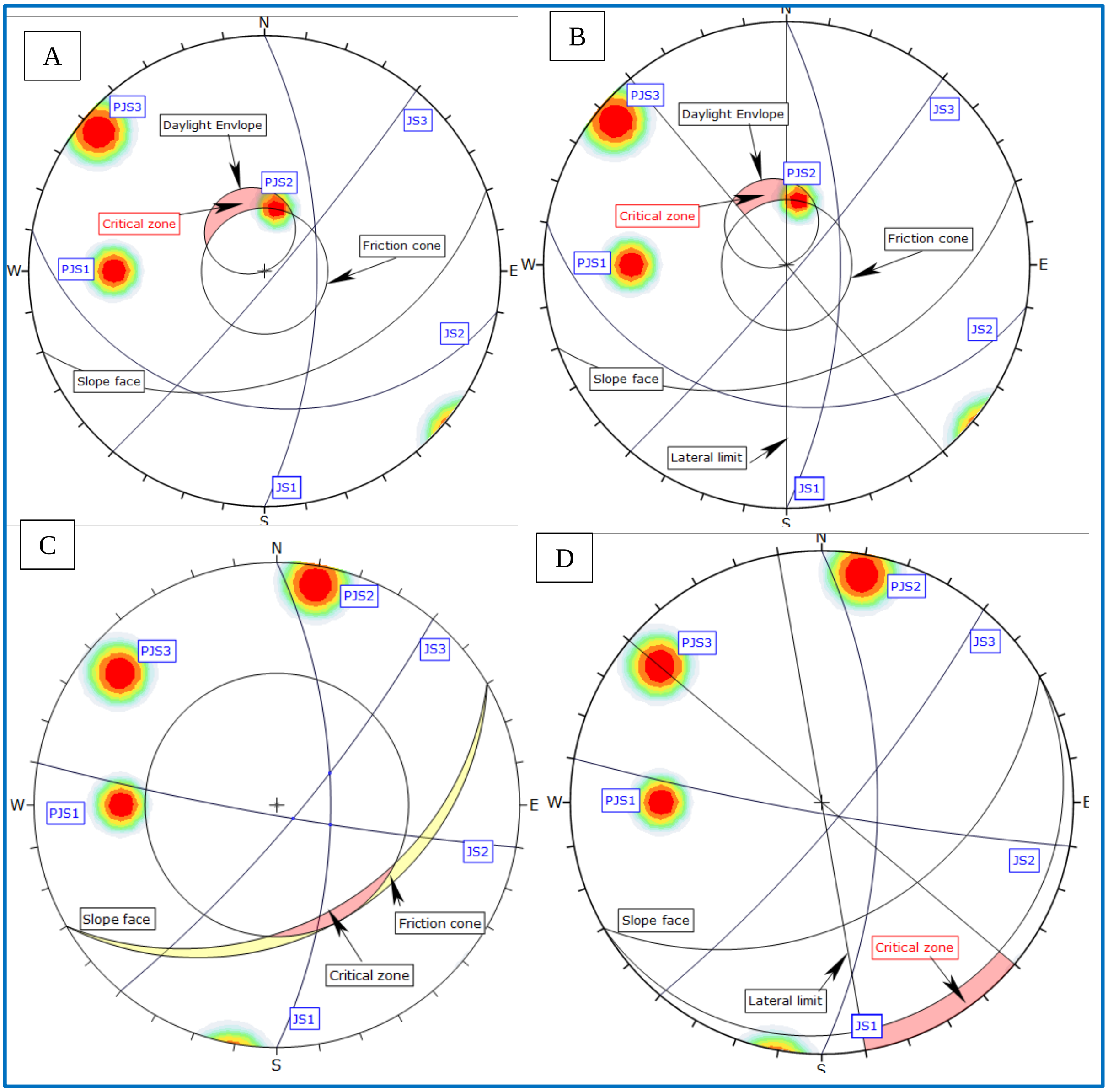

Figure 45 Kinematic analyses of right abutment RASS1(A) Checking for Planar mode of failure with no lateral limit (B) Checking for Planar mode of failure with lateral limit (C) Checking for Wedge mode of failure (D) Checking for Toppling mode of failure.

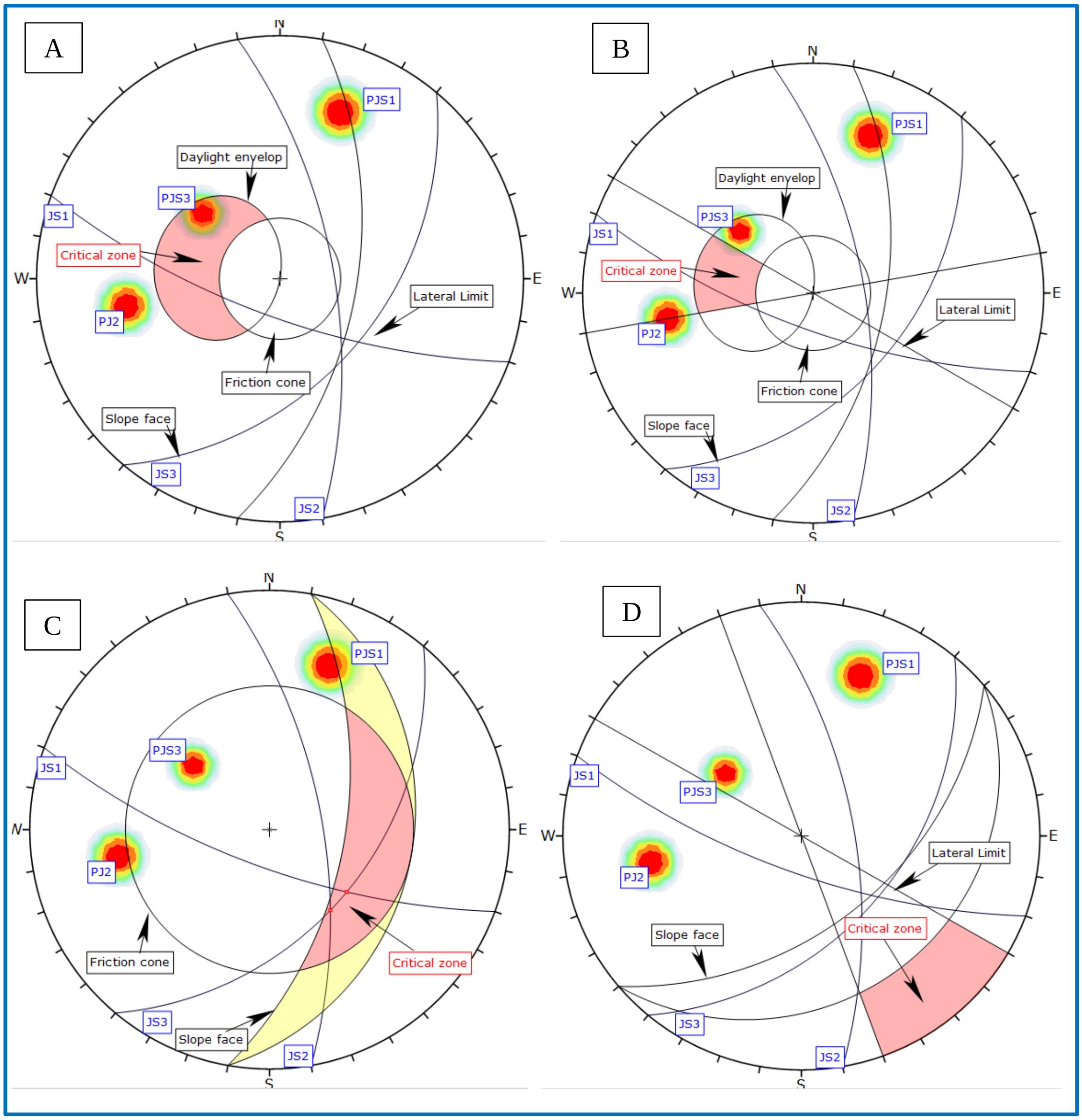

Figure 46 Kinematic analyses for left abutment at LASS1 (A) Checking for Planar mode of failure with no lateral limit (B) Checking for Planar mode of failure with lateral limit (C) Checking for Wedge mode of failure (D) Checking for Toppling mode of failure.

5.8.1.2 Stability Analysis using Deterministic Method

The findings of the kinematic analysis showed that the joint sets JS3 on the left abutment at the LASS1 induced a planar mode of failure, and joint set JS3 with JS1 and JS2 caused a wedge mode of failure. Similar to the left abutment slope section there was planar mode of failure on the right abutment at joint set JS2. The possibility of kinematic instability was therefore found, and deterministic methods were applied for additional stability study in terms of FOS (Park and West, 2001). As a result, using the RocPlane programme (Rocscience, 2004), the factor of safety (FOS) has been examined for each planar mode of failure.

Table 32 lists the input parameter utilised by the RocPlane programme. The factor of safety (FOS) was calculated using the friction angle and cohesive shear strength parameters, which were computed using the RocData programme. In the field, the slope's geometry and discontinuity orientation were established. Waviness is a factor that may be taken into account when estimating the failure plane's shear strength. It explains the failure plane surface's undulations, which may be seen at distances between 1 and 10 metres (Rocsience, 2004). The term of wavness is defined as the failure plane's average dip minus its minimum dip. The effective shear strength of the failure plane will always be higher for waviness angles larger than zero.

Table 35 Input parameters used in RocPlane software for determination of FOS at critical slope sections having a plane mode of failure

Slope section	Potential joint plane	UCS (MPa)	Input parameters of RocData software for Barton-Bandis failure criteria.					Output result of RocData software	
			JCS (MPa)	JR C	$\phi r^{(0)}$	γ(MN/m3)	H(m)	C(Mpa)	$\phi^{(0)}$
RASS1	JS2	83.6	62.7	5	32	0.023	25	0.018	38.02
LASS1	JS1	46.77	23.4	6	28.5	0.019	15	0.012	38.4
	JS2	43.5	21.75	6	27.5	0.019	15	0.011	37.15
	JS3	30.2	15.1	8	24.2	0.019	15	0.015	35.7

The FOS was calculated under both static conditions (without earthquake loading) and dynamic conditions (with the application of an earthquake load) by dry conditions when 0%, moderate saturated conditions when 50%, and fully saturated conditions when 100%, of the joints are filled with water. FOS was interpreted for study area according to Wyllie and Norrish (1996). They claimed that when FOS = 1, the driving and opposing forces are in equilibrium, and that when FOS > 1, the slope is stable, while FOS < 1, the slope is unstable. Accordingly, the analysis of findings showed that the slope was stable and the FOS is more than one at the LASS1 and RASS1 for joint sets 3 (JS3) and 2 (JS2), respectively, when dry to moderately static and dynamic conditions are assumed (Table 33). However, in these specific slope sections, the FOS decreased to less than one under fully saturated static and dynamic conditions (Table 33), which results in the slope to become unstable (Wyllie and Norrish, 1996). This showed that the area's stability was mostly dependent on water pressure.

Additionally, using RocPlane software, slope geometries at the LASS1, as shown in Figure 49a, were plotted in 2D and 3D view in figure 49b with joint set JS3 failure planes when the slope was assumed to be totally filled in water and a seismic force with a magnitude of 6.15t/m was applied to the failure plane. The lowest factor of safety for JS3 at this specific slope section, under the assumption of a completely saturated state, is 0.05, with resisting and driving horizontal forces of 2.55 t/m and 49.28 t/m, respectively (Figure 48a). Similar to this, the minimum factor of safety is 0.44 at the RASS1 for joint set JS2 as shown in Figure 49b when the slope was assumed to be fully saturated with water, when the horizontal seismic force was expected to occur, and when water pressure was applied to the failure plane with magnitudes of 40.63t/m and 357.32t/m respectively. Furthermore, the analysis result at the right abutment slope section 1 (RASS1) for joint set JS2 showed that the FOS is 0 with resisting and driving a horizontal force of 0t/m and 255.99t/m, respectively, when the slope were subject to horizontal seismic acceleration with magnitude of 40.63t/m and when the slope were assumed to be fully saturated or water pressure applied to the failure plane with magnitude of 404.10t/m.

Table 36 The factor of safety determine at critical slope sections on right abutment

Slope section	Potentioal failure plane	FOS					
		Static			Dynamic		
		Dry	Moderately	Fully Saturated	Dry	Moderately	Fully Saturated
RASS1	JS2	2	1.62	0.56	1.67	1.32	0.44
LASS1	JS3	Dry	Moderately	Fully Saturated	Dry	Moderately	Fully Saturated
		1.74	1.39	0.23	1.46	1.14	0.05

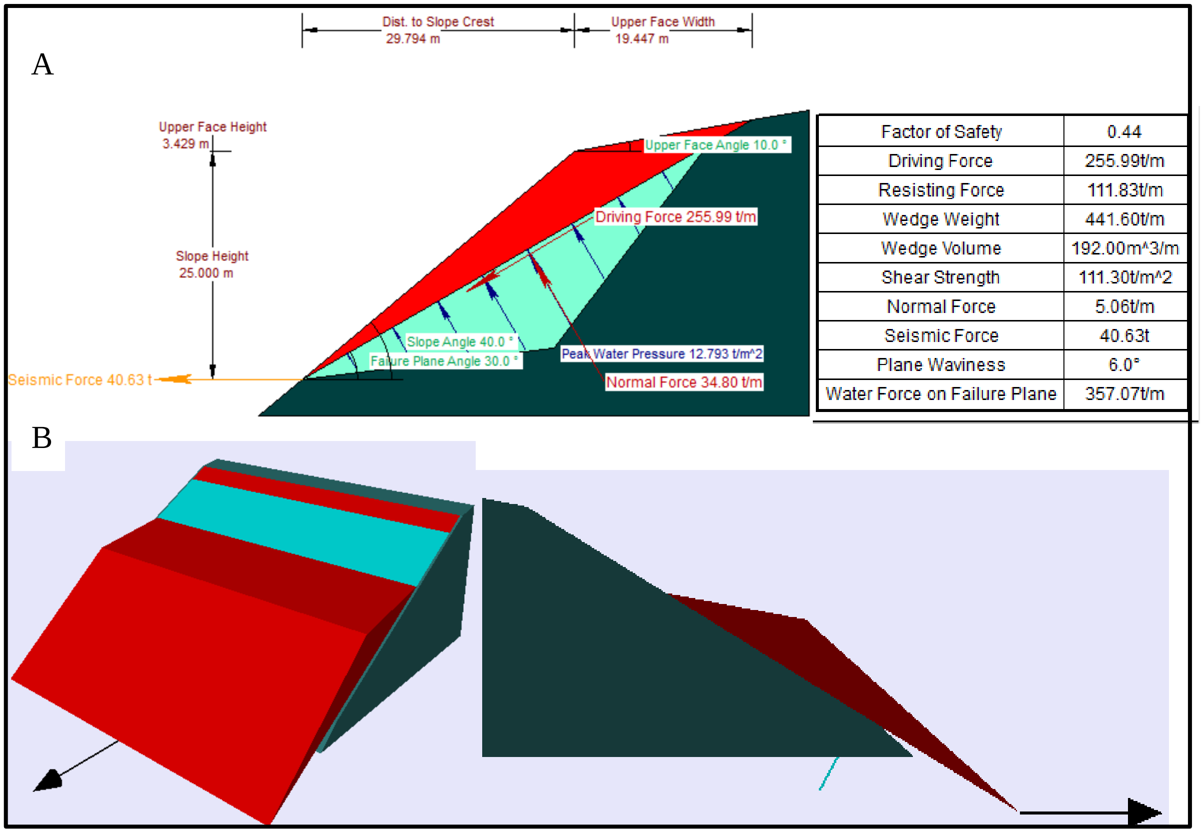

Figure 47 Slope stability analysis results from RocPlane software under dynamic fully saturated condition at the right abutment RASS1 slope section showing the 2D side view with forces acting on failure plane J2 (A). Side and perspective 3D view of slope section (B).

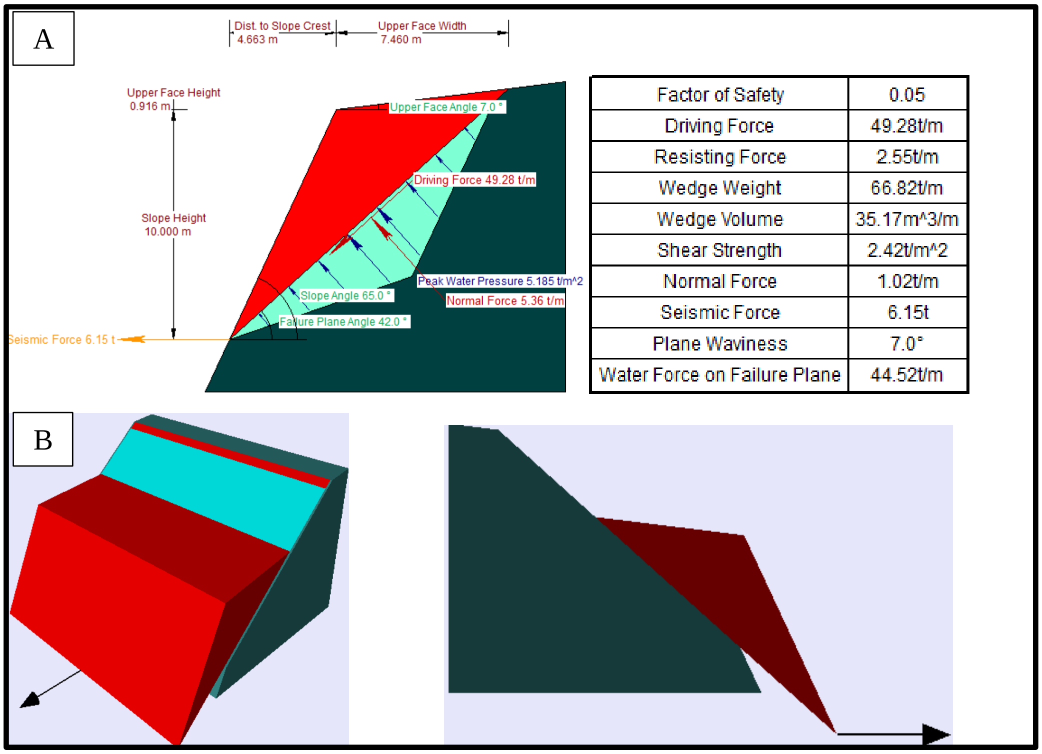

Figure 48 Slope stability analysis results from RocPlane software under dynamic fully saturated condition at the right abutment RASS1 slope section showing the 2D side view with forces acting on failure plane J2 (A). Side and perspective 3D view of slope section (B).

Table 37 FOS for wedge mode of failure on the left abutment.

Slope section	Potential failure plane	FOS					
		Static			Dynamic		
		Dry	Moderatel y	Full Saturated	Dry	Moderately	Full Saturated
LASS1	JS3 and JS1	5.72	3.74	2.33	5	3.3	2.13
	JS3 and JS2	8.7	8.5	5.1	7.6	7.4	4.8

FOS for wedge modes of failure on the left abutment at slope section LASS1 determined by swedge software were shown on the table 34. Accordingly, the analysis's findings showed that the slope was stable and the FOS is more than one for both wedge mode of failure JS1 with JS3 and JS2 with JS3, when dry and saturated static and dynamic conditions are assumed.

However, in these specific slope sections, the FOS decreased under saturated static and dynamic conditions.

The lowest factor of safety for JS3 with JS1wedge failure at this specific slope section, under the assumption of a completely saturated and dymamic state, is 2.13, with resisting and driving horizontal forces of 859.05 t/m and 402.19 t/m, respectively (Figure 50a). Similarly for JS3 with JS2 wedge failure under the assumption of a completely saturated and dymamic state, is 4.8, with resisting and driving horizontal forces of 859.05 t/m and 402.19 t/m, respectively

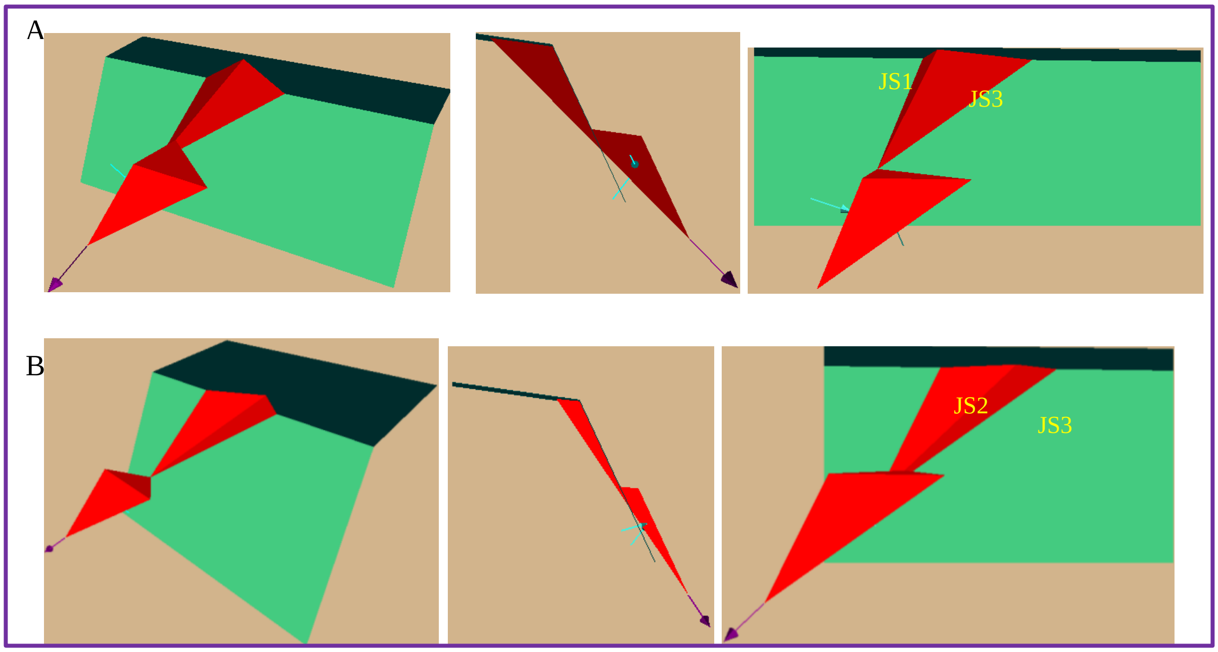

Figure 49 Wedge modes failure along JS3 with JS1 (A) and along JS3 with JS2 (B) at different view on the left abutment.

5.8.2 Stabilization Method for Left and Right Abutment Slope

According to the analytical results, the slope was generally found to be unstable under saturated conditions and stable under dry to moderately dry conditions at both the LASS1 and RASS1 slope sections. This showed that, in contrast to seismic activity, pore water pressure considerably contributed to the instability of these specific slope sections. The geometry of the slope and the direction of the discontinuity were the additional factors affecting the stability of these specific slope sections. Therefore, these specific slope portions required appropriate corrective action to avoid the failure of the dam abutments.

The proposed stabilization methods are modifying the slope geometry and constructing drainage systems to improve the FOS. The natural slope angle of the right abutment is 40^0 as shown in the figure 46 and from the kinematic analysis the maximum safe angle for slope section RASS1 was 33^0. Similarly the maximum safe angle for slope section LASS1 was 49^0 and 48^0 for planar and wedge mode of failure respectively. Therefor cut the slope with maximum safe angle makes the slope stable. The drainage system also reduce the weight and anticipated pore water pressure by free exit of water entered in the slope

5.8.2 Stability Analysis for non-Structurally (Rock mass) Controlled Slope Section

The stability analysis of highly weathered and fractured slope sections of the reservoir area at RRSS1 was carried out using Limit Equilibrium Method (LEM). The LEM methods are based on force and moment equilibrium .

5.8.2.1 Slope Stability Analysis by LEM

Through the calculation of the factor of safety under various anticipated conditions, including dry condition, before the impoundment of water in the reservoir and saturated condition, after the impoundment of water into the reservoir, under static and dynamic conditions, was carried out. The factor of safety determined under static condition represents the stability status without considering the effect of earthquake load while the effect of seismic/earthquake load was taken into account for the factor of safety determined under dynamic condition.

The limit equilibrium stability study was carried out using slide software and the GLE/Morgenstern-Price technique, with the shear strength parameters, rock unit weight, and slope geometry taken into consideration as input parameters (Table 38). The unit weight of the rock was established in the lab and the shear strength parameters (cohesion and friction angle) of the rock used in the analysis were derived from Hoek-Brown failure criteria using RocLab software (Table 14). In the field, measurements of the slope's height and slope angle were also made. During the stability analysis, external loads including groundwater conditions and horizontal seismic acceleration were also taken into account. The research area was discovered to be in seismic risk zone, and analyses took into account the horizontal seismic load coefficient with magnitude (α) = 0.092g (ES EN 19981: 2015). Table 38 lists the input parameters utilised in the analysis.

Figure 50 Unstable slope section in the reservoir area RRSS1.

Table 38 Input parameter of slide software for the slope section on the reservoir area at RRSS1.

Material	Input parameters			Slope geometry		α (g)
	c (MN/m2)	ϕ(°)	γ (kN/m3)	Height (m)	Angle(°)	
Ignimbrite	2.712	31	23.45	25	30	0.092
Basalt	2.6	28.27	27.3	25	30	0.092

The analysed result from slide software both at static and dynamic dry condition were stable or FOS were greater than one. However FOS become less than one, when the area was saturated at both satic and dynamic condition. The result indicated that, the stability of slope section is highly subjected to the water entered to the slope than the horizontal seismic activities.

Table 39 FOS calculated from slide software for reservoir slope section.

Slope section	FOS					
	Static			Dynamic		
	Dry	Moderately Saturated	Full Saturated	Dry	Moderately Saturated	Full Saturated
RRSS 1	1.33	0.68	0.654	1.06	0.55	0.502
Where **RRSS1** is right reservoir slope section one						

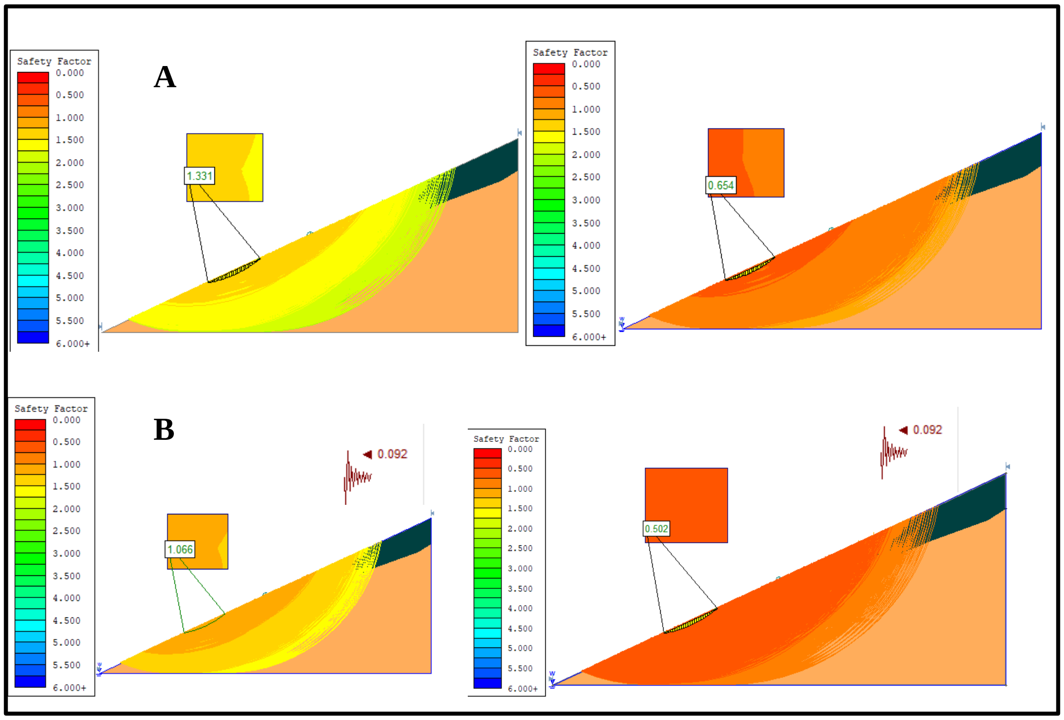

Figure 51 Slope stability analysis using limit equllibrium method by slide software on the reservoir slope sections at static conditons (A) and dynamic condition (B) for both dry and saturated conditions.

5.8.2.2 Slope Stability Analysis by FEM

To confirm the stability of the particular slope sections under various anticipated conditions, the slope stability analysis of RRSS1 slope sections was further evaluated using the finite element method in terms of the critical strength reduction factor (SRF). The critical strength reduction factor is equivalent to the "safety factor" of the slope (Pandit et al., 2016).

The stability examination in this method was done utilizing Phase2 version 8.0 software. The shear strength reduction choice in Phase2 software was utilized in order to perform a finite element slope stability analysis and compute a critical strength reduction factor. With the exception of Young's modulus (Erm) and the Poisson's ratio (v), the input parameters used in this method are identical to those used in the limit equilibrium method. The young's modulus (Erm), which was utilized in the analysis, was assessed from disturbance factor (D), geological strength index (GSI) and intact modulus (Ei), while the Poisson's ratio (v) was taken from puplished works by taking 0.25 for this study (Gercek, 2007) . The input parameters used in stability analysis by FEM were given in Table 41.

Table 40 Input parameters for finite element stability analysis to calculate critical SRF

Rock units	Input parameters					Slope geometery		α (g)
	C (MPa)	ϕ (°)	γ (KN/m3)	Erm (MPa)	V	Height (m)	Angle (°)	
Layer 1 (Basalt)	2.71	31	27.3	6997	0.3	25	30	0.092
Layer 2 (Ignimbrite)	2.6	28.3	23.5	4181	0.25	25	30	0.092

The analyses result showed that, the critical strength reduction factor (SRF) at the reservoir slope section 1 (RRSS1) are 1.35 and 1.15 when the slope was assumed as static dry and dynamic dry conditions respectively (Table 42 and Figure 52). In addition, when the slope was assumed to be in a saturated condition, the critical strength factor are 0.7 and 0.49 during static and dynamic conditions respectively (Table 43 and Figure 52). The critical SRF or FOS is less than one and this indicated that slope was unstable while when the slope is assumed to be at dry conditions, the critical SRF or FOS was greater than one and the slope was stable according to Christian (2004).

Table 41 Estimated strength reduction factor by Phase2 software under static and dynamic conditions.

Slope section	Critical **SRF** under different anticipated conditions			
	Static		Dynamic	
	Dry	Saturated	Dry	Saturated
RRSS1	1.35	0.7	1.15	0.49
Where **RRSS1** is right reservoir slope section one				

From, the factor of safety results determined by FE were in a very good agreement with those computed by the limit equilibrium methods. Furthermore, the slip failure surfaces were some difference for both techniques. As stated in Cheng et al. (2007) the values of E and v have a very small influence on the computed factor of safety values and the location of critical failure surface by FEM using Phase2 software. Generally , it can be concluded that the results of both

FE and LE methods were in good agreement under different anticipated conditions and when simple slope geometry and heterogeneous material were considered.

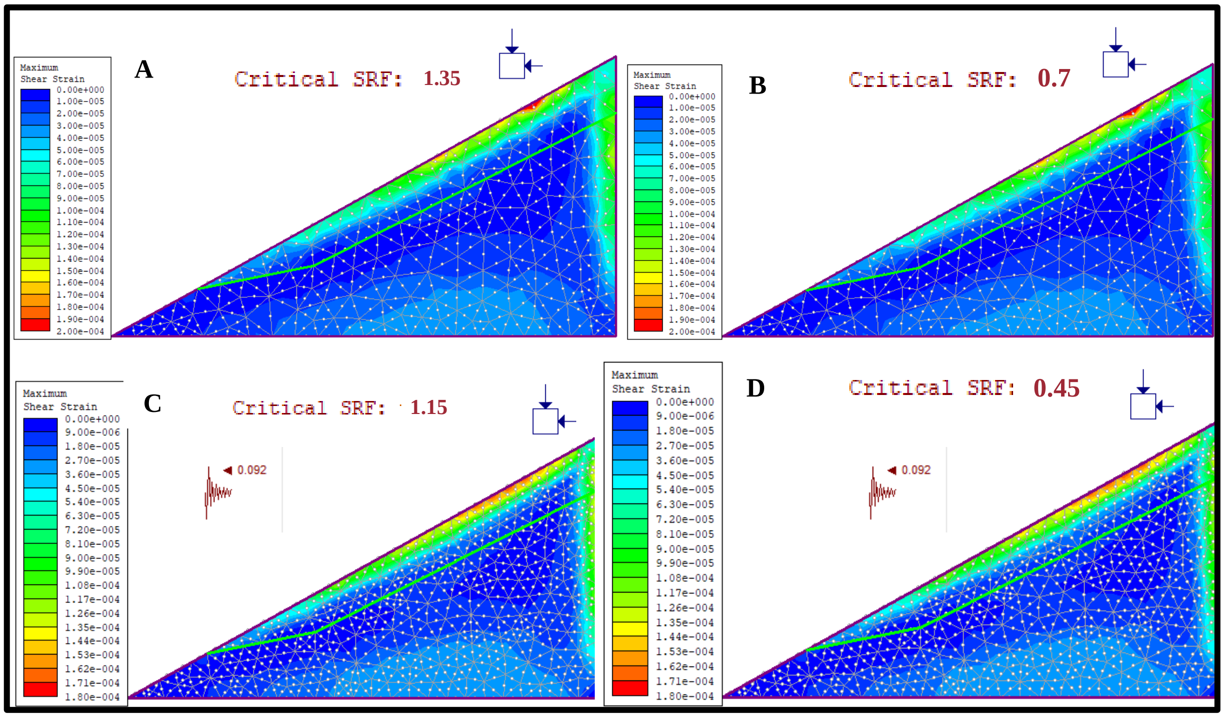

Figure 52 Slope stability analysis result from finite element method using the Phase2 software for reservoir area at RRSS1 under A) static dry condition, B) static saturated condition, C) dynamic dry condition and D) dynamic saturated condition

The method of stabilization recommended for the slope section is modifying the slope geometery with the slope angle 24^0 and 20m slope height and utilize drainage holes. Additionally grouting method is used for increasing the shear resistance of the slope. If five end anchored with 200KN capacity and 10m length was used FOS become greater than one as shown in the figure 53, but this method is costy compared to the other methods.

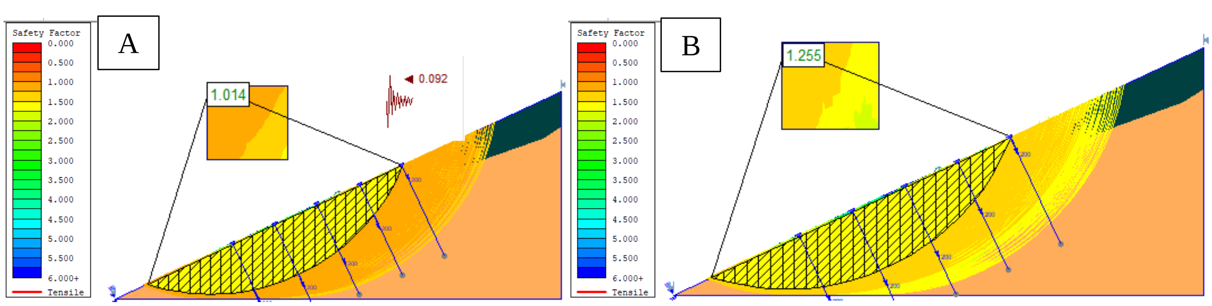

Figure 53 FOS is greater than one with anchore at dynamic (A) and static condition (B).

CHAPTER SIX

6. CONCLUSION AND RECOMMENDATIONS

6.1. Conclusion

Engineering geological characterization the dam site can be investigated and evaluated using integrated field and laboratory assessments of engineering geological conditions. The study's primary findings led to the following conclusions;

- Alluvial and residual soils, which are predominately silt soils, and ignimbrite rocks are the dominant lithological units in the dam site and reservoir area. Basaltic rocks and tuff rocks also found in some part of the area. The area is characterized by gently to moderately sloppy area.
- The rock masses that make up both abutments are found to be moderately to slightly weathered, highly fractured, and joined rocks with three sets of tectonic joints. The majority of joint set orientations favour the leakage path as it crossed the dam axis in a direction that is almost parallel to the river flow.
- The RQD estimated from joint volumetric count (JV) revealed that the rocks exposed at both abutment slopes have poor to fair rock qualities and fair to good in the reservoir area. Similarly, the RQD determined from core logs revealed that for left abutments the average RQD falls poor to good rock and for the right abutment RQD value falls from poor to fair. Generally the RQD value from different drilling area ranges from poor to good quality as the rock mass forms the abutments of the dam was characterized by high degree of fracturing and moderately weathering.
- According to in-situ Schmidt hammer values, the strength of intact rock falls in the range of 61.65 MPa to 109.39 MPa for the right abutment and 24.54 MPa to 54.95 MPa for the left abutment. The UCS value ranges from 21.12 MPa to 123.12 MPa as determined from point load laboratory testing. As a result, the rock that makes up the dam's foundation, abutments and reservoir has a very low to medium strength.

- From the rock mass rating, the quality of the rock masses at the dam site ranges from fair to good, with RMR values between 48 and 70. The GSI value determines from RMR value, which varies from 50 to 72. The calculated cohesion and friction angle varies from 2.7 to 4.97 and from 27.92 to 34.79, respectively, using GSI and UCS values. Furthermore, the modulus deformation ranges from 4.2 to 54.
- The findings of the kinematic analysis showed that the slope was possibly unstable and planar modes of failure at the RASS1, because joint set two (JS2) and planar and wedge modes of failure at the LASS1,because of joint set (JS1,JS2,JS3) at left and right abutments, respectively.
- The left and right abutment of the dam is unstable under both static and dynamic saturated conditions with a safety factor of less than one, according to deterministic slope stability analysis. Contrarily, the right and left abutment of the dam has a safety factor greater than one and is stable under both static and dynamic dry to moderately dry condition circumstances. Therefore, in comparison to seismic activity, pore water pressure greatly contributed to the destabilisation of these specific slope portions.
- The limit equilibrium method was used to perform stability assessments of the RRSS1 slope section under various situations at the reservoir area. The analysis's findings showed that the slope portion of the RRSS1 was unstable under moderately to fully saturated conditions and stable under dry conditions both in static and dynamic conditions ones. Therefore, in destabilising this specific slope portion, the impacts of pore water pressure are more significant.
- According to the results of the hydraulic conductivity analysis based on surface discontinuity spacing and aperture data, the rock mass has moderate to high permeability values at both the dam's abutments and in the reservoir area. As a result, considerable leakage will be anticipated following the impoundment of the reservoir, particularly through both dam abutments.
- There have been two types of in-situ permeability tests performed: a falling head test for the topmost rock that has undergone complete weathering and a packer test for the rock mass below the surface. The classification obtained from the "falling head" test indicates that pervious in each rock units. The Lugeon value varies from 0 to 2 with a

class range of impervious to semi pervious rock mass, according to the packer test results. The permeability of the rock mass, however, decreases with depth.

- The soil thickness at the dam site some parts of the reservoir area ranges from 0.40m to 2.8m. A soil laboratory test revealed that clayey silt soils predominate in the research area, with an average liquid limit of larger than 50%, indicating that the soils have a significant plasticity properties. A test for soil permeability showed that the soils in the reservoir area and dam axis have relatively low permeabilities and can hold water after impoundment. Because of this, the reservoir location has extremely little seepage and is nearly watertight.

6.2 Recommendations

The dam site foundation at mainly characterized clayey silt organic and silty clay soil and 0.5-2m highly to completely weathered ignimbrite rock must be excavated and put the foundation on fractured ignimbrite rock after ground improvement with grouting. The result from the bearing capacity of geotechnical units possess very low safe bearing capacity and different bearning capacity at right and left abutment. Therefore, proper ground improvement including consolidation grouting up to the depth of 25m must be conducted.

The results of the water tightness analysis indicate that there are several conditions under which the dam site is low to high permeable. The following are some ground improvement techniques for this:

- The results of the discontinuity survey show that the vertical and sub-vertical columnar joints dominate the ignimbrite rocks on the right abutment and reservoir areas. Discontinuity conditions such as spacing, opening, infilling, and persistence may facilitate seepage through the foundation. In order to reduce the possibility of seepage through the discontinuities, the area should be lined with an impervious material, such as clay blanket.
- The falling head test on the rock unit with the highest degree of weathering revealed that the unit is pervious. Grouting suggested to improved the water tightness problem caused by this pervious unit up to a depth of 25 at ASHBH-02, up to 20m depth at ASHBH-01 and up to 12m at ASHBH-03.
- There are zones of low to moderately permeable rock mass, according to the packer test result. Therefore, curtain grouting is required in these permeable zones. Particular focus should be applied to the river beds at ASHBH-02 because there is alluvial deposite and extend up to highly fractured and weathered ignimbrite rocks at a depth of 25 metres.

Some parts of the area is not stable, according to the results of the stability analysis. This study offered the following stabilization method.

- The planar mode of failure was discovered at the slope sections LASS1 and RASS1. Consequently, changing slope geometry, rockbolts, anchors and drain holes are suggested as corrective solutions to stop the sliding and stabilise those slope parts. The stability analysis result for the RRSS1 slope sections showed that the slope is unstable primarily under conditions of full saturation. In order to decrease the slope angles in these slope sections, the study advised first removing the failing material, followed by the recommendation to use shotcrete to strengthen the stability of the slope. To reduce the pore water pressure that is accumulating beneath the shotcrete surface, there must be enough drain holes provided for the shotcrete surface.

- Consolidation Grouting with the intended slope geometry and a long the foundation with low bearing capacity rocks can help boost the material strength and the stability condition can be improved.

Some common issues, these are essential for the safety of the dam recommended by this study are:-

- Siltation of reservoirs is one of the major issues that contribute to reservoir falling and reduce the dam's life span, although this issue was not covered in the study. In order to analysis the reservoir siltation issues and prolong the functional life of the dam and reservoir, it is highly recommended that to study further.
- The proposed dam site is situated at the eastern flank of the main Ethiopian rift. Consequently, there is, may be indicate some horizontal ground acceleration. Therefore, it needs to give attention during the design and construction.
- Further analysis was recommended by this study for the planning and implementation of corrective procedures like caurtin and consolidation grouting, clay blanketing, rock bolts, anchors, and shotcrete.

REFERENCE

Abdulkadir, M. (2009). Assessment of Micro-Dam Irrigation Projects and Runoff Predictions for Un-gauged Catchments in Northern Ethiopia, Ph.D. Dissertation, Muenster University, Germany.

Abramson, L., Lee, T., Sharma, S. and Boyce, GM. (2002). Slope Stability Concepts. Slope Stabilization and Stabilization Methods, Second edition, published by John Willey and Sons, Inc., 329- 461.

Abrehet, M. (2017). Embankment Dam Safety Monitoring through Seepage Analysis. Unpublished, MSc thesis, Addis Ababa University, Addis Ababa Ethiopia

Adamo, N., Al-Ansari, N., Sissakian, V., Laue, J. and Knutsson, S. (2020). Dam safety problems related to seepage. *Journal of Earth Sciences and Geotechnical Engineering*, *10*(6), pp.191-239.

Ajalloeian, R. and Azimian, A. (2013). Geotechnical engineering assessment of the nargesi damsite, Southwest Iran. *Geotechnical and Geological Engineering*, *31*, pp.1369-1392.

Ajalloeian, R., Habibi., V., Sharifipour, M. and Azimian, A. (2012). Evaluation of Engineering Geology Properties of Jamishan Dam Site with Emphasis on Its groutability. EJGE 17,2777-2793.

Allen, A. and Tadesse, G. (20030. Geological setting and tectonic subdivision of the Neoproterozoic orogenic belt of Tuludimtu, western Ethiopia. *Journal of African Earth Sciences*, *36*(4), pp.329-343.

Anon, Q. (1977). The description of rock masses for engineering purposes. *Quarterly Journal of Engineering Geology,*, *10*, 355-399.Arora, J.S., 2004. *Introduction to optimum design*. Elsevier.

Arora, K. R. (2008). *Soil Mechanics and Foundation Engineering (Geotechnical Engineering): In SI Units*. Standard publishers..

Asmelash, A. and Claudia, M. (2015). Engineering-Geological Properties of Carbonates and Shale: Their Implications for Dam Construction in Mekelle, Northern Ethiopia. Momona Ethiopian Journal of Science, 1, 64-84.

ASTM. (2001). Standard test method for determination of rock hardness by rebound hammer method. ASTM Stand. 04.09 (D 5873-00).

ASTM, A. (1995). Standard Test Method for Determination of the Point Load Strength Index of Rock, D5731-95.

ASTM, D. (1998). Standard Test Method for Specific Gravity. *American Society for Testing and Materials (ASTM)*.

Aydin, A. and Basu, A. (2005). The Schmidt hammer in rock material characterization. *Engineering geology*, *81*(1), pp.1-14.

Barani, H.R., Lashkaripour, G. and Ghafoori, M. (2014). Predictive permeability model of faults in crystalline rocks; verification by joint hydraulic factor (JH) obtained from water pressure tests. *Journal of Earth System Science*, *123*, pp.1325-1334.

Barjasteh, A. (2019). The impact of active faulting on the geotechnical properties of the Upper Gotvand Dam, southwest Iran. *Bulletin of Engineering Geology and the Environment*, *78*(2), pp.709-722.

Barton, N. (1978). Suggested methods for the quantitative description of discontinuities in rock masses. International Society of Rock Mechanics Commission on Standardization of Laboratory and Field Tests, International Journal of Rock Mechanics and Mining Sciences and Geomechanical Abstracts, 15, 319–368

Barton, N. and Choubey, V. (1977). The shear strength of rock joints in theory and practice. *Rock mechanics*, *10*, pp.1-54.

Basahel, H. and Mitri, H. (2019). Probabilistic assessment of rock slopes stability using the response surface approach–a case study. *International Journal of Mining Science and Technology*, *29*(3), pp.357-370.

Barzegari,G. (2017).Geotechnical Evaluation of Dam Foundation with Special Reference to In Situ Permeability: A Case Study. Geotech. Geol Eng. 35(3), 991-1011

Bell, F.G, (2007). *Engineering geology*. Elsevier.

Bell, A.L. (1915). THE LATERAL PRESSURE AND RESISTANCE OF CLAY AND THE SUPPORTING POWER OF CLAY FOUNDATIONS. In *Minutes of the Proceedings of the Institution of Civil Engineers* (Vol. 199, No. 1915, pp. 233-272). Thomas Telford-ICE Virtual Library.

Berhane, G., Martens, K., Al Farrah, N. and Walraevens, K. (2013). Water leakage investigation of micro-dam reservoirs in Mesozoic sedimentary sequences in Northern Ethiopia. *Journal of African Earth Sciences*, *79*, pp.98-110.

Berhanu Temesgen, et al. (1999). Landslide Hazard on the Slopes of Dabicho Ridge, Wondo Genet Area. The Case of June 18, 1996 Event. Sinet.

Bieniawski, Z.T. (1973). Engineering classification of jointed rock masses. *Civil Engineering Siviele Ingenieurswese*, *1973*(12), pp.335-343.

Bieniawski, Z.T. (1989). Engineering rock mass classifications: a complete manual for engineers and geologists in mining, civil, and petroleum engineering: New York, Wiley, xii, 251

Bishop, A.W. (1956). The use of slip circles in stability analysis of slopes. Geotechnique, 5(1), 7-17

Chen, Y., Cao, P., Chen, R. and Teng, Y. (2010). Effect of water–rock interaction on the morphology of a rock surface. *International Journal of Rock Mechanics and Mining Sciences*, *47*(5), pp.816-822.

Bowles, J.E. (1996). Foundation Analysis and Design. 5th Edition, The McGraw-Hill Companies, Inc., New York

Broch, E. and Franklin, J.A. (1972). November. The point-load strength test. In *International Journal of Rock Mechanics and Mining Sciences & Geomechanics Abstracts* (Vol. 9, No. 6, pp. 669-676). Pergamon.

Christian, J.T. (2004). Geotechnical engineering reliability: How well do we know what we are doing?. *Journal of geotechnical and geoenvironmental engineering*, *130*(10), pp.985-1003.

Daniel, G. (2017). Engineering rock mass characterization - An integrated approach through Rock Mass Classification and Seismic Refraction - A case of TAMS Hydroelectric Power Dam Project in Gambella, Ethiopia. Unpublished, MSc thesis, Addis Ababa University, Addis Ababa Ethiopia. pp125

Deere, D.U. (1968). Geological consideration. *Rock mechanics in engineering practice*.

Deere, D.U., Miller, R.P. (1966). Engineering classification and index properties for intact rocks. Tech Report. Air Force Weapons Lab., New Mexico, No. AFNLTR, pp. 65-116. Kirtland

Duncan, J.M. (2000). Factors of safety and reliability in geotechnical engineering. *Journal of geotechnical and geoenvironmental engineering*, *126*(4), pp.307-316.

Eberhardt, E. (2003). Rock slope stability analysis–utilization of advanced numerical techniques. *Earth and Ocean sciences at UBC*, *41*.

ECDSWC. (2022). Ethiopian Construction Design & Supervision Works Corporation Water & Energy Design & Supervision Works Sector, Unpublished Geotechnical Report

El-Naqa, A. (2000). The hydraulic conductivity of the fractures intersecting Cambrian sandstone rock masses, central Jordan. *Environmental Geology*, *40*, pp.973-982.

Fell, R., MacGregor, P., Stapledon, D., Bell, G. and Foster, M. (2015). Geotechnical engineering of dams (2nd ed), Taylor & Francis Group, London

Fell, R., MacGregor, P., Stapledon, D., & Bell, G. (2005). Geotechnical Engineering of Dams. In Geotechnical Engineering of Dams. https://doi.org/10.1201/noe0415364409

Fellenius, W. (1936). Calculation of the stability of earth dams. In *Proc. of the second congress on large dams* (Vol. 4, pp. 445-463).

Gangopadhyay, s. (1993). Geotechnical Problems of Dam Site and Their Solution With Reference To the Projects of Eastern India Proceedings: Third International Conference on Case Histories in Geotechnical Engineering, St. Louis, Missouri, June 1-4, 1993, paper No. 2.43.

Gardi, S., Al-Heety, R. & Mawlood, Z. (2013). 2D Electrical Resistivity Tomography for the Investigation of the Subsurface Structures at the Shaqlawa Proposed Dam Site at Erbil Governorate, NE Iraq.

Ghobadi, M.H., Khanlari, G.R. and Djalali, H., 2005. Seepage Problems in the Right Abutment of the ShahidAbbaspour Dam, Southern Iran. Engineering Geology, Vol. 82, Issue 2. Elsevier, Pp. 119–126

Gurocak, Z. and Alemdag, S. (2012). "Assessment of Permeability and Injection Depth at the Atasu Dam Site (Turkey) Based on Experimental and Numerical Analyses. "Bulletin of engineering geology and the Environment 71(2):221- 29 doi:10.1007/s10064-011-0400-9

Hamm, S.Y., Kim, M., Cheong, J.Y., Kim, J.Y., Son, M. and Kim, T.W. (2007). Relationship between hydraulic conductivity and fracture properties estimated from packer tests and borehole data in a fractured granite. *Engineering Geology*, *92*(1-2), pp.73-87.

Hoek, E. and Bray, J. D. (1981). Rock slope engineering. CRC Press

Hoek, E. and Brown, E.T. (2002). Practical estimates of rock mass strength. *International journal of rock mechanics and mining sciences*, *34*(8), pp.1165-1186.

Hoek, E. and Brown, E.T. (1980). Empirical strength criterion for rock masses. *Journal of the geotechnical engineering division*, *106*(9), pp.1013-1035.

Hoek, E. and Brown, E.T. (1997). Practical estimates of rock mass strength. *International journal of rock mechanics and mining sciences*, *34*(8), pp.1165-1186.

Houlsby, A.C. (1976). Routine interpretation of the Lugeon water-test. *Quarterly Journal of Engineering Geology and Hydrogeology*, *9*(4), pp.303-313.

ISRM. (1978). Rock Characterization, Testing and Monitoring – ISRM Suggested methods, Pergamon Press, Oxford, E.T. Brown (ed), pp211

Janbu, N. (1996). Slope stability evaluation in engineering practice. In *Proc., 7th Int. Symp. on Landslides, Trondheim* (Vol. 1, pp. 17-34).

Janbu, N. (1954). Stability analysis of slopes with dimensionless parameters. *(No Title)*.

Johansson. (1997). Seepage monitoring in Embankment Dams. Doctoral thesis, Royal Institute of Technology, Sweden, p 50

Johnson, K.T. (1998). Experimental determination of partition coefficients for rare earth and high-field-strength elements between clinopyroxene, garnet, and basaltic melt at high pressures. *Contributions to Mineralogy and Petrology*, *133*(1-2), pp.60-68.

Kamal, L.B.L. (2007). Investigation of water leakage mechanisms in the karst Dam site, Saman alawewa, Sri Lanka. PhD Thesis, Saga University, Saga, Japan (unpublished)

Kazmin, V. (1973). Geological map of Ethiopia (scale 1: 2,000,000). *Geological Survey of Ethiopia, Addis Ababa*.

Lee CH, Farmer I. (1993). Fluid flow in discontinuous rocks. Chapman & Hall, New York.

Leulalem, S.B., Kifle W. and Nata, T., 2016. "Geological and Geotechnical Investigations of Axum Dam Site, Tigray, Northern Ethiopia". International Journal of Scientific & Technology Researcher 4(8):84–111

Louis, C.L. (1974). Introduction to rock hydraulics. *BULL BRGM, III,* (4).

Marinos, P. and Hoek, E. (2000) November. GSI: a geologically friendly tool for rock mass strength estimation. In *ISRM international symposium* (pp. ISRM-IS). ISRM.

Mengesha, T., Tadiwos, C. and Werkneh, H. (1996). Explanation of the geological map of Ethiopia, Ethiopian institute of geological surveys. *Addis Ababa, 3,* p.79.

Merla, G., Abbate. E., Canuti, P., Sagu, M. and Tacconi, P. (1973). Geological map of Ethiopia and Somalia. Explanatory notes (1979). Consiglio Nazionale delle Ricerche, Frirenze, Ital

Ministry of Construction. (2015) Ethiopian building Standards based on Euro Norms (ES EN 19998:2015) and Design of Structures for Earthquake Resistance. Part1, General Rules and Seismic Actions for Building, Urban development and construction, Addis Ababa, pp. 1–7

Mitchell, M. J., & Parkinson, D. (1976). Fungal feeding or Oribatid mites (Acari: Cryptostigmata) in an aspen woodland soil. *Ecology*, *57*(2), 302-312.

Mohammad, S.K. (2012). Geological aspects of seepage problem and its management at Khanpur dam project, Pakistan. Journal of Himalayan Earth Sciences, 45(1):77-81

Morgenstern, N. and Price, V. (1965). The Analysis of the Stability of General Slip Surfaces. Geotechnique, Vol. 15 (No. 1), pp. 77-93

Mozafari, M., Raeisi, E. and Zare, M. (2011). Water leakage paths in the Doosti Dam, Turkmenistan and Iran. Environ Earth Sci. doi: 10.1007/s12665-011-1069-x

Nappi, M., Esposito, L., Piscopo, V. and Rega, G. (2005). Hydraulic characterisation of some arenaceous rocks of Molise (Southern Italy) through outcropping measurements and Lugeon tests. *Engineering geology*, *81*(1), pp.54-64.

Osgoui, R.R. and Oreste, P. (2010). Elasto-plastic analytical model for the design of grouted bolts in a Hoek–Brown medium. *International journal for numerical and analytical methods in geomechanics*, *34*(16), pp.1651-1686.

Palmstrom, A. (2009). Combining the RMR, Q, and RMi Classification Systems. Oslo, Norway, pp. 400

Palmstrom, A. and Broch, E. (2006). Use and misuse of rock mass classification systems with particular reference to the Q-system. *Tunnelling and underground space technology*, *21*(6), pp.575-593.

Palmström, A. (1986). The volumetric joint count as a measure of rock mass jointing. *Annals of the Israel Physical Society*, *8*, pp.1-18.

Pantelidis, L. (2009). Rock slope stability assessment through rock mass classification systems. *International Journal of Rock Mechanics and Mining Sciences*, *46*(2), pp.315-325.

Park, H. and West, T.R. (2001). Development of a probabilistic approach for rock wedge failure. *Engineering Geology*, *59*(3-4), pp.233-251.

Preene, M. (2018). Design and interpretation of packer permeability tests for geotechnical purposes. Quarterly Journal of Engineering Geology and Hydrogeology, 52(2), 182–200. doi: 10.1144/qjegh2018

Prince, T., Sound, W., West, T. R., & Cho, K. H. (2007). Rock Slope Stability of the VMT. East, 556.

Raghuvanshi, T.K. (2017). Plane failure in rock slopes–A review on stability analysis techniques. *Journal of King Saud University-Science*, *31*(1), pp.101-109.

Robin, F., Patric, M., David, S. and Graeme, B., 2005. Geotechnical Engineering of Dams.A.ABalkema Publisher Lienden, Netherlands

Rocscience. (2004). Dips 6.0, http://www.rocscience.com/software/dips

Rocscience. (2004). Rocdata 3.0, http://www.rocscience.com/software/rocdata

Rocscience. (2004). Slide 6.0, http://www.rocscience.com/software/slide

Rocscience. (2004). RocPlane 2.0, http://www.rocscience.com/software/rocplane

RocScience, R. (2002). Rocscience inc. *Toronto, Canada*.

Ramana, K.V. (1993). Humid tropical expansive soils of Trinidad: their geotechnical properties and areal distribution. *Engineering Geology*, *34*(1-2), pp.27-44.

Sen, Z. and Essa, E.A. (1992). Rock Quality Charts for Long –Normally. Distributed Block Size, Int. J.Rock Mech. Min. Sci& Geomech. Abstr. ,Pergamon, Vol.29, No.1, pp.1-12.

Sen, Z.and Sadagah, H.B. (2002). Modified rock mass classification system by continuous rating. Engineering Geology.67:269–280

Sharghi, Y., Siahkoohi, H., Alinia, F. and Moarefvan, P. (2010). Estimation of Lugeon number at the abutments of Bakhtyari dam site using seismic tomography. Aust J Basic Appl Sci 4(2):274–285

Sharma, S.K. (1973). Stability analysis of embankments and slopes. *Geotechnique*, *23*(3), pp.423-433.

Snow, D.T. (1965). *A parallel plate model of fractured permeable media*. University of California, Berkeley.

Spencer, E. (1967). A method of analysis of the stability of embankments assuming parallel inter-slice forces. *Geotechnique*, *17*(1), pp.11-26.

Tefera, M., Chernet, T. and Haro, W. (1996). *Explanation of the geological map of Ethiopia*. Geological Survey of Ethiopia.

Tenalem, A. and Tamiru, A. (2001). Principles of hydrogeology. *Department of Earth Sciences, AAU, Addis Ababa*.

Tiruneh, M. (2005). Reservoir Operational Planning of Irrigation Dams for MicroHydropower Development. A Case Study Conducted on Haiba Micro irrigation Earth Dam in Tigray Regional State. M.Sc. thesis, Addis Ababa University,Ethiopia.

Warner, J. (2004). Practical Handbook of Grouting: Soil, Rock, and Structures. John Wiley & Sons, Hoboken, NJ, USA

Wyllie, D.C. and Mah, C.W. (2004). Rock Slope Engineering 4thEd. The Institution of Mining and Metallurgi Londo

USBR. (1987). Design of Small Dams. United States Department of the Interior, Bureau 145 of Reclamation, Denver

APPENDIX

Appendix 1. Natural moisture content of the soil samples.

Location	Sample code	Sample interval(m)	Mass of can (gm)	Moist soil weight (gm)	Dry weight of soil (gm)	Moisture content (%)
Left Abutment	ASHTP-01A	0-0.7	22.96	85.18	72.5	17.5
		0.7-1.5	22.80	96.9	81.2	19.4
In River Bed	ASHTP-02	0-0.5	21.72	68.69	54.2	26.75
Right Abutment	ASHTP-03A	0-2	21.7	59.9	45.3	32.4
	ASHTP-03B	0-0.6	22.95	79.06	64.9	21.83
Reservoir Area	ASHTP-04A	0-0.44	21.72	95.81	83.20	15.15
	ASHTP-04B	0.44-1	22.89	74.14	56.24	37.4

Appendix 2. Specific Gravity of soil Samples Analysis Determined from Laboratory

Location	Sample code	Sample interval(m)	WO	WA	WB	Specific gravity
Left Abutment	ASHTP-01A	0-0.7	10	126.65	144.45	2.78
	ASHTP-01B	0.7-1.5	10	128.36	143.96	2.56
In River Bed	ASHTP-02	0-0.5	10	127.5	144.5	2.70
Right	ASHTP-03A	0-2	10	126.48	142.78	2.63

Abutment	ASHTP-03B	0-0.6	10	124.22	139.82	2.56
Reservoir Area	ASHTP-04A	0-0.44	10	138.21	144.15	2.46
	ASHTP-04B	0.44-1	10	126.01	143.51	2.75
	ASHTP-04C	1-1.65	10	137.87	143.64	2.37

Appendix 3. Soil Particle Size Analysis Result

Sample code	Sieve Size (mm)/ Passing								Hydrometer (%)			
	at 25	at 19	at 12.5	at 10	at 5	at 2	at 0.425	at 0.075	Sand	Silt	Clay	Type of soil
ASHTP-01A	100.0	100.0	100.0	100.0	100	98.6	95.50	91.9	16	23	61	Fine grain size
ASHTP-01B	100.0	100.0	100.0	100.0	97.8	93.5	88.30	75.8	20	42	38	Fine grain size
ASHTP-02	100.0	100.0	100.0	99.6	99.0	97.7	93.94	89.0	18	30	52	Fine grain size
ASHTP-03A	100.0	100.0	100.0	100.0	99.2	89.7	78.40	69.6	32	34	34	Fine grain size
ASHTP-03B	100.0	100.0	98.6	98.6	98.2	97.9	91.3	76.5	37	33	30	Fine grain size
ASHTP-04A	100	100	100	99.6	99	97.7	93.94	89	16.5	42	40	Fine grain size
ASHTP-04B	100	100	100	100	99.2	89.7	78.4	69.6	21.4	40	34.5	Fine grain size

Appendix 4. Shear stress parameter estimation graphs of soil sample.

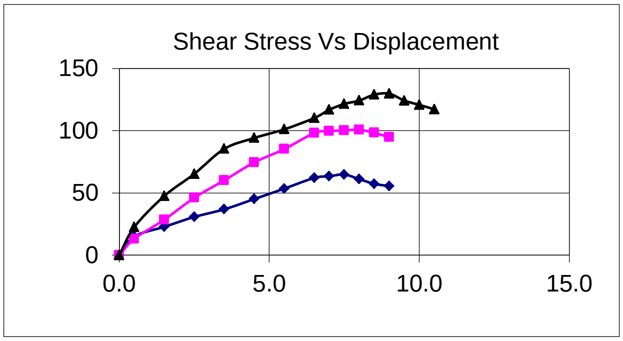

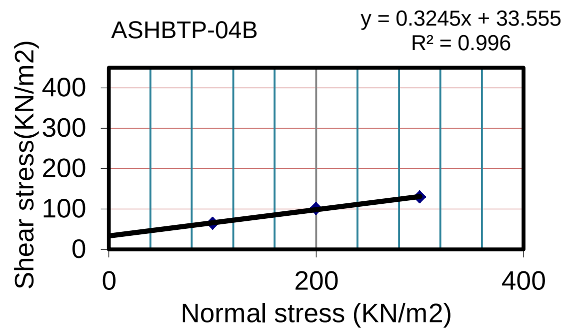

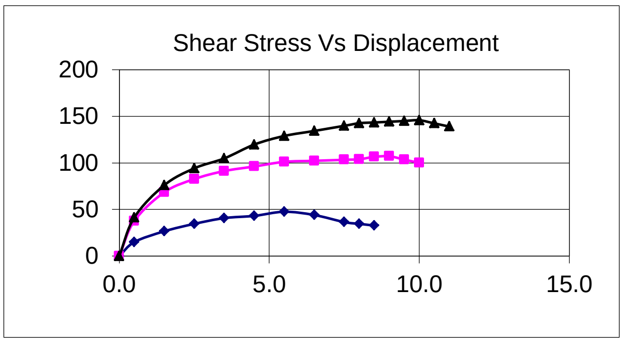

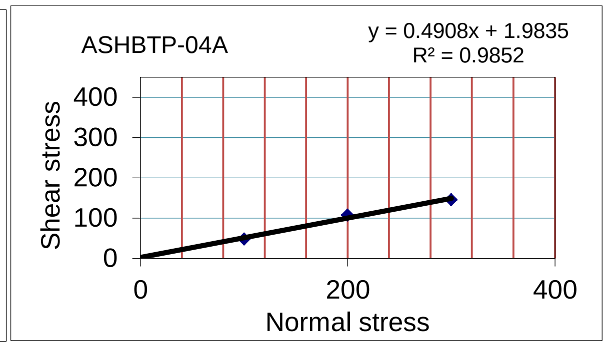

Appendix 5. Bearing Capacity Factors- Nc, Nq, NϒꞋ. For Ø = 10-500 for soil samples.

Ø	N_c	N_q	N_Υ	Ø	N_c	N_q	N_Υ
0	5.1.3	1.00	0.00	26	22.25	11.85	12.54
1	5.38	1.09	0.07	27	23.94	13.20	14.47
2	5.63	1.20	0.24	28	25.80	14.72	16.72
2	5.90	1.31	0.34	29	27.86	16.44	19.34
4	6.19	1.43	0.45	30	30.14	18.40	22.40
5	6.49	1.57	0.57	31	32.67	20.63	25.99
6	6.81	1.72	0.71	32	35.49	23.18	30.22
7	7.16	1.88	0.86	33	38.64	26.09	35.19
8	7.53	2.06	1.03	34	42.16	29.44	41.06
9	7.92	2.25	1.22	35	46.12	33.30	48.03
10	8.35	2.47	1.44	36	50.59	37.75	56.31
11	8.80	2.71	1.69	37	55.63	42.92	66.19
12	9.28	2.97	1.97	38	61.35	48.93	78.03
13	9.91	3.26	2.29	39	67.87	55.96	92.25
14	10.37	3.59	2.65	40	75.31	64.20	109.41
15	10.98	3.94	3.06	41	83.86	73.90	130.22
16	11.63	4.34	3.53	42	93.71	85.38	155.55
17	12.34	4.77	3.67	43	105.11	99.02	186.54
18	13.10	5.26	4.07	44	118.37	115.31	224.64
19	13.93	5.80	4.68	45	133.88	134.88	271.76
20	14.83	6.40	5.39	46	152.10	158.51	330.35
21	15.82	7.07	6.20	47	173.64	187.21	403.67
22	16.88	7.82	7.13	48	199.26	222.31	496.01
23	18.05	8.66	8.20	49	229.93	265.51	613.16
24	19.32	9.60	9.44	50	266.89	319.07	762.89
25	20.72	10.66	10.88				

Appendix 6. RQD of different rock samples from different borehole locations.

BH.ID	Location	Coordinates		Total depth(m)	Interval depth(m)	Average RQD	Rock Quality
		Northing	Easting				
ASHBH-1	Left Abutment	852212	517554	36	0- 0.40	0	Very poor
					0.40- 2.3	61	Good
					2.3- 3.70	0	Very poor
					3.70- 9.00	88	Very good
					9.00- 20.5	58.4	Fair
					20.5- 21.7	34	Poor
					21.7-24.80	60	Good
					24.80-31.7	0	Very poor
					31.7-35	65.5	Good
ASHBH-2	Near to river bed	852212	517560	29	4.30- 6.0	30	Poor
					6.0-17.0	0	Very poor
					17- 20	45	Fair
					20- 23	57.5	Fair
					23- 29	0	Very poor
ASHBH-3	Right Abutment	852272	517554	44	0.5-7.10	0	Very poor
					7.10-14.20	72.5	Good
					14.2- 19	0	Very poor
					19-20	30	Poor
					20-24	0	Very poor
					24-26	0	Very poor
					27.7-32	0	Very poor
					32-35	34	Poor
					35-44	0	Very poor
ASHBH-4	Intake	852054	517628	20	0.70- 3.4	49.67	Fair
					3.4- 5.6	49	Fair
					6- 11	0	Very poor
					11-12.5	78	Good
					12.5-16	0	Very poor
					16-18	50	Fair
					18-20	0	Very poor
ASHBH-5	Dam & S.W junction	852440	517567	15	0-15	0	Very poor
ASHBH-6	S.W(chutte)	852822	517418	15	0.5- 4.6	48	Fair

Appendix 7. Subsurface discontinuity surevy of differnent rock units from different borehole locations.

Borehole-ID	Depth	Orientation W.r.t dam axis	Spacing (cm)	Apertur e(mm)	Filling material	Roughness condition	Discontinuity type
ASHBH-01	0.4-2.6	Normal	35.0	tight		Rough	Fracture
	2.6-3.7						Soil formation
	3.7-9.0	Normal	70.0	<2	Ca/Fe	Rough	Fracture joint
	9-20.5	Normal/parallel		<3	Ca/Fe	Rough	Fracture joint
	20.5- 32						Soil formation
	32-36	Normal	100	<1	SC	Rough	Fracture
ASHBH-02	0.4-7.0	Norma, oblique, and parallel	<5	>5		Rough	Fracture joint
	7.0-17.0						Soil formation
	17.0-23	Normal	15	2	SC	Rough	Fractured joint
	23-29						Soil formation
ASHBH-03	9-14.20	Oblique, Normal	13.0	2.0	Ca/Fe	Rough	Fracture joint
	14.20-32	Parallel, Oblique & Normal	10.0	2.0	Ca/Fe	Rough	Fracture joint
	32-44						Soft formation
ASHBH-04	0.6-4.6	Oblique & Normal	6.0	>4	Ca/Fe	Rough	Fractures
	4.6-20						Soft formation
ASHBH-06	0.5-11.2	Oblique, Normal & Parallel	5.0	>5	Ca	Rough	Fracture joint
	11.2-20						Soft formation

Appendix 8. Subsurface discontinuity surevy of differnent rock units from different borehole locations.

Location	Observation point	Schmidt Rebound Value	Average RN	Mean of RN by discarding those differing from the average by more than 7 units	UCS (MPa)
Right abutment	RAS1	29, 30, 31, 33, 35, 39, 40, 42, 43, 43, 45, 48	40	40.54	104.71
		48,35,45,47,50,51,49,47,46,45,	46.3	46.90	109.39

		39,33,42,43,45,38,39,45,45,41,	41.0	45.5	100
	RAS2	24,31,39,38,36,33,37,34,22,34	32.7	35.75	61.65
		41,37,34,39,32,38,33,42,45,30	37.1	37.66	67.60
		38,45,40,36,32,39,40,37,35,38	38	38	70.79
	RAS3	29, 30, 31, 33, 35, 39, 40, 42, 43, 43, 45, 48	38.1	40.81	79.43
Left abutment	LAS1	20,32,37,30,32,33,34,30,22,36	30.8	33.3	54.95
		31,34,37,30,32,33,34,30,22,34	31.7	32	51.28
	LAS2	29,13,19,18,16,15,17,21,15,18,14	19.6	17.54	24.54
		35,32,37,30,32,33,34,30,22,37	32.2	33.63	44.67
	LAS3	30,33,37,30,32,33,34,30,23,35	31.7	32.6	42.66
		33,32,38,31,32,33,34,30,24,33	33	34.2	46.77
		29,32,37,32,32,33,34,30,21,28	30.4	32.7	43.65
Reservoir	RRS1 Right side	41,37,34,39,32,38,33,42,45,30	37.1	37.90	54.95
		39, 30, 31, 33, 35, 39, 40, 42, 43, 43, 45, 48	40.5	41	63
		30,34,37,35,32,33,34,30,23,33	32.1	33.58	44.67

	RRS2 Right side	40,32,44,43,45,38,39,47,46,45,	41.9	43	69.18
		39,33,42,43,45,38,39,46,47,39,	41.1	42.90	67.6
		27,32,37,30,32,33,34,30,20,36	31.1	32.08	41.68

Appendix 9. Rock mass rating (RMR) values and classification of rocks at the dam site (After Bieniawski, 1989).

	UCS(Mpa)		RQD(%)		Spacing (cm)		Discontinuity condition						Ground water condition		Orientation	RMR value	Rock mass class	Deformation modules Ed = 2RMR-100
Section points	Avg. UCS	Rating	Avg. RQD	Rating	Avg. Value	Rating	Avg.Aperture(cm)	Persistence(cm)	Filling	Weathering Degree	Roughness	Rating	Condition	Rating	Rating			
RAS 1	104.7	12	59.45	13	25	10	No	50	No	S.W	S.R	25	Dry	15	-7	68	Good	50
RAS 2	66.68	7	63.42	13	29	10	No	98	No	S.W	S.R	25	Dry	15	-7	63	Good	40
RAS 3	79.43	7	41.3	8	24	10	No	65	No	S.W	S.R	25	Dry	15	-7	58	Fair	30
LAS 1	53.12	7	52.2	13	23	10	<0.1	92	No	S.W	S.R	25	Dry	15	-7	63	Good	40
LAS 2	34.60	4	31.3	8	15	8	3	20	Soil	M.W	R	20	Dry	15	-7	48	Fair	10
LAS 3	44.36	4	47.5	8	20	8	<0.1	30	No	S.W	S.R	20	Dry	15	-7	48	Fair	10
RRS 1	54.2	7	94.2	20	85	15	2	37	Soil	S.W	S.R	20	Dry	15	-7	70	Good	54
RRS 2	59.48	7	61.7	13	44	8	No	22	No	S.W	S.R	20	Dry	15	-7	56	Fair	26
RRS	49	4	41.5	8	17	8	1.5	31	soil	M.W	R	20	Dry	15	-7	48	Fair	10

3																		

Appendix 10. Estimated shear strength parameters of rock mass using RocData software.

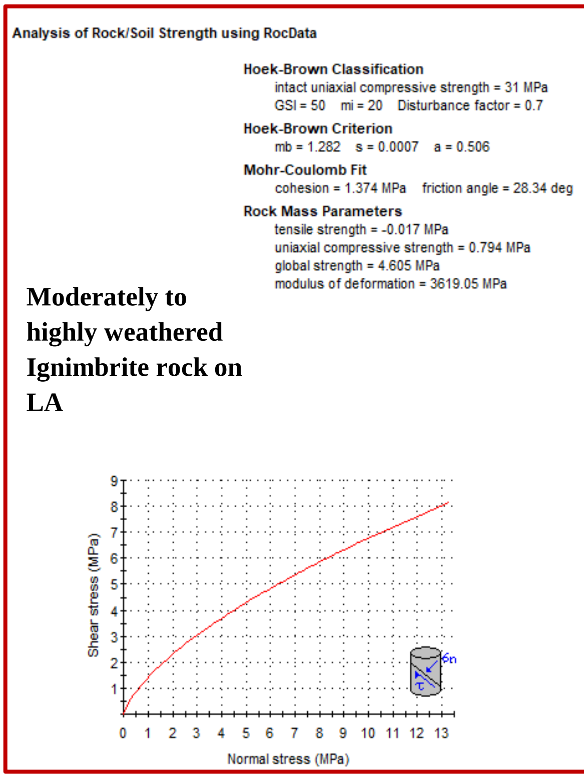

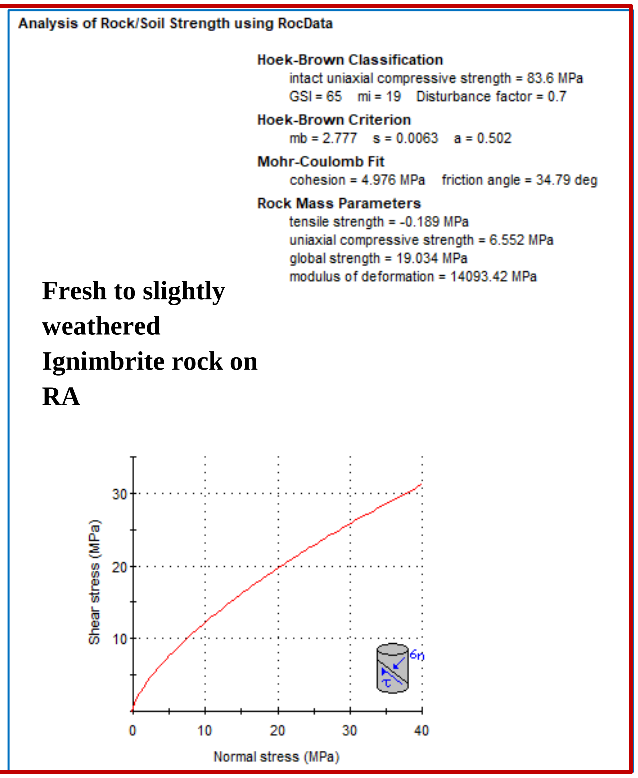

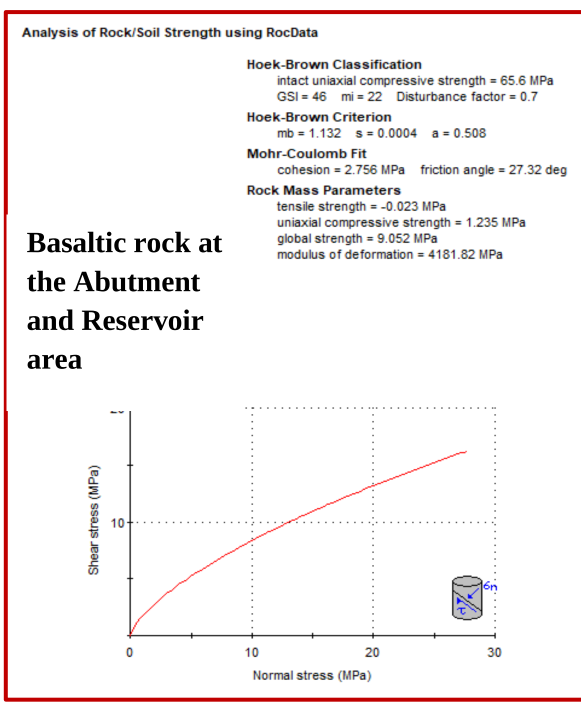

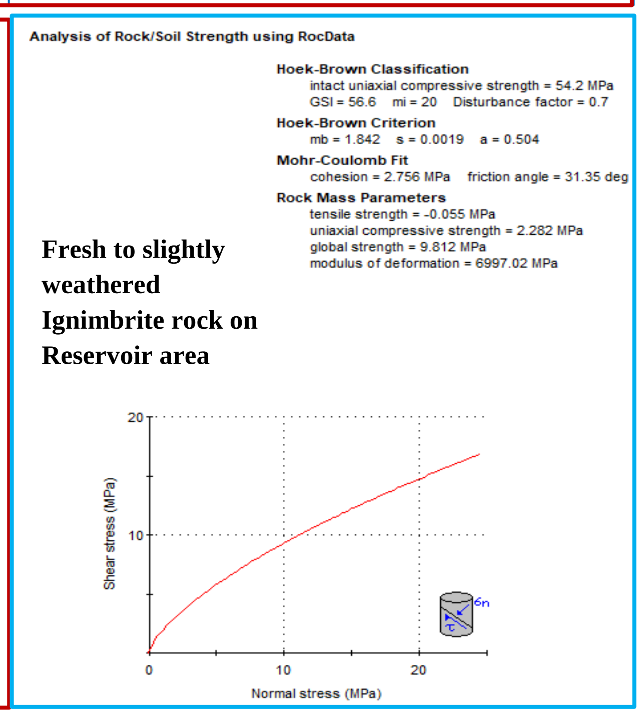

Appendix 11 Estimated shear strength parameters of joints along failure planes using RocData software at LASS1 for JS1, JS2 and JS3 on left abutment, and at RASS1 for JS2 on right abutment.

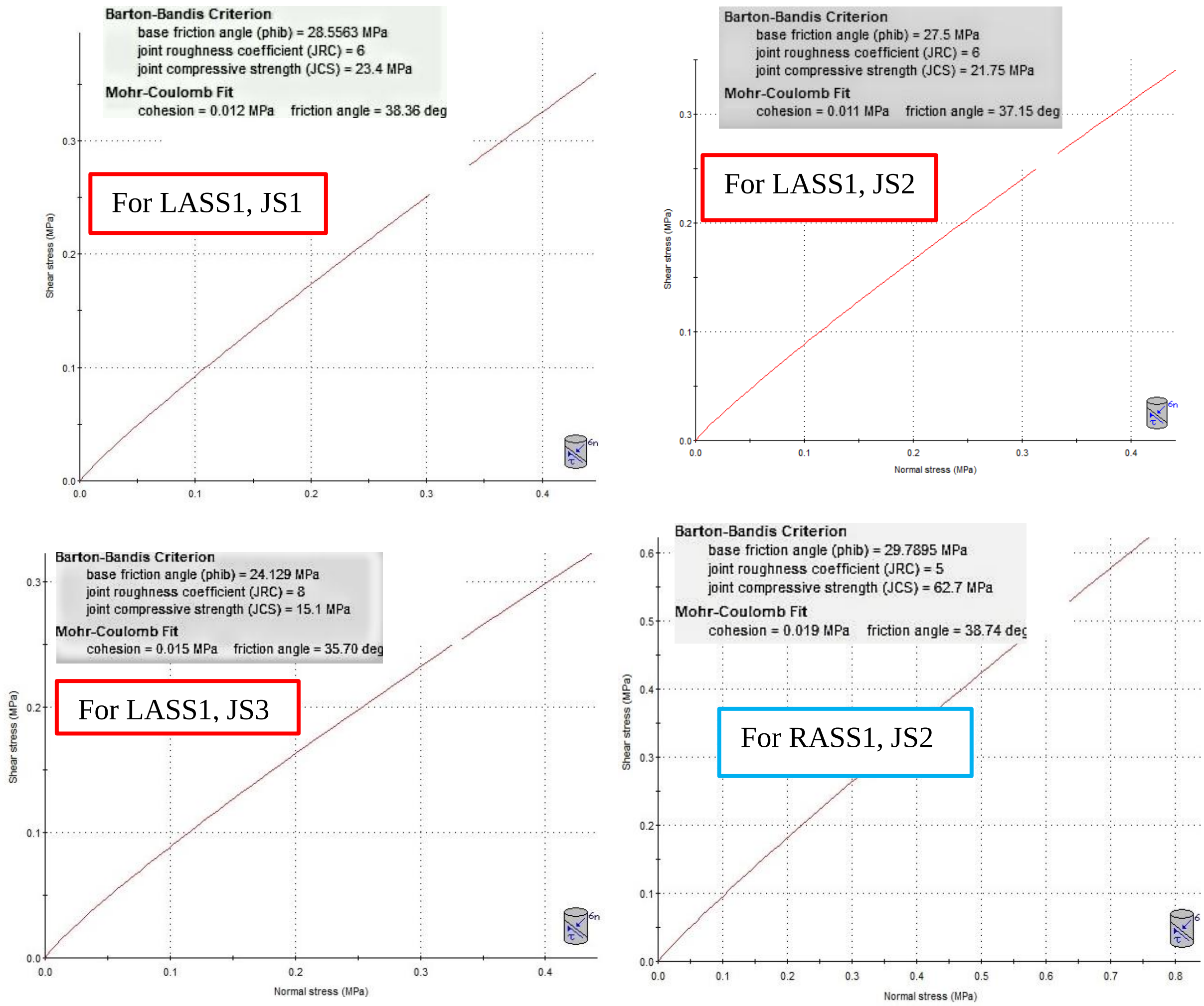

Appendix 12 Coeficient of Permeability of soils according to (USBR, 1987)

Coefficient of permeability (cm/sec)	Degree of permeability	USBR classification
Greater than 10^{0}	Very high	Pervious
10^{-2} to 10^{0}	High	
10^{-4} to 10^{-2}	Medium	
10^{-6} to 10^{-4}	Low	Semi pervious
10^{-8} to 10^{-6}	Very low	Impervious
Less than 10^{-8}	Impermeable	

Appendix 13. Packer test classification based on Lugeon value

Lugeon value range	Classification (Canoglu et al., 2017)
<1	Impermeable
1-5	Low permeable
5-25	Permeable
>25	Highly permeable

Appendix 14 Classification of UCS of rock according to Deere and Miller (1966).

Unconfined Compressive Strength (UCS) (MPa)	Description of streangth
Over 224	Very High Strength
112-224	High streangth
56-112	Medium streangth
28-56	Low streangth
Less than 28	Very low streangth

Appendix 15 Classification of rock mass based on modulus of deformation according to (Serafim & Pereira,1983)

Class	Modulus of deformation (Gpa)	Description of deformation
1	<5	Very high
2	5-15	High
3	15-30	Moderate
4	30-60	Low
5	>60	Very low

Appendix 16. Plasticity characteristics of soil (Burmister, 1947)

Plasticity Index (PI)	Plasticity Characterstics
0	Non-Plastic
1-5	Slightly Plastic
5-10	Low plastic
10-20	Medium plastic
20-40	Highly plastic
>40	Very high plastic

Appendex 17 Reperesentative core samples from different boreholes.

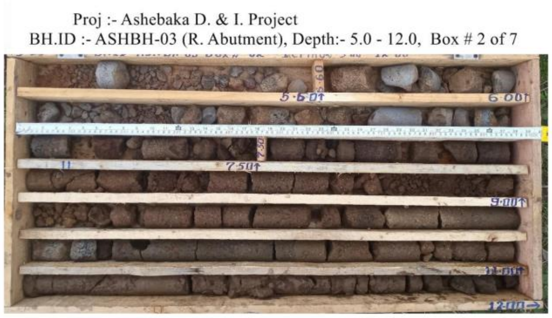

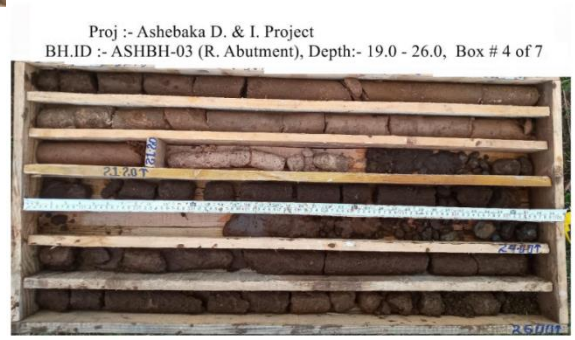

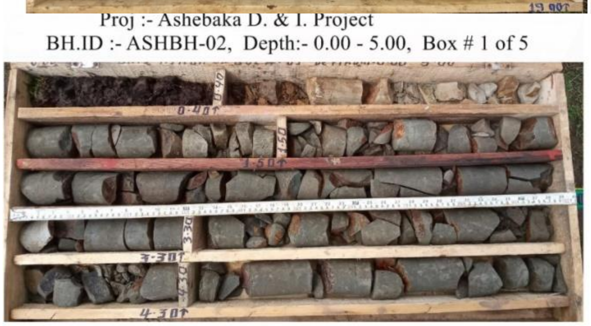

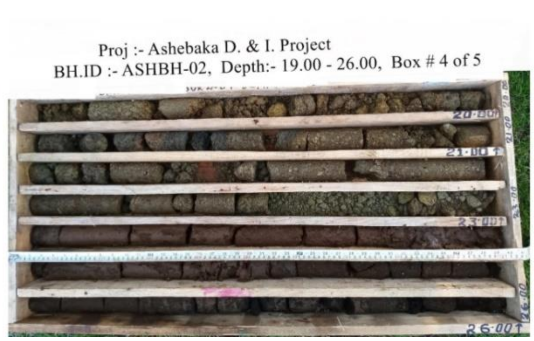

ASHBH-04

ASHBH-05

ASHBH-06

Appendix 17 Factors depend on the existing relationship between discontinuities affecting the rock mass and the slope for SMR

Case of slope Failure		Very Favorable	Favorable	Fair	Unfavorable	Very Unfavorable
P	$(\alpha_j - \alpha_s)$	>30°	30 - 20°	20 - 10°	10 - 5°	<5°
T	$(\alpha_j - \alpha_s - 180^\circ)$	>30°	30 - 20°	20 - 10°	10 - 5°	<5°
W	$(\alpha_i - \alpha_s)$	>30°	30 - 20°	20 - 10°	10 - 5°	<5°
P/W/T	F_1	0.15	0.40	0.70	0.85	1.00
P	(β_j)	<20°	20 - 30°	30 - 35°	35 - 45°	>45°
W	(β_i)	<20°	20 - 30°	30 - 35°	35 - 45°	>45°
P/W	F_2	0.15	0.40	0.70	0.85	1.00
T	F_2	1.0	1.0	1.0	1.0	1.0
P	$(\beta_j - \beta_s)$	>10°	10 - 0°	0°	0–(-10°)	<-10°
W	$(\beta_i - \beta_s)$	>10°	10 - 0°	0°	0–(-10°)	<-10°
T	$(\beta_j + \beta_s)$	<110°	10 - 120°	>120°	>120°	-
P/W/T	F_3	0	- 6	- 25	- 50	- 60

Method	Natural slope	Presplitting	Smooth blasting	Blasting/Ripping	Deficient blasting
F4	+15	+10	+8	0	-8

Appendix 18 Various stability classes as per SMR values (Romana, 1985)

Class No.	V	IV	III	II	I
SMR Value	0-20	21-40	41-60	61-80	81-100
Rock Mass Description	Very bad	Bad	Normal	Good	Very good
Stability	Completely Unstable	Unstable	Partially stable	Stable	Completely stable
Failures	Big Planar or Soil like or Circular	Planar or Big Wedges	Planar along some joint and many wedges	Some Block failure	No Failure
Probability of Failure	0.9	0.6	0.4	0.2	0

Research Fund Acknowledgement

This research thesis was funded by Adama Science and Technology University under the garant number of ASTU/SM-R/698/23,Adama Ethiopia.